UNIVERSITEIT VAN PRETORIA
UNIVERSITY OF PRETORIA
YUNIBESITHI YA PRETORIA

**The role of the kisspeptin receptor, KISS1R, in breast cancer cell proliferation, invasion and migration**

By

**Udochi Felicia Azubuike**

Submitted in partial fulfilment of the requirements for the Master of Science degree in Human Physiology

in the

Department of Physiology

Faculty of Health Sciences

UNIVERSITY OF PRETORIA

2021

## ABSTRACT

Kisspeptin receptor, also known as KISS1R, is the endogenous receptor for the ligand peptide, kisspeptin. It is a G-protein coupled receptor that couples through the Gα$_{q/11}$ pathway. It has been shown that KISS1R activation by kisspeptin results in the activation of phospholipase C, calcium mobilization and ERK1/2 phosphorylation. Moreover, kisspeptin production has been linked to inhibition of metastasis in many cancers. However, in breast cancer, conflicting studies have shown that kisspeptin and KISS1R may play pro-metastatic or anti-metastatic roles. The aim of this study was to decipher the role of endogenous KISS1R in breast cancer cell proliferation, invasion and migration. Firstly, endogenous protein expression of the receptor was determined in 3 breast cancer cell lines by western blotting. Secondly, the signalling potential of the receptor was determined by assessing ERK1/2 phosphorylation after stimulation of cells with the ligand, KP-10. The effects of KP-10 stimulation on the growth rate and migration speed of the cell lines were assessed using crystal violet staining and scratch assay, respectively. Lastly, the last exon, exon 5 of the *KISS1R* gene in the BT-20 and MDA-MB-231 cell lines was assessed by Sanger sequencing. The results show that KISS1R protein is expressed in all the breast cancer cell lines tested albeit at significantly different levels. The non-metastatic BT-20 cell line express a much higher level of KISS1R compared to the metastatic MDA-MB-231 cell line or the migratory, MCF-7 cell line. Furthermore, ERK1/2 phosphorylation analysis after ligand stimulation suggests that only BT-20 cells muster a KISS1R response while no ERK1/2 phosphorylation is seen in MDA-MB-231 cells. The temporal nature of the ERK1/2 response suggests that it is a β-arrestin related activation of ERK1/2. Interestingly, β-arrestin1/2 expression analysis shows high levels of β-arrestin1/2 expression in BT-20 cells but very little in MDA-MB-231 cells. Physiologically, treatment with the KISS1R ligand, KP-10, had no significant impact on cell growth and migration. However, under serum free culture conditions, there was an increase in the migration of MDA-MB-231 cell line treated with KP-10, compared to the untreated control. In the BT-20 and MDA-MB-231 cell lines, a *KISS1R* variant was identified which was characterized by a c.1091T>A in exon 5, resulting in the substitution of leucine to histidine (p.L364H) in the C-terminus or cytoplasmic tail of the receptor. Overall, our data suggest that KISS1R expression correlates with the migratory potential

of the cells and the KISS1R in the BT-20 cells activates ERK1/2 through a G-protein independent mechanism.

**Keywords**: KISS1R, ERK1/2, kisspeptin, KP-10, Breast cancer, BT-20, MDA-MB-231

**DECLARATION**

I declare that this dissertation I am submitting for the Master of Science degree in Human Physiology, is my work and where I used other sources, I referenced them properly. This dissertation has not been previously submitted by me for another degree either at the University of Pretoria or another university.

Udochi Felicia Azubuike

## ACKNOWLEDGEMENTS

**Table of Content**

# Table of Figures

## List of Appendix Figures

# List of Tables

**List of Abbreviations**

| | |
|---|---|
| μl | microliter |
| μM | micromolar |
| Ab | antibody |
| d | day (s) |
| DAPI | 4'.6'-diamidino-2-phenylindole |
| EMT | epithelial-to-mesenchymal-transition |
| ER | endoplasmic reticulum |
| ER$^+$ | Oestrogen receptor positive |
| ERK1/2 | extracellular signal regulated kinase 1/2 |
| FCS | fetal calf serum |
| HEK293 | human embryonic kidney 293 cell line |
| HER2$^+$ | human epidermal growth factor receptor 2 |
| HepG2 | hepatocellular carcinoma cell line |
| h | hour(s) |
| g | gram |
| GPCR | G-protein coupled receptor |
| G$\alpha_{q/11}$ | G protein alpha subunit for $G_q$ and $G_{11}$ subfamilies |
| kD | kilodalton |
| kb | kilobase |
| KISS1R | Kisspeptin 1 receptor |
| KP-10 | kisspeptin-10 |
| M | molar |
| MW | molecular weight |
| min | minute |
| ml | millilitre |
| NCBI | National Centre for Biotechnology Information |
| PCR | polymerase chain reaction |

PR$^+$                  progesterone receptor positive

s                       seconds

TNBC                    triple negative breast cancer

# Chapter 1 LITERATURE REVIEW

## 1.1. Cancer

Cancer is a non-communicable disease that is characterized by uncontrolled cell growth in one or more body organs.[1] It is an ancient disease that has been described as far back as 3500 BCE, where it was discovered in Egyptian mummies and fossil bones, and described in 2 Egyptian papyri. In the one papyrus, the Edwin Smith surgical papyrus, about 48 cancer cases were described and 8 of them were like breast cancer. In one of the breast cancer cases, case 39, breast cancer was described as a protruding head in a patient's breast, and it was reported to be an untreatable disease. [2,3] In the second papyrus, the Ebers papyrus, cancer was described as swollen tumour vessels. [4] Over time, more suggestions and descriptions of the cancer disease were made. In 460 BCE, Hippocrates (460-370 B.C), the father of modern medicine, described cancer as a humoral disease. He predicted that the body has 4 humours: phlegm, blood, black bile, and yellow bile, and suggested that breast cancer was due to black bile in the breast and it should not be treated. Rather, it should be allowed to harden, rupture, and release the black bile to other parts of the body. He was the one that called cancer "Karkinos", which is a Greek word that means crab. Apart from the breast tumour, he also described skin, cervical, stomach and rectal cancers.[4] Although cancer is an ancient disease, its prevalence has increased in current years due to the increase in the aging population and presence of many carcinogens in the environment resulting from modernization and industrialization.[5]

Presently, cancer is the second  leading cause of death after cardiovascular diseases,[6] with 7.6 million people dying from cancer in 2008 and it is anticipated that by 2030 the number of deaths will rise to 13.1 million.[7] Cancer research has led to an improvement in the 5 year survival rates of cancer patients. This improvement is attributed to better cancer detection techniques and screening. Due to improvements in screening, many cancers can be detected in their early treatable stage. However, in most cases, 90% of cancer related deaths are caused by the development of metastasis and there is currently no preventative therapy for metastasis.[8]

According to the World Health Organization (2018) [9], lung cancer is the most commonly diagnosed (accounts for 11.6% of total cancer cases) and leading cause of death (accounts for 18.4% of total cancer deaths) in the world, followed by female breast cancer, colorectal cancer and prostate cancer, which have incidence rates of 11.6%, 10.2% and 7.1%, respectively. The global distribution of the cases and deaths for the 10 most common cancer in the world is shown in Figure 1.1.
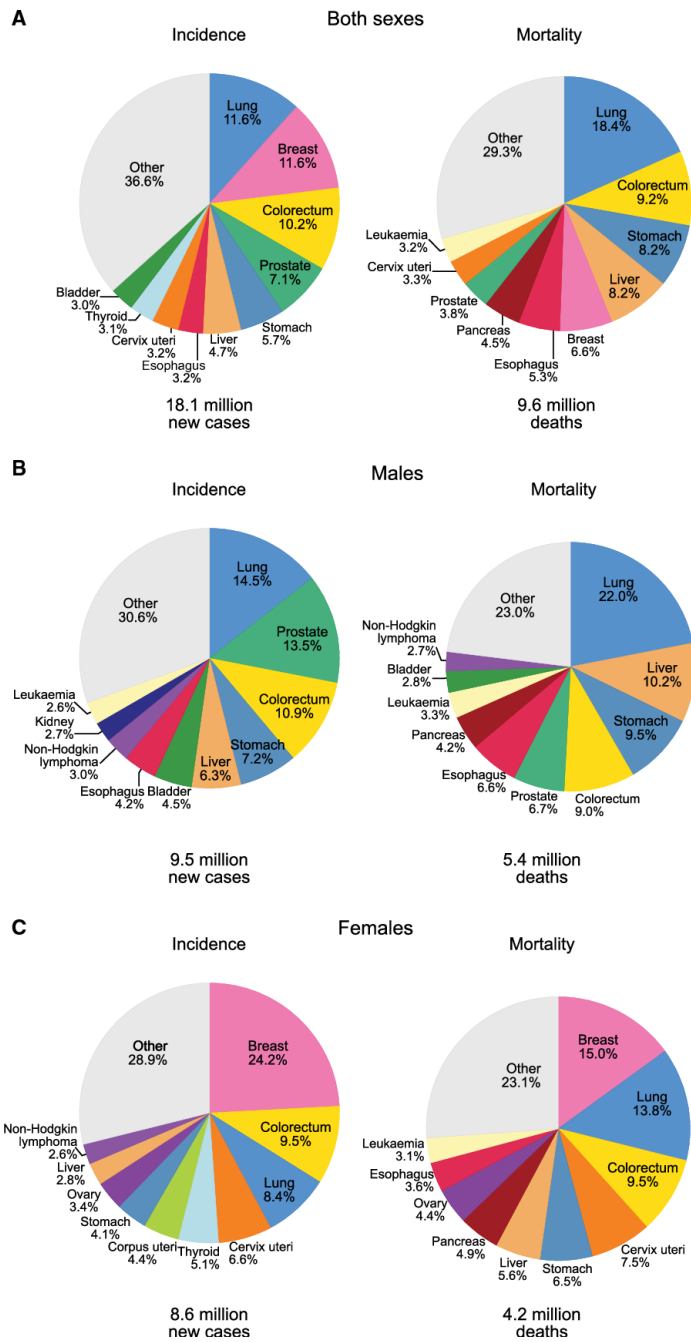
Figure 1.1: The global distribution of the incidence and mortality for the 10 most common cancers in 2018 in both genders (A), in males (B) and in females (C).[9]

4

## 1.2.  Cancer biology

Under normal physiological conditions, cells grow and divide to form new cells when the body needs them. When the cells get old or become damaged, they are destroyed through programmed cell death (apoptosis) and the dead cells get replaced by new cells. However, during cancer, this pattern of cell growth, division and apoptosis is disrupted because the cells start to grow uncontrollably (even when they are not needed). The cells become resistant to apoptosis and so the cells that were supposed to die, live, and new cells grow when they are not required. These cells divide non-stop and form growths that are known as solid tumours.[10] There are different cancer types and they have this common attribute of growing, dividing and re-dividing continuously.[6]

Cancer is a genetic disease that occurs when there are changes in the genes that control cell growth and division.  Some of these changes can be inherited mutations in genes mostly involved in DNA repair such as BRCA1 and BRCA2. This makes some people more susceptible to contracting cancer. Other changes can be somatic mutations caused by exposure to environmental factors such as smoke from cigarettes, and radiation.[6]

Genetic changes that result in cancer mostly affect 3 types of genes: proto-oncogenes, tumour suppressor genes and DNA repair genes. The proto-oncogenes are genes that control normal cell growth and division. However, when they are mutated (gain-of-function mutation) they become constitutively active and become cancer causing genes (oncogenes).[11] One example is the *Kras* gene whose mutation has been involved in 30 to 40% of colorectal cancers.[12] Tumour suppressor genes such as *TP53* are also involved in normal cell growth and preventing uncontrolled cell growth. When they acquire inactivating mutations, they lose their function and cells grow uncontrollably. DNA repair genes or stability genes are genes that repair damage in the DNA such as excised nucleotides and mismatched nucleotide pairs, which occur during normal DNA replication or when cells are exposed to mutagens. Therefore, when they acquire inactivating mutations, this leads to increased mutations in other genes and the accumulation of these mutations results in cancer. [10,11]

Tumours exhibit aberrant cell proliferation and can be either benign or malignant. [13] In cancer pathology, it is important to be able to distinguish between benign and malignant tumours. Benign tumours do not invade surrounding tissues, they remain confined to their original location and they are called non-cancerous tumours. They can be treated either through surgery, chemotherapy, or radiotherapy. When treated, they do not grow back. However, compared to benign tumours in other parts of the body, benign brain tumours can be life threatening.[13,14] On the other hand, malignant tumours have the ability to invade normal tissues and spread through the lymphatic and circulatory system to other parts of the body.[13,14] Only malignant tumours are called cancers.[13,14] Benign and malignant tumours are classified based on the type of cell that they arise from. Most types of cancer fall into one of the 5 categories; carcinomas, sarcomas, leukaemia, lymphomas, and myelomas.[13] Carcinomas arise from epithelial cells, while sarcomas arise from connective tissues like bone, muscle and fibrous tissue, and lymphomas, leukaemia and myelomas are from cells of the immune system and blood forming cells, respectively.[13]

The cancer disease consists of many molecular components that are constantly evolving. Therefore, explaining the events that drive cancer genesis and progression is still a major challenge for clinicians and researchers.[15] In 2000, Hanahan and Weinberg gave a detailed logical framework for the functional study of cancer. They demonstrated 6 characteristics that cancer cells acquire during tumorigenesis and tumour development. These were called the 'hallmarks of cancer'. These hallmarks of cancer differentiate cancer cells from normal cells. The first 6 hallmarks include: sustaining proliferative signalling, evading growth suppressors, resisting cell death, enabling replicative immortality, inducing angiogenesis and activating invasion and metastasis.[16] In 2011, Hanahan and Weinberg extended the original 6 hallmarks, as they identified 2 characteristics that are important for the acquisition of the 6 hallmarks. They are inflammation, and genome instability and mutation. Other emerging potential hallmarks that are recognized include the deregulation of cellular energetics and avoidance of immune destruction.[17]

1.3.  <u>Breast cancer</u>

Breast cancer is a group of heterogeneous tumours that originate from the epithelial cells that line the milk ducts.[18] As previously mentioned, breast cancer is an ancient disease that was first described in one of the Egyptian papyri.[4]

Our understanding of breast cancer and its treatment has greatly evolved over centuries from being an untreatable systemic disease to a heterogeneous group of diseases that can be treated if diagnosed early. After the description of breast cancer in the Edwin Smith Papyrus as an incurable disease, in 460 B.C Hippocrates described breast cancer as a black bile with crab-like tumours that should not be treated, but should be allowed to harden, rupture and release the black bile to the different parts of the body.[4] In 203 C. E, a Greek physician known as Galen described breast cancer as a disease that is common in menopausal females and females with abnormal menstrual cycles and suggested that it should be treated using sulphuric acid, castor oil and opium. He also suggested that the affected breast should be excised using hot cautery.[4,19] During the middle Ages, breast cancer was treated through surgery by either lumpectomy or mastectomy. Later on, in the 18th century, through epidemiological studies, it was observed that breast cancer was more common in nuns than in married women and this observation was attributed to childbearing. Therefore, it was theorized that breast cancer was caused by childlessness as well as depressive mental disorders and breast inflammation filled with pus. In the late 18th century the French surgeon, Henry LeDran, theorized that breast cancer was a localized disease that has the potential to spread through the vasculature to other parts of the body as the disease progresses.[19] By the 19th century, breast cancer was observed to be a hormone dependent disease. It was observed that in premenopausal women with breast cancer, the growth of the tumour fluctuated with the menstrual cycle. While in postmenopausal women, tumour growth was slower.[4] Many of the advances in breast cancer were made in the 20th century. Firstly, more treatment options such as radiotherapy and chemotherapy, were identified. Secondly, it was established that breast cancer is a hereditary disease. Thirdly, before the 20th century, breast cancer was detected only through physical examination such as palpitation and nipple inversion and retraction; this was replaced by mammography, after the discovery of X-ray.[4] Fourthly, it

was discovered that surgery is not enough to treat breast cancer, especially after the tumour cells have disseminated to other parts of the body.[19] Fifthly, it was shown that a combination of lumpectomy surgery, radiation therapy, and chemotherapy was more effective than radical mastectomy, in treating breast cancer. It was also in the 20th century that Tamoxifen was discovered as an anti-oestrogen drug that can be used to treat oestrogen receptor positive breast cancers. Trastuzumab or Herceptin, was discovered as a monoclonal antibody drug that can be used to treat breast cancers with Human epidermal growth factor receptor 2 (HER2) amplifications. Another striking discovery was the increased risk of breast cancer in individuals with family history of mutations in the breast cancer tumour suppressor genes: *BRCA1* and *BRCA2*.[4] In the 21st century, with the advent of the human genome sequenced in 2003, more methods of studying breast cancer as well as new therapeutic and diagnostic tools have been and are still being discovered. One of the tools for studying breast cancer which was discovered in the 21st century is The Cancer Genome Atlas (TCGA), which uses bioinformatics and large-scale genome sequencing to find cancer-related mutations. It has helped to understand the molecular basis of cancer. Breast cancer classification based on gene expression profiling was discovered in the 21st century. Moreover, various genetic tests have been developed such as the Oncotype DX Breast Cancer Assay that can stratify breast cancers to allow more directed treatment decisions.[4]

Worldwide, breast cancer is the most diagnosed and leading cause of cancer related death in women.[20] Each year breast cancer accounts for 23% (1.38 million women) of cancer diagnoses and 14% (458 000 women) of cancer deaths.[21] Studies have shown that breast cancer has a higher incidence in developed countries. However, half of the diagnoses and over 50% of breast cancer deaths occur in developing countries. It affects both males and females but females are at a higher risk of the disease.[4] Some of the most important risk factors for breast cancer are gender, age (breast cancer incidence increases with age), late or no childbearing, short breastfeeding time, use of birth controls or contraceptives (women who use hormonal contraceptives are more prone to contracting breast cancer compared to women that have never used hormonal contraceptives [22]), race (Caucasian women are more at risk of developing breast cancer although African women are more likely to die from the disease), obesity, excessive

alcohol consumption, and hormone replacement therapy after menopause.[23] Also, a person with a mother, sister or daughter that has been diagnosed with breast cancer is at a higher risk of developing breast cancer due to the presence of cancer gene variations.[23] For instance, inherited mutations in the breast cancer associated genes, *BRCA1* and *BRCA2*, accounts for 5-10% of breast cancers.[23]

Since 1989, there has been a decline in breast cancer mortality in premenopausal women.[24] This is most likely as a result of early detection and improved treatments in developed economies.[24] Such improved treatments include chemotherapy using Doxorubicin, which has shown great response with limited resistance.[24]

Based on the histopathological features of the primary tumour, breast cancer can be classified based on the presence or absence of the oestrogen receptor (ER) and the progesterone receptor (PR), and on the overexpression of HER2 oncogene. This system of classification helps to determine the optimal treatment options for each patient. In this system of classification, therapy is targeted against specific cancer drivers. For instance, a patient with ER positive breast cancer will be given anti-oestrogen therapies such as Tamoxifen, while a patient with HER2 breast cancer will be given anti-HER2 therapies such as Herceptin. [21]

Another way in which breast cancer can be classified is based on molecular profiling. Breast cancer can be subdivided into at least 5 subtypes: Luminal A, Luminal B, HER2, basal like and normal-like breast cancer.[23] The subtypes are based on the presence or absence of ER and PR or the overexpression of HER2, and levels of the cell proliferation marker, Ki-67, as shown in Table 1.1.

Table 1.1: Classification of breast cancer based on molecular profiling.

| Subtype | Features | Description |
|---|---|---|
| **Luminal A breast cancer** | ER+, PR+, HER2- and low level of Ki-67 | Accounts for 40% of all breast cancers and it grows slowly and responds to hormone therapy.[23] |
| **Luminal B breast cancer** | ER+ or PR+, HER2+ and high levels of Ki-67 | Accounts for less than 20% of all breast cancers. It grows faster than Luminal A cancer and has a slightly worse prognosis.[23] |
| **HER2 positive breast cancer** | ER-, PR- and overexpression of HER2 | Accounts for 15-20% of breast cancer patients. It grows faster than the Luminal cancers and has a worse prognosis. However, it can be treated with targeted therapies like Herceptin, which target the HER2 protein.[23] |
| **Basal-like breast cancer or triple-negative breast cancer (TNBC)** | ER-, PR-, and HER2- | It accounts for 20% of all breast cancers.[23] It is often diagnosed in women below 50 years of age.[25] |
| **Normal-like breast cancer** | ER+, PR+, HER2- and low Ki-67. | It has similar features to Luminal A but its prognosis is worse than Luminal A. [23,26] |

*+, present; -, absent; ER, oestrogen receptor; PR, progesterone receptor; HER2, Human epidermal growth factor receptor 2; Ki-67 is a marker for cell proliferation.*

Triple negative breast cancer (TNBC) is an aggressive type of breast cancer that has a short progression time and metastasizes early. As a result of these factors, patients with TNBC have a poor overall survival. There are currently no targeted therapies for TNBC

due to lack of identified targets for this subtype, although about 20% of the patients are responsive to standard chemotherapies.[27] Therefore, lots of research are currently ongoing to find a specific therapy for TNBC.

## 1.4.  Breast cancer biology

Breast cancer is initiated by mutations in genes that result in uncontrolled growth. Mutations in 2 gene families are essential. These families are proto-oncogenes and tumour-suppressor genes.[11,28,29] Deleterious mutations in a proto-oncogene such as *HER2 also known as ErbB2* causes it to be permanently active due to a loss of regulatory motifs leading to increased cell proliferation. The function of tumour-suppressor genes such as *BRCA1* and *BRCA2* is to control cell division, repair DNA mismatches and induce apoptosis in compromised cells. Mutations in these tumour-suppressor genes inactivates them resulting in loss of cell division suppression leading to uncontrolled growth.[11,29]

Breast cancer is a heterogeneous group of diseases as discussed above. There are two main types of heterogeneity: intra-tumour heterogeneity and inter-tumour heterogeneity which is characterised by the hormone receptors status of different tumours. Intra-tumour heterogeneity occurs when there are molecular, phenotypic and functional variations within a individual patient's tumour.[20] According to Charles Darwin, in the Origin of Species, "It has been proven experimentally that if a plot of ground is sown with one species of grass, and a similar plot of ground is sown with several distinct genera of grasses, a greater number of plants and a greater weight of dry herbage will be raised in the latter case than in the former". [20,30,31] This shows how diversity makes communities to be more productive. Just like the diversity in the different ecological systems, diversity in tumours occurs as a result of both co-operation and competition among the tumour cells and this makes the tumours more resistant to therapies.[20] Thus, tumour heterogeneity has made cancer treatment difficult due to the intra and inter-patient variation.

## 1.5.   Introduction to metastasis

Breast cancer metastasis is the cause of almost all breast cancer related mortality.[21] Metastasis is a multi-step process that involves a series of events or adaptations that occur sequentially but are interrelated.[32,33] There are 7 processes that are essential for metastasis to occur: tumour cell detachment from the primary tumour, invasion into the surrounding tissue, migration to the vasculature, intravasation of an arteriole, extravasation at a distant site, survival in the tissue and expansion to form a secondary tumour.[34] Metastatic breast cancers are also called stage 4 or advanced breast cancers, and it can be seen in lymph nodes around the armpit and in distant organs including the lung, liver, bone and brain.[23,35] A summary of the process of metastasis is shown in Figure 1.2.
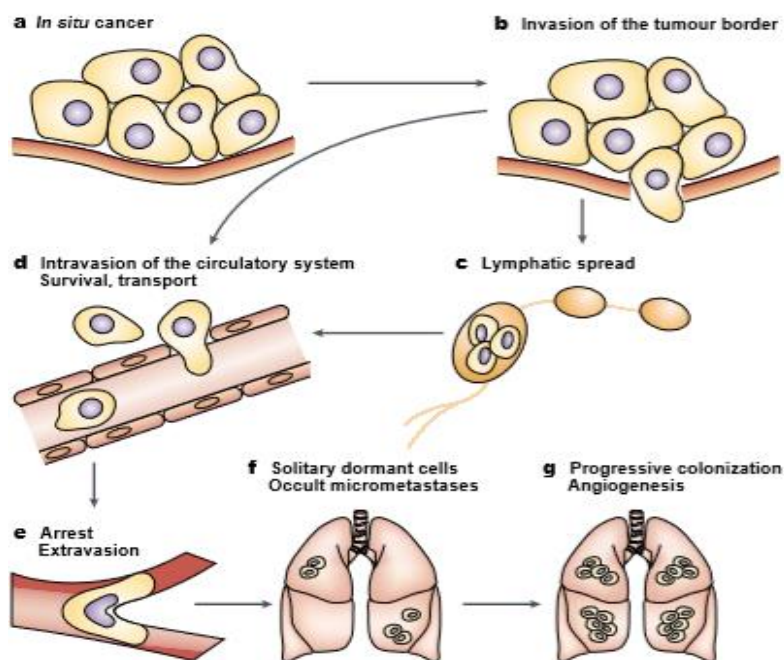


Figure 1.2: Summary of the metastasis process.

During metastasis, (a) cancer cells that have undergone epithelial-mesenchymal transition detach from the primary tumour, (b) invade the basement membrane, (c and d) intravasate into the lymphatic and circulatory

system, evade attack by the immune system, (e) extravasate at distant capillary beds, (f) invade and proliferate in distant organs, (g) these metastatic cells form a microenvironment that facilitates angiogenesis and proliferation, leading to a macroscopic, malignant, secondary tumour.[33,34,36]

Cancer cells metastasize to preferential organs. To explain this preference of cancer cells to specific organs, in 1889 the English surgeon Stephen Paget proposed a theory called the "seed and soil theory". According to the seed and soil theory metastasis only occurs when the right tumour cell "seed" is planted in the suitable target organ "soil".[37] Most solid tumours originate from epithelial cells which are separated from the stroma by a basal lamina and are connected to each other through cell-to-cell adhesion molecules. When a tumour progresses from an *in situ* to an invasive carcinoma, epithelial cells lose the ability to adhere to each other and they invade the basement membrane. This is due to a process called epithelial-to-mesenchymal transition (EMT).[38]

The process of breast cancer metastasis begins when cancer epithelial cells of the primary tumour undergo EMT. In EMT, epithelial cells which were well differentiated, polarized, and organized cells, are changed into cells that are undifferentiated, isolated and mesenchymal, with migratory and invasive behaviour.[32] Such mesenchymal cells are elongated and fibroblast-like in shape and are able to secrete enzymes such as matrix metalloproteinases (MMP), that degrade the extracellular matrix (ECM) and allow the cells to invade the surrounding connective tissue.[26]

## 1.6.  Epithelial to Mesenchymal Transition (EMT)

EMT is the essential first step in metastasis. During EMT there is a change in cell-to-cell adhesion and cell adhesion to the ECM. The family of transmembrane glycoproteins called cadherins are important in mediating cell-to-cell adhesion.[39] There are over 20 members of the cadherin family and they function in a homotypic manner, such that E-cadherins in epithelial cells only recognise and bind to other E-cadherins on neighbouring cells in trans or to E-cadherin on the same cells in cis.[40] Cells undergoing EMT down-

13

regulate E-cadherin expression allowing cells to dissociate from their cell-to-cell junctions.[41] At the same time, expression of the mesenchymal marker N-cadherin is increased.[42] Other mesenchymal markers that are expressed by the mesenchymal cells after EMT are: alpha smooth muscle Actin (α-SMA), fibroblast-specific protein 1 (FSP1), vimentin and desmin.[43] EMT is activated by transcriptional repressors of E-cadherin such as Snail, Twist, Zinc finger E-box binding homeobox 1 (ZEB1) and Slug, which are also involved in embryogenesis.[44] For example, the transcription factors, ZEB1 and ZEB2 proteins with their zinc finger domains can bind directly to the promoter and induce the expression of mesenchymal marker genes and suppress the expression of E-cadherin and other epithelial markers.[45] These transcription repressors are involved in signalling pathways such as receptor tyrosine kinases (RTKs), transforming growth factor beta (TGFβ) superfamily, Notch and Wnt signalling pathway. TGFβ signalling activates the expression of EMT transcription factors, Snail and Slug, ZEB1 and ZEB2, and Twist through a receptor mediated pathway. The ligand binds to the receptor, activating it. Active receptor phosphorylates Smad2 and Smad3, which in turn bind to Smad4 and forms a complex.[46] These enter the nucleus and directly bind to the regulatory promoter sequence of Snail and induces its transcription. This in turn forms an active Smad2/3, Smad4 and Snail complex which binds to the regulatory promoter sequences of the genes that encode epithelial junction proteins, E-cadherin and occludin, causing TGFβ-induced repression of expression.[47]

Another group of glycoproteins called integrins are important for cell adhesion to the ECM. Integrins are a family of 24 transmembrane heterodimers that are produced from a combination of 18α integrin and 8β integrin subunits.[48] Some integrins interact with specific ligands in the ECM i.e. α5β1 integrins only bind to fibronectin, while other integrins such as αvβ3 are promiscuous and bind to diverse ligands such as fibrinogen, and vitronectin.[48] Switching integrin expression allows cells to adhere and migrate on ECM mixtures that are different to the epithelial ECM of the primary tumour. Integrins also act as mediators of adhesion dependent survival. During EMT, the pro-survival pathways are altered to allow cells to detach without entering apoptosis. Therefore, primary tumour cells that have undergone EMT have improved migration and are resistant to anoikis.[49]

However, when they have arrived at their target site they revert to their epithelial phenotype through mesenchymal to epithelial transition (MET).

EMT is completed when the basement membrane is degraded and mesenchymal cells migrate away from the epithelial layer, thereby invading the basement membrane into the stroma.[26]

## 1.7. Invasion and migration

Invasion and migration are two important processes in the metastatic cascade. Loss of cell-to-cell adhesion through EMT is a prerequisite for invasion.[38] But to invade distant tissues metastatic cells have to be migratory.[38] Up-regulation of α5β1 integrin has been linked to cancer invasiveness during cancer metastasis.[32] Some integrins also promote invasion by activating proto-oncogenes such as *P13K* and *Src*.[49] *Src* is under the control of integrins and activates and releases matrix metalloproteinases (MMPs) which degrade the basement membrane and ECM.[48] This allows the primary tumour cells to invade surrounding tissue.

Tumour cells can migrate using similar mechanisms and migration modes as seen in normal cells during physiological processes such as leukocyte migration and collective migration during early development.[50] Cell migration can be divided into 2 different forms: single-cell migration and collective or coordinated migration.[32,39] While single cells migrate independently, collective cells are attached to each other and they migrate as a group or sheet. Coordinated migration occurs mostly in epithelial and endothelial cells while single cell migration occurs in leukocytes and fibroblasts during inflammation.[32,39] Metastatic tumour cells use both collective and single cell migration during invasive growth and metastasis.[50]

During single cell migration, the tumour cells can migrate in either of two ways: (1) Protease-dependent mesenchymal migration or (2) Protease-independent amoeboid-like migration.[32] In protease-dependent mesenchymal migration, the mesenchymal cells take

advantage of their elongated, fibroblast-like shape to move through the ECM that has been degraded by MMPs secreted by the cells.[32,39] Cells moving by mesenchymal migration migrate slowly due to the need for ECM degradation. Such cells adhere strongly to the surrounding ECM and create a path for invasion using ECM degrading proteases.[51] Mesenchymal migration involves the following 5 steps: 1. Formation of a pseudopod protrusion due to Actin cytoskeleton contraction under the control of GTPases Rac1 and Cdc42. 2. Formation of focal adhesions containing β1 and β3 integrins. 3. Proteolytic enzyme activation at the cell-matrix interface which leads to the destruction and remodelling of the ECM. 4. Change in Actin cytoskeleton polarization under myosin II mediated control and 5. Trailing edge detachment and movement towards the defects formed in the matrix structure.[50]

The second type of single cell migration is protease-independent amoeboid migration. It has a similar behavioural and movement pattern as an amoeba, a single celled organism. Amoeboid tumour cells only weakly attach to the ECM through non-integrin adhesion using selectin instead of integrin based adhesions.[50] The tumour cells in amoeboid migration move through pores and spaces between the fibres of the ECM due to a lack of proteolytic enzymes.[50] This movement through small pores also causes the deformation of the nucleus. During amoeboid migration, Rho kinase signalling is activated which allows the cells to squeeze through the matrix.[32,39] Rho-family GTPases are small GTP binding proteins that play an important role in the reorganization of the Actin cytoskeleton. Active RhoA binds to and activates the effector, ROCK, which in turn phosphorylates and activates downstream effectors such as myosin light chain (MLC) which leads to the contraction of Actin-myosin.[52] This causes a change in conformation so that the activated Rho proteins control cell morphology and behaviour.[52]

Tumour cells can transition between mesenchymal and amoeboid migration to adapt to changing environmental conditions. For example, reduced stiffness or density of the ECM can induce the transition from mesenchymal to amoeboid.[51]

During collective migration cells migrate as a group that are connected to each other through adherens junctions formed around cadherins.[53] The group of moving cells are polarised so that they have a leading edge, containing integrins and proteases. Studies

have shown that there is a difference in gene expression and morphology of cells in the leading edge and those following them, which are called the trailing edge.[53] The cells at the leading edge are usually mesenchymal-like with weaker cell-cell adhesions and protrusions adhering to the ECM via pseudopodia and invadopodia while the following cells collectively form rosette-like tubular structures with tight junctions between them. [50]

## 1.8.    Circulation

Breast cancer cells circulating in the blood or lymphatic vessel survive by being resistant to anoikis (programmed cell death due to detachment from the ECM), resisting shear forces of the blood flow and evading the immune system. One way in which cancer cells can protect themselves from shear forces and detection by the immune system is through the formation of small emboli consisting of tumour cells covered by platelets.[26] Cancer cells can also evade immune system surveillance by modulating the antigen presenting process. This happens when the antigen processing machinery that controls the major histocompatibility complex I pathway is downregulated. As a result of this, the expression of the tumour antigen is downregulated and this enhances tumour metastasis because cytotoxic T lymphocytes are unable to recognise the antigens on the tumour cells.[54]

## 1.9.    Extravasation to a distant organ

Metastatic tumour cells that survived the harsh conditions of the vascular environment extravasate into the target tissue or organ. Extravasation is when tumour cells exit the vasculature. For successful extravasation, tumour cells need to attach to and move through the endothelial layer of the arteriole. This depends on changes in endothelial architecture including receptor expression and cell-to-cell contacts.[55]

Tumour cell extravasation requires three sequential steps. Firstly, the cells attach loosely to the vascular endothelial cells through an interaction between the cell surface ligands such as lectins found on the cancer cell and selectins, the protein receptors expressed on the endothelium. Following the initial weak interaction, integrin dependent binding ensues allowing the cancer cell to spread on the endothelium and produce protrusions that invade the cell layer.

The tumour cells do not migrate randomly to any organ, they are guided by signals which are delivered by the vascular endothelium. This was observed by Paget in 1889 [56], who noticed the preferential dissemination of tumour cells 'seeding' to target organs 'soil'. In 2001, Balkwill and Mantovani [57] showed that these metastatic tumour cells may use chemokine gradients to spread to different parts of the body.[55] For example, the stromal-cell derived factor (SDF)-1α is a chemokine that is expressed in organs that are the first destination for breast cancer metastasis.[55]  Also, breast cancer tissues express the chemokine receptor, CXCR4 at high levels, while the organs that it preferentially metastasizes to (bone marrow, lung, lymph nodes and liver) express the ligand, CXCL12, at higher levels compared to other tissues like the stomach, kidney and skin.[58] Breast cancer metastasis to the bone occurs with an incidence rate of 65-75%.[37] This has been attributed to some features of the bone such as acidic pH, cytokines, high extracellular calcium concentration and growth factors, which provide homing signals for the cancer cells.[37]

## 1.10.  Survival and outgrowth

The tumour cells in the new microenvironment have to adapt to the new environment, which has stroma components, tissue organization and matrix composition that are different from their original or primary site.[26] They also express certain chemokine receptors such as chemokine receptor 4 (CXCR4), which binds to locally produced CXCL12 and activates pro-survival and proliferation pathways.[59]

To survive in their new environment, they induce the production of new blood vessels through which they can get nutrients from the blood. This process is called angiogenesis. Angiogenesis is regulated by the balance between pro-angiogenic and anti-angiogenic factors.[60] Angiogenesis can be induced by tumour cell expression of angiogenic proteins in response to hypoxia and nutrient starvation.

Thus, cancer progression and especially metastasis is a process largely driven by adaptation to changing environments and survival in hostile ones. Many of the receptors that detect such changes are important targets of research to investigate whether modulation of these can inhibit the metastatic success of breast cancer cells. Of course, the largest receptor family is the G-protein coupled receptor family with many members implicated in cancer.

## 1.11.  G-Protein Coupled Receptors (GPCRs)

Cells react to extracellular stimuli such as light and pressure through different physical, chemical, and biological signals. However, the plasma membrane acts as a barrier preventing external molecules from entering the cell. Therefore, there are cell surface receptors that sense these extracellular stimuli and provide the appropriate cellular response. One of these cell surface receptor families is the G-protein coupled receptors (GPCRs).[61] GPCRs are the most commonly expressed and largest family of cell surface receptors in eukaryotes with over 800 members identified in humans.[62] They are called GPCRs because of their interaction with guanine nucleotide binding regulatory proteins (G-proteins), when the receptor is activated.[61] GPCRs regulate several physiological processes such as inflammation, muscle contraction, immunity, endocrine and exocrine secretion, cell-cell communication, hormonal signalling, sensory transduction and neurone transmission.[63,64] Structurally, they consist of a transmembrane spanning domain consisting of seven transmembrane helixes, which is connected by three intracellular and three extracellular loops.[62] They also have an extracellular N-terminus

and intracellular C-terminus. GPCRs couple to a heterotrimeric complex of GTP binding G-proteins.[65] The heterotrimeric G-proteins have three subunits which are: α, β, and γ subunits. The Gα proteins have four subfamilies; $G\alpha_s$, $G\alpha_{i/o}$, $G\alpha_q$ and $G\alpha_{12/13}$, each of which functions to activate different subsets of effectors. $G\alpha_s$ and $G\alpha_{i/o}$ regulate intracellular concentrations of cyclic adenosine monophosphate (cAMP) by activating ($G\alpha_s$) or inhibiting ($G\alpha_{i/o}$) adenylyl cyclases. The $G\alpha_q$ subfamily activates phospholipase C (PLC) which generates the second messengers inositol-1,4,5-triphosphate (IP3) and diacylglycerol (DAG) from the substrate phosphatidylinositol 4,5-biphosphate.[66] $G\alpha_{12/13}$ activate small GTPase Rho.[67]

GPCRs respond to extracellular stimuli by changing their conformation, transducing the extracellular signal to an intracellular response. In its inactive state Gα is coupled with GDP and associated with the heterodimer Gβγ. Upon ligand binding, the GPCR becomes activated and undergoes conformational change.[62] The GPCR acts as a guanosine nucleotide exchange factor (GEF), that exchanges the GDP bound to the Gα subunit for GTP promoting dissociation of the Gα subunit from the Gβγ heterodimer.[68] The activated Gα and Gβγ proteins interact with an effector such as phospholipase C (PLC) or adenylyl cyclase enzymes, which generates second messengers such as diacylglycerol (DAG) or inositol-1,4,5-triphosphate (IP3). The activation of second messengers induces a physiological response through pathways leading to altered gene expression in the nucleus of the cell.[69] The reaction is inactivated by the GTPase activity of Gα which converts the bound GTP to GDP and the Gα subunit re-associates with the Gβγ dimer.[68] Other signalling pathways that are activated by GPCRs include the β-arrestin pathway, G-protein gated ion channels such as calcium channels, protein tyrosine kinase (PTK) pathway, extracellular signal-regulated kinase (ERK/MAPK) pathway, AKT pathway, and Rho pathway.[70]

Another important event that happens upon ligand binding to GPCR, is receptor internalization. This is necessary to prevent the receptor from being active continuously. Therefore, upon stimulation by agonists, GPCRs activate a group of receptor serine/threonine kinases called G-protein coupled receptor kinases (GRKs). These kinases phosphorylate agonist bound GPCRs at their C-terminus and/or the third

intracellular loop. Subsequently, regulatory proteins called β-arrestin1 and 2 bind to the phosphorylated receptor and cause receptor internalization. Receptor internalization can stop receptor signalling although cases have been reported of internalised receptor activating specific signalling pathways.[71] Receptor internalization occurs in the endocytic compartment where the receptor is dephosphorylated and either recycled back to the plasma membrane or degraded in the lysosome.[61] It is however, now also clear that internalised receptors can still signal further complicating the mechanisms of signal regulation.

GPCRs are important in the pharmaceutical industry as drug targets for different diseases such as pain, diabetes, obesity, Parkinson's disease, Alzheimer's disease and cardiovascular disease.[70] About 40% of the drugs in the market target GPCRs.[70]

GPCRs are important in cell proliferation and migration. The already mentioned chemokine receptor, CXCR4, which is expressed by metastatic breast cancer cells, is a GPCR that promotes metastasis.[72]

## 1.12.  Kisspeptin and KISS1R

Kisspeptin is a neuropeptide that is encoded by the *KISS1* gene, which was first discovered as an anti-metastasis gene in 1996.[73] In that study, it was shown by Northern blotting that *KISS1* mRNA was expressed in non-metastatic melanoma cells but not in metastatic melanoma cells. That study showed that when human metastatic melanoma cancer cell lines, C8161 and MelJuso, overexpressing KISS1 cDNA were transplanted into athymic nude mice, metastasis was suppressed. They also showed that *KISS1* was located on chromosome 1 and a gene on chromosome 6 was regulating its activity.[73]

The initial product of the *KISS1* translation is a 145 amino acid product, prepro-kisspeptin, which is then proteolytically  cleaved further to produce shorter peptides: kisspeptin 54, kisspeptin 14, kisspeptin 13 and kisspeptin 10, as shown in Figure 1.3A.[74] The shorter peptides; kisspeptin 14, kisspeptin 13 and kisspeptin 10, are thought to be degradation

products of kisspeptin-54 since there are no cleavage sites to explain the presence of the shorter peptides. The 10 amino acids at the carboxyl terminal of each kisspeptin is the minimum length that is required to activate the kisspeptin receptor.[75] All 4 peptides are collectively called kisspeptins, and *in vitro*, they have the same affinity and efficacy for the kisspeptin receptor.[76] They belong to the RF amide family of neuropeptides that end with the sequence Arg-Phe-NH$_2$.[77]

Under normal physiological conditions, *KISS1* is expressed in various tissues in the body such as the testes, ovary, pancreas, pituitary and the intestine.[78] It is also highly expressed in the placenta where it regulates growth, migration and invasion. Kisspeptin is the natural ligand of the G protein coupled receptor, GPR54, which is now called KISS1 or kisspeptin receptor (KISS1R).[78]

KISS1R, also referred to as GPR54, AXOR12, metastin receptor and hOT7T175, was discovered in 1999 by Lee *et al*. It was detected in rat brain cDNA and genomic DNA amplified by polymerase chain reaction (PCR) using degenerate primers that were based on conserved transmembrane regions 3 and 7. Through sequencing, it was shown to have conserved residues and consensus sequences of GPCRs that belong to the Rhodopsin superfamily. These conserved residues include an asparagine in transmembrane 1, an aspartate in transmembrane 2 and prolines in transmembrane 4 to 7. Consensus sequences for 3 N-linked glycosylation sites in its extracellular amino terminus as well as protein kinase A and protein kinase C phosphorylation motifs in the second intracellular loop and third extracellular loop. It was also shown to have 3 possible palmitoylation cysteine sites on the carboxyl tail.[79]

Although it was classified as a member of the galanin receptor family, it showed no specific binding with galanin and it was only 45% homologous to galanin. Since its ligand was not known (it was an orphan receptor), it was called GPR54.[79] However, in 2001, three independent groups; Kotani *et al*. 2001 [76]; Ohtaki *et al*. 2001 [80]; Muir, *et al*. 2001 [81], showed that kisspeptin is the endogenous ligand for GPR54, hence the name, kisspeptin receptor, KISS1R. Through Northern blotting and *in situ* hybridization analyses, it was shown that KISS1R is expressed in various areas of the brain such as the amygdala,

hippocampus, hypothalamus, midbrain, pons, thalamus, cortex and striatum as well as peripheral tissues such as the liver, pancreas and the intestine.[73]

KISS1R is located on chromosome 19 in humans.[75] It consists of 5 coding exons and 4 introns and an open reading frame that is 1197 base pairs long, which translates to a 398 amino acid sequence protein. It has 7 transmembrane domains with 3 intracellular and 3 extracellular loops and an extracellular N-terminus and a cytoplasmic C-terminus, as shown in Figure 1.3B.[77]



Figure 1.3: The structure of kisspeptin and KISS1R.

(A) The initial product of the KISS1 gene transcription is a 145 amino acid, pre-pro-kisspeptin, which is then cleaved proteolytically to kisspeptin (Kp) 54, Kp-14, Kp-13 and Kp-10. Kp-10 is the minimal length that is necessary to activate the kisspeptin receptor. (B). The structure of KISS1R from GPCRdb.[77,82] KISS1R as a GPCR has 7 helices spanning the membrane, it has 3 intracellular loops (ICL), 3 extracellular loops (ECL), an amino-terminal extracellular ( N-term) and a carboxyl-terminal cytoplasmic domain  (C-term). The black arrows on the N-terminus indicate the 3-N linked glycosylation sites of the receptor. The last 10 amino

acids, as shown by the arrow is the target sequence for the KISS1R 1213 and 1210 antibodies that were used for this study.

The binding of kisspeptin to KISS1R results in the activation of the $G\alpha_{q/11}$ class of G-proteins which in turn activates phospholipase C leading to the hydrolysis of phosphatidylinositol-4,5-bisphosphate into inositol triphosphate and diacylglycerol, which are secondary intracellular messengers.[77] These secondary intracellular messengers cause the release of calcium and activate protein kinase C, respectively.[77] Figure 1.4 shows the process of KISS1R signalling through the $G\alpha_{q/11}$ pathway.
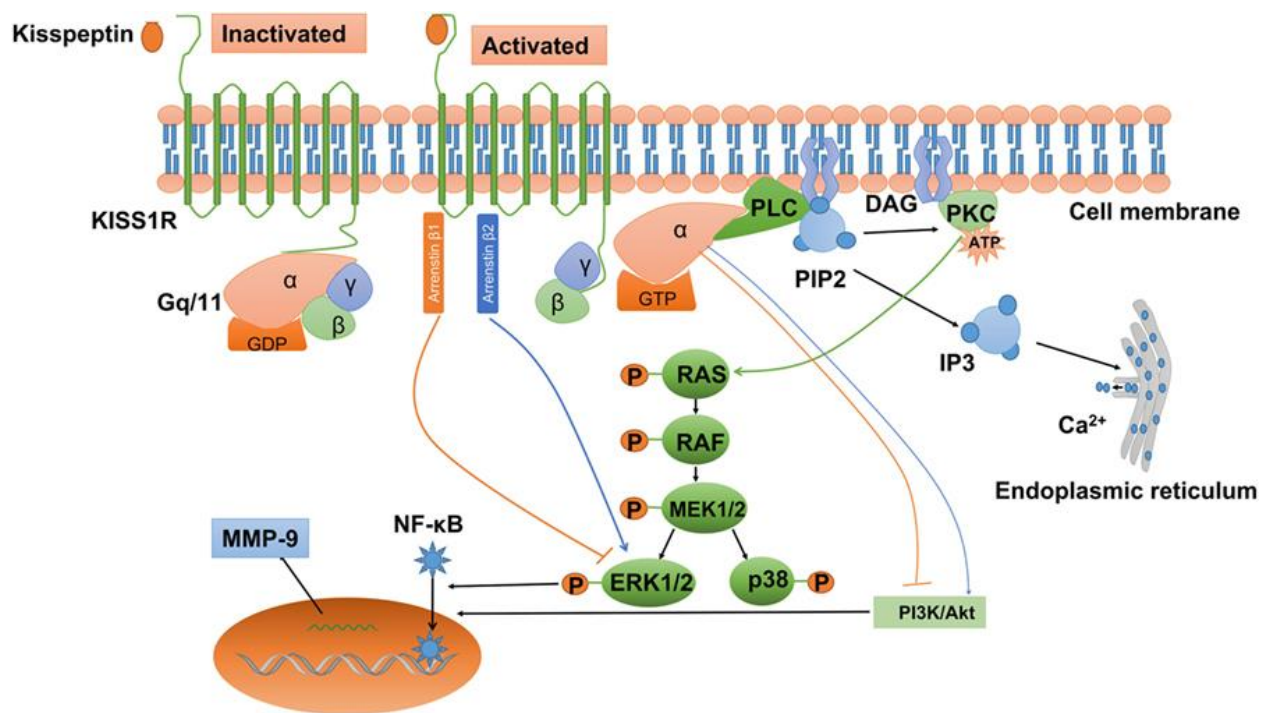


Figure 1.4: Activation of KISS1R by its endogenous ligand, kisspeptin.

Binding of kisspeptin to KISS1R results in the in the activation of various downstream effectors such as phospholipase C (PLC), inositol-1,4,5-triphosphate (IP3) and diacylglycerol (DAG). IP3 release results in calcium ion release from the endoplasmic reticulum.[69]

Activation of KISS1R by kisspeptin also results in the phosphorylation and activation of extracellular signal-regulated protein kinase 1 and 2 (ERK1/2) and p38 mitogen-activated

protein kinase (p38MAP Kinase), activation of the Akt pathway, reorganization of stress fibres in the cell and inhibition of cell movement by inducing focal adhesion kinase.[74,75]

Although Kisspeptin was first discovered as a metastasis suppressor, its best characterised physiological function is in the regulation of gonadotropin-releasing hormone (GnRH) secretion thereby controlling the neuroendocrine-reproductive axis.[74] It is secreted along with other neuropeptides like neurokinin B (NKB) and dynorphin (DYN) to regulate the release of GnRH from the hypothalamus.[74] The GnRH in turn stimulates the release of gonadotrophic hormones; luteinizing hormone (LH) and follicle stimulating hormone (FSH), from the anterior pituitary gland. The gonadotrophin hormones then stimulate the gonads (ovaries and testes), to produce the sex hormones (oestrogen and testosterone). It may also act directly on the pituitary and the gonads.[74] Kisspeptin also plays a regulatory role in folliculogenesis and spermatogenesis.[83] During folliculogenesis, kisspeptin negatively regulates prenatal follicles by inducing the synthesis of anti-Mullerian hormone (an ovarian reserve marker) and decreasing FSH sensitivity by inhibiting the expression of FSH receptor (FSHR).[83,84] In spermatogenesis, kisspeptin inhibits chemotaxis and migration, which are important in early stage spermatogenesis. Then in late stage spermatogenesis, kisspeptin induces changes in sperm motility and sperm hyperactivation.[83,85] The kisspeptin/KISS1R system plays an important role in reproduction as individuals with inactivating mutations in KISS1R have been shown to have hypogonadotropic hypogonadism, which has symptoms such as deficient LH and FSH secretion, which results in delayed puberty and infertility.[75] Also, in transgenic mice that lacked KISS1/KISS1R there was no sexual maturity and the gonads developed poorly and they were infertile.[77]

Kisspeptin and KISS1R have been shown to suppress metastasis in other cancers like colorectal cancer [86], bladder cancer [87], oesophageal cancer [88], prostate cancer [89], ovarian cancer [90], pancreatic cancer.[91] Kisspeptin signalling to KISS1R has been shown to suppress metastasis in these cancers by repressing matrix metalloproteinase 9 (MMP-9) activity thereby inhibiting cancer cell invasion and migration.[92] In colorectal cancer, Ji *et al.* (2014), showed that KISS1 and KISS1R mRNA expression decreased in higher grade tumours.[86] Also, there was a significant decrease in expression of KISS1R mRNA in

tumour tissues compared to normal background tissues. The study also showed that in patients undergoing chemo-radio therapy, there was higher KISS1R expression compared to those patients without therapy. KISS1 expression also correlated negatively with tumour metastasis and invasion.[86]

In breast cancer, the role of kisspeptin and KISS1R is not yet clearly understood. Studies by Stark and colleagues (2005)[93] showed that *KISS1* mRNA expression was lower in the brain metastases of breast cancer patients compared to the primary tumours. However, studies by Martin *et al.* (2005) [94], Cvetkovic *et al.* (2013)[95], Goertzen *et al.* (2016)[96], and Blake *et al.* (2017)[97] show that KISS1 and KISS1R protein are highly expressed in metastatic breast cancer cells compared to primary tumours. This high expression has been correlated with aggressive behaviours such as increased invasion and migration in metastatic breast cancer cells *in vitro*.[95] In breast cancer cell lines, activation of KISS1R by kisspeptin promotes EMT and invadopodia formation (F-actin rich protrusions that are formed by tumour cells to degrade the matrix), which allows increased migration and invasion.[96,97] One study suggests that the loss of the oestrogen receptor alpha (ERα) in breast cancer cells allows the pro-metastatic signalling of KISS1R to occur.[97]

In conclusion, contradicting reports suggest a pro- or anti-metastatic role for KISS1R in breast cancer in contrast to the anti-metastatic role in other cancers. Through this study we hope to determine the expression of endogenous KISS1R in breast cancer cell lines that are either metastatic or non-metastatic and how KISS1R activation by kisspeptin either inhibit or promote growth and migration in breast cancer.

# Chapter 2 MATERIALS AND METHODS

Table 2.1: General buffers and solutions.

| Name | Composition |
| --- | --- |
| 10× Phosphate buffered saline (PBS) | 1.37 M NaCl, 27 mM KCl, 18 mM $KH_2PO_4$, 100 mM $Na_2HPO_4$ pH 7.4. For all assays, it was diluted to 1× using 900 ml of ultra-pure water and 100 ml of the 10× stock, pH 7.4. |
| 2× Freeze media | 20% (v/v) DMSO, 80% (v/v) FCS |
| Radioimmunoprecipitation assay (RIPA) lysis buffer | 25 mM HEPES, 150 mM NaCl, 1 mM EDTA, 1% (v/v) Igepal/NP40, 1% (w/v) SDS, pH 7.4 |
| 1× Towbin transfer buffer | 25 mM Tris base, 192 mM glycine, 20% (v/v) methanol, pH 8.3 |
| PBS+ | 137 mM NaCl, 2.7 mM KCl, 1.8 mM $KH_2PO_4$, 10 mM $Na_2HPO_4$, 0.9 M $CaCl_2$, 0.5 M $MgCl_2$ |
| PBS Tween 0.2% (v/v) | 137 mM NaCl, 2.7 mM KCl, 1.8 mM $KH_2PO_4$, 10 mM $Na_2HPO_4$, 0.2% (v/v) Tween20 |
| Blocking solution for western blotting | 5% (w/v) skimmed milk in PBS Tween |
| Blocking solution for ERK1/2 phosphorylation assay | 5% (w/v) bovine serum albumin in PBS Tween |
| 4× sample loading buffer | 150 mM Tris HCl (pH 7.0), 25% (v/v) glycerol, 12% (w/v) SDS, 0.05% (w/v) bromophenol blue, 6% (v/v) β-mercaptoethanol |
| 50× Tris-Acetate-EDTA (TAE) | 2 M Tris, 50 mM Na EDTA, 1 M Acetic acid, pH 8.5 |
| 1× TAE | 40 mM Tris, 1 mM Na EDTA, 20 mM Acetic acid, pH 8.5 |

## 2.1 Cell Culture

## Materials

Table 2.2: List of materials used in cell culture.

| Material | Supplier | City and country | Catalogue number | Note |
|---|---|---|---|---|
| MDA-MB-231 | ATCC | Virginia, USA | HTB-26$^{TM}$ | A triple negative, metastatic breast cancer cell line. |
| MCF7 | ATCC | Virginia, USA | HTB-22$^{TM}$ | An oestrogen receptor positive breast cancer cell line. |
| BT-20 | ATCC | Virginia, USA | HTB-19$^{TM}$ | A triple negative non-metastatic breast cancer cell line. |
| HEK293 | ATCC | Virginia, USA | CRL-1573$^{TM}$ | A mammalian cell line that is used for the heterologous expression of proteins. |

| | | | | |
|---|---|---|---|---|
| HepG2 | ATCC | Virginia, USA | HB-8065™ | A human hepatocellular carcinoma cell line. |
| GT1-7 | Sigma-Aldrich | Missouri, USA | SCC116 | A mouse GnRH secreting neuronal cell line. |
| Dulbecco's modified eagle's medium (DMEM) | Invitrogen | California, USA | 10566016 | DMEM media was supplemented with 10% FBS. |
| Ham's F-12 media (F-12) | Invitrogen | California, USA | 21765029 | Supplemented with 10% FBS and 1% glutamine. |
| Minimum essential media (MEM) | Invitrogen | California, USA | 21090022 | Supplemented with 10% FBS and 1% glutamine. |
| Foetal calf serum (FCS) | Invitrogen | California, USA | 10499044 | It was heat inactivated by heating at $60^0$C for 1 hour. |
| 1 × trypsin-EDTA | Invitrogen | California, USA | 252000072 | |

| | | | | |
|---|---|---|---|---|
| Glutamine GlutaMax I-100✕) | Invitrogen | California, USA | 35050061 | |
| 75 cm$^2$ tissue culture (T-75) flasks | Greiner Bio-One | Kremsmünster, Austria | 658170 | |
| 6-well tissue culture plates | Greiner Bio-One | Kremsmünster, Austria | 657160 | |
| 12-well tissue culture plates | Greiner Bio-One | Kremsmünster, Austria | 665180 | |
| 24-well tissue culture plates | Greiner Bio-One | Kremsmünster, Austria | 662160 | |
| 96-well tissue culture plates | Greiner Bio-One | Kremsmünster, Austria | 655180 | |
| Trypan blue solution | Gibco | California, USA | 15250061 | |
| Countess$^{TM}$ Automated Cell Counter | Invitrogen | California, USA | AMQAX1000 | |
| X-tremeGENE$^{TM}$ HP DNA transfection reagent | Roche | Basel, Switzerland | 06366546001 | |

| Polyethylenimine (PEI) | Sigma-Aldrich | Missouri, USA | 408727 | |
|---|---|---|---|---|
| Cryogenic vials (Cryo vials) | Greiner Bio-One | Kremsmünster, Austria | 126263 | |
| Freezing container/ Mr Frosty™ | ThermoFisher Scientific | Massachusetts, USA | 51000001 | |

Methods

The HEK293, GT1-7, HepG2, MCF7 and MDA-MB-231 cell lines were maintained in DMEM media supplemented with 10% FCS in a humidified incubator with 5% $CO_2$ at 37ºC. The BT-20 cell line was cultured in DMEM media (supplemented with 10% FCS) mixed with F12 media (supplemented with 10% FCS and 1% L-glutamine) in a 1:1 ratio, in a humidified incubator with 5% $CO_2$ at 37ºC. The cells were passaged twice a week and were cultured in T-75 flasks. Before passaging the cells, the media and 1 × PBS were warmed to 37ºC. The cells were passaged by aspirating the growth media and rinsing the cell monolayer once with 10 ml of 1× PBS after which the cells were incubated for 3 min for HEK293, GT1-7 and HepG2 cells, and 8 min for the 3 breast cancer cell lines, with 1 ml trypsin-EDTA at 37ºC. Afterwards, 9 ml of media was added to the cells and transferred into 15 ml Falcon tubes. The cell suspension was centrifuged at a speed of 300 ×g (Centrifuge 5702, Eppendorf, Hamburg) for 3 min. The media was aspirated, and cells were resuspended in growth medium and 1 ml of the cell suspension was transferred into T-75 flask containing 10 ml of fresh DMEM or DMEM-F12 media, using a sterile serological pipette. The cells were maintained, and all incubations were performed at 37ºC with 5% $CO_2$ in a humidified incubator (95% relative humidity).

In order to maintain stock, the cells were cryopreserved in liquid nitrogen. Prior to freezing the cells, the cells were passaged as described above, but after centrifugation 1 ml of the

cells in culture media were suspended in 1 ml of cryopreservation media and transferred into cryovials. The cryovials were put in a freezing container and kept at $-80^{0}C$ overnight. The following day the cells were moved to liquid nitrogen storage.

Cells to be seeded for different assays were trypsinised and resuspended in their respective culture media. The viable cell numbers were counted using the automated cell counter. The automated cell counter is a cell counting device that uses trypan blue to count cells and measure cell viability. Therefore, 10 μl of the suspended cells was mixed with 10 μl of trypan blue solution. Then 10 μl of the mixture was transferred into a Countess cell counting chamber slide and the slide was inserted into the slide port and the number of dead and living cells per millilitre displayed on the screen was used to calculate the number of viable cells per ml required for each assay.

Transfection of HEK293 cells

HEK293 cells were seeded at a density of $2 \times 10^{5}$ cells/ml in a 6 well tissue culture plate and incubated at 37ºC with 5% $CO_2$ overnight. The following day, the cells were transfected with the plasmid DNA expression vector with either FLAG-tagged KISS1R or empty pcDNA3.1 vector, using the X-tremeGENE™ HP DNA transfection reagent following the manufacturer's protocol using a 2:1 ratio of X-tremeGENE™ to DNA. Therefore, for every 1 μg of DNA, 2 μl of X-tremeGENE™ was used. The transfection was done in serum free DMEM media.

In another experiment, HEK293 cells were transiently transfected with either FLAG-tagged KISS1R or pLKO GFP plasmid (as negative control) using polyethylenimine (PEI) transfection reagent, in a 3:1 ratio of PEI to DNA in serum free media. Therefore, for every 1 μg of DNA, 3 μl of PEI was used. Firstly, 1 μg of either the Flag tagged KISS1R or pLKO GFP DNA was added to serum free media and mixed by vortexing. Thereafter, PEI was added to the mixture and mixed briefly by vortexing. Subsequently, the cocktail was kept at room temperature for 15 min before being added to the HEK293 cells.

## 2.2 Western Blot analysis

### Materials

Table 2.3:  List of primary and secondary antibodies used for western blotting.

| Name of antibody | Species | Supplier, state and country | Concentration | Catalogue number |
|---|---|---|---|---|
| KISS1R, R2 1213 | Rabbit | Prof R. Millar | Unknown concentration but it was used at 1:1000 dilution | Directed against last 10 aa sequence on the C-terminal of KISS1R. See Figure 2.1 |
| phospho-ERK1/2 antibody | Rabbit | CST, Massachusetts, USA | 0.25 µg/ml | 9101S |
| β-Actin | Mouse | Sigma-Aldrich, Missouri, USA | 1 µg/ml | A2228 |
| β-Tubulin | Mouse | Sigma-Aldrich, Missouri, USA | Unknown concentration but it was used at 1:1000 dilution | T5293 |
| Haemagglutinin (HA) Tag | Mouse | Life Technologies, California, USA | 0.5 µg/ml | 32-6700 |
| Goat anti Rabbit conjugated to horseradish peroxidase | Goat | Bio-Rad, California, USA | Unknown concentration but it was used at 1:10000 dilution | 1662408 |

| Goat anti Mouse conjugated to horseradish peroxidase | Goat | Bio-Rad, California, USA | Unknown concentration but it was used at 1:10000 dilution | 1706517 |
|---|---|---|---|---|
| β-Arrestin 1/2 | Rabbit | CST, Massachusetts, USA | Unknown concentration but it was used at 1:1000 dilution | 4674S |
| Anti-β-Arrestin 1 mAb | Mouse | Transduction Laboratories | 0.25 µg/ml | A47520 |
| Anti-β-Arrestin 2 mAb | Mouse | Transduction Laboratories | 0.25 µg/ml | A46120 |

Target sequence of the KISS1R antibody

Human   $^{341}$CAPRRPRRPRRPGPSDPAAPHAELLRLGSHPAPARAQKPGSSGLAARGLCVLGEDNAPL$^{398}$

Mouse   $^{340}$CCRQRQRRPHTSAHSDRAATHTVPHSRAAHPVRIRS—PEPGNPVVRSPCAQSERTASL$^{394}$
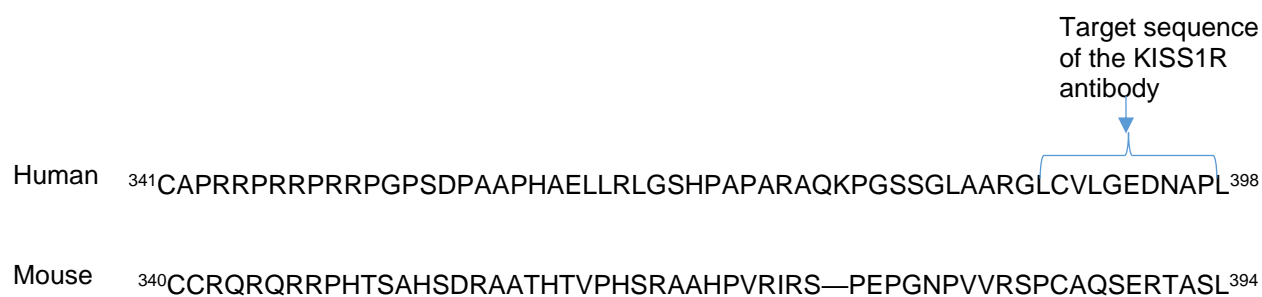
Figure 2.1: The cytoplasmic tail of the Human and Mouse KISS1R.[128]

The arrow indicates the epitope for the KISS1R antibodies, Rabbit 1213 and Rabbit 1210.

Table 2.4: List of materials used for Western blotting.

| Name | Supplier | City and Country | Catalogue number |
|------|----------|------------------|------------------|
| Complete EDTA-free protease inhibitor cocktail tablets | Roche | Basel, Switzerland | 04693124001 |
| Phosphatase inhibitor cocktail tablets | Roche | Basel, Switzerland | 04906837001 |
| 4-15% Mini-PROTEAN® TGX Stain-free™ Protein 15 well gels | Bio-Rad | California, USA | 4568086 |
| Novex 4-20% Tris-Glycine mini 10 well Gels | Invitrogen | California, USA | XP04200BOX |
| Novex 4-20% Tris-Glycine mini 15 well Gels | Invitrogen | California, USA | XP04205BOX |
| Polyvinylidene difluoride (PVDF) membrane | Amersham GE Healthcare | Amersham, UK | 10600023 |
| 4× lithium dodecyl sulphate (LDS) and 10× reducing agent | Invitrogen | California, USA | LDS; NP007 Reducing agent; NP0004 |
| Endoglycosidase H (Endo H) | New England Biolab (NEB) | Massachusetts, USA | P0702S |
| Peptide-N-Glycosidase F (PNGase F) | New England Biolab (NEB) | Massachusetts, USA | P0704S |
| 10 × Glycoprotein Denaturing Buffer (5% SDS and 400 mM DTT) | New England Biolab (NEB) | Massachusetts, USA | B1704S |
| 10 × GlycoBuffer 3 (500 mM sodium acetate, pH 6 at RT) | New England Biolab (NEB) | Massachusetts, USA | B1720S |
| 10 × GlycoBuffer 2 (500 mM sodium phosphate, pH 7.5 at RT) | New England Biolab (NEB) | Massachusetts, USA | B3704S |
| NP-40 (Igepal) | Sigma-Aldrich | Missouri, USA | I8896 |

| Tunicamycin (in 100% DMSO) | Sigma-Aldrich | Missouri, USA | T7765 |
|---|---|---|---|
| Dimethyl sulfoxide (DMSO) | Sigma-Aldrich | Missouri, USA | D8418 |
| Bicinchoninic Acid (BCA) protein quantification | Thermo Fisher Scientific | Massachusetts, USA | 23225 |
| Clarity Western ECL substrate | Bio-Rad | California, USA | 1705061 |
| ProSieve™ Color Protein Marker | Lonza | Basel, Switzerland | 50550 |
| BLUelf Prestained Protein ladder | GeneDirex | Taiwan, China | PM008-0600 |

N/B: The RIPA lysis buffer used for protein extraction was prepared by in house and the protocol is in Table 2.1.

Methods

Protein extraction

HEK293 cells transfected with either flag-tagged-KISS1R (HEK293-FLAG-KISS1R) or empty pcDNA3.1 (HEK293-empty-pcDNA3.1), MCF7 and MDA-MB-231 were seeded at a density of $2 \times 10^5$ cells/ml, while BT-20 cells were seeded at a density of $4 \times 10^5$ cells/ml into 6 well tissue culture plates at 37ºC in a humidified incubator with 5% $CO_2$. After overnight incubation lysate preparation was performed on ice by aspirating the culture media and washing the cell monolayer with 1 ml of ice-cold PBS supplemented with calcium and magnesium (PBS+). The cells were lysed with RIPA lysis buffer supplemented with protease inhibitors. After adding 150 µl of the RIPA lysis buffer, the cells were scraped off the plate using a syringe stopper and transferred into 1.5 ml microcentrifuge tubes. The cell suspension was passed through a 1 ml gauge needle to lyse the cells and incubated on ice for 15 min. Subsequently, the protein lysates were cleared by centrifugation at 16 602 ×g (Sigma 1-14K centrifuge, Sigma Laborzentrifuge,

Osterode) for 10 min at 4ºC. The supernatant was transferred into new 1.5 ml microcentrifuge tubes (Eppendorf, Hamburg).

Protein quantification

Protein concentration was determined using the Pierce$^{TM}$ BCA protein assay kit, following the manufacturer's instruction. Protein standards (0-2000 μg/ml) were made using bovine serum albumin (BSA) dissolved in ultrapure water and used to create a standard curve. The concentration of the protein was obtained by measuring the absorbance at 540 nm using the microplate reader (Bio-Rad, California). Protein concentration was calculated using the values obtained from the standard curve.

Western blotting

The protein lysates were prepared for western blotting by mixing equal amount (12 μg) of BT-20, MCF7, MDA-MB-231, HEK-FLAG-KISS1R, HEK-empty-pcDNA3.1, GT1-7 and HepG2 cell lysates with equal volume of LDS and reducing agent in a final concentration of 1×. The GT1-7 and HepG2 lysates were obtained as gifts from Ms Schwulst and Mr Ellero. The protein lysates were separated on 4-15% Mini-PROTEAN® TGX Stain-free$^{TM}$ protein gels using Bio-Rad gel apparatus for 1 h 30 min at 120 volts. After protein separation, the gels were imaged on the ChemiDoc (Bio-Rad) imager using the stain-free application in the Image lab software 6.0 (Bio-Rad). The protein gel was blotted onto PVDF membranes using the Bio-Rad wet transfer apparatus. The PVDF membranes were activated by soaking for at least 30 s in 100% methanol. The filter papers and sponges were soaked in 1 × Towbin transfer buffer. A transfer sandwich was assembled in the order; sponge → filter paper → gel → membrane → filter paper → sponge, as shown in Figure 2.1, in a gel holder cassette.

Figure 2.2: An illustration of how the components of a Western blot transfer were assembled.

(Image credit: Abcam, https://www.abcam.com/protocols/general-western-blot-protocol).[98]

The transfer was performed on ice at 90 V for 1 h 30 min. After transfer, the membranes were immediately transferred to blocking solution and incubated for 1 h at room temperature with gentle agitation on a roller. The membranes were washed 3 times with PBS Tween at 5 min intervals with gentle agitation on a roller. This was followed by incubation with the primary antibody, KISS1R 1213 (1:1000). The primary antibody was prepared in 2.5% (w/v) BSA in PBS Tween. After overnight incubation, the membranes were washed 3 times with PBS Tween at 5 min intervals and then incubated with secondary antibody, Goat anti-rabbit IgG conjugated to horseradish peroxidase (1:10 000) for 1 h. The secondary antibody was prepared in 5% (w/v) skimmed milk in PBS Tween. This was followed by three 5 min washes in PBS Tween at room temperature with gentle agitation. Afterwards, the membranes were incubated with the chemiluminescent detection reagents, Clarity Western ECL substrate and Clarity ECL luminol in a 1:1 ratio for 1 min before image acquisition. Image acquisition was performed using the multichannel image, chemiluminescence and colorimetric application in the Image Lab 6.0 software. The chemiluminescence application was manually adjusted to 30 s to enable proper image acquisition. The bands were analysed by densitometric analysis using the Image Lab software. The data was normalized to total protein captured on the gel.

<u>Deglycosylation analysis</u>

BT-20 cellular proteins were deglycosylated using the antibiotic tunicamycin, which inhibits glycosylation and the deglycosylation enzymes, Endo H and PNGase F. Endo H selectively removes unprocessed high mannose chains while PNGase F selectively removes N-linked glycosyl chains. Therefore, BT-20 cells were harvested using RIPA lysis buffer supplemented with protease inhibitor following the protein extraction method described above. Thereafter, the lysates were treated using EndoH or PNGase F. Firstly, 20 μg of the BT-20 lysate was mixed with 1 × Glycoprotein Denaturing Buffer and denatured at 100ºC for 10 min. Thereafter, for Endo H treatment, 1 × GlycoBuffer 3 and 1 U of Endo H was added to the denatured protein. A mock control was included which had everything in the reaction but the Endo H.  For the PNGase F treated lysates, after denaturation, the denatured proteins were briefly placed on ice, and centrifuged for 10 s. Subsequently, 1 × GlycoBuffer 2, 1% NP-40 and PNGase F was added to the denatured protein. A mock control was also included which contained everything in the reaction but PNGase F. Afterwards, the Endo H and PNGase F treated BT-20 lysates along with their respective mock controls were incubated for 16 hours at 37ºC. Thereafter, the lysates were separated on an SDS-PAGE gel and blotted onto a PVDF membrane following the method described above.

In a subsequent experiment, BT-20 cell lysates were deglycosylated with Endo H and PNGase F alongside HEK293 cells transfected with HA-NK3R, as a positive control. After lysate preparation, the HEK293-HA-NK3R and the BT-20 lysates were treated with Endo H and PNGase F enzymes, with a slight modification to the method described above. After adding 1 × Glycoprotein Denaturing buffer to the lysates, they were incubated at room temperature for 30 min to denature. The subsequent steps were the same as described previously. Also, a no enzyme control (mock control) was included for each enzyme treatment.

For the tunicamycin treatment, BT-20 cells were seeded at a density of $4 \times 10^5$ cells/ml into a 6 well tissue culture plate at 37ºC in a humidified incubator with 5% $CO_2$. The following day, the media was replaced with media containing 5 mg/ml of tunicamycin dissolved in 100% DMSO and then incubated again for 16 h. Untreated controls were

included. Both the tunicamycin treated and untreated controls were lysed on ice with RIPA lysis buffer supplemented with protease inhibitor, following the protein extraction method described above.

The treated BT-20 lysates as well as the treated HEK293-HA-NK3R lysates were analysed by Western blotting, following the same Western blotting protocol described above. However, for the HEK293-HA-NK3R blot, a mouse monoclonal anti-HA primary antibody (0.5 μg/ml) was used to detect NK3R and the blot was incubated overnight with the primary antibody prepared in 2.5% (w/v) BSA in PBS Tween. This was followed by a 1 hr incubation with the secondary antibody, Goat anti-mouse IgG conjugated to horseradish peroxidase (1:10 000). The secondary antibody was prepared in 5% (w/v) skimmed milk in PBS Tween.

Table 2.5: KISS1R agonist, antagonist and vehicle.

| Name | Source | Note |
|---|---|---|
| Human kisspeptin 10 (Tyr-Asn-Trp-Asn-Ser-Phe-Gly-Leu-Arg-Phe-NH$_2$) (KP-10) | Sigma-Aldrich, Missouri, USA | Dissolved in 20% PG. Diluted in DMEM. |
| KISS1R antagonist, ((D-Ala)-Asn-Trp-Asn-Gly-Phe-Gly-(D-Trp)-Arg-Phe-NH$_2$) P234 | Sigma-Aldrich, Missouri, USA | Dissolved in 20% PG. Diluted in DMEM. |
| Propylene glycol (PG) | Sigma-Aldrich, Missouri, USA | 100% propylene glycol diluted to 20% with PBS. |

ERK phosphorylation analysis

The BT-20 and MDA-MB-231 cells were seeded at densities of $1.5 \times 10^5$ cells/ml and $1.2 \times 10^5$ cells/ml, respectively, in 12 well tissue culture plates and grown overnight at 37ºC in a humidified incubator with 5% $CO_2$. The following day, the media was replaced with serum-free medium for 4 h at 37ºC. Subsequently, the cells were stimulated with either 100 nM KP-10 or 0.02% propylene glycol (PG), for 5, 10, 30, 45 or 60 min at 37ºC. An unstimulated control was included, which was not stimulated with either KP-10 or PG. Afterwards, the cells were placed on ice. They were washed once with PBS+ and lysed with RIPA lysis buffer containing protease and phosphatase inhibitors, following the protein extraction and quantification method described above. Equal amounts (5 µg) of the protein lysates were mixed with 4 × loading buffer to a final concentration of 1x and resolved on 4-15% Mini-PROTEAN® TGX Stain-free$^{TM}$ protein gels and transferred unto PVDF membranes following method described above in the Western blot protocol. Blocked membranes were incubated overnight at 4ºC with rabbit anti-phospho-ERK1/2 antibody (0.25 µg/ml). Subsequently, membranes were processed as described above. The bands were analysed by densitometric analysis using the Image Lab software. The data was normalized to total protein.

To determine maximal ERK1/2 phosphorylation levels in BT-20 and MDA-MB-231 cell lines, cells were stimulated with serum after starvation. The starved cells were stimulated with 10% serum media for 5, 10 , 30 , 45, 60 and 120 min. They were analysed by western blotting following the method described. The experiment was repeated 2 times and the second repeat was done using the Novex 4-12%Tris-Glycine mini-Gels and the Invitrogen gel apparatus. β-Actin was used as a loading control. Therefore, after detection of phosphorylated ERK1/2, the membrane was washed 3 times at 10 min interval with PBS Tween and then re-probed with either human β-Actin or Tubulin antibody for 1 h. This was followed by incubation with the secondary antibody, horseradish peroxidase conjugated goat anti-mouse, for 1 h. Afterwards, the membrane was washed 3 times at 5 min interval and the bands were visualized as described above. The data was normalized to β-Actin.

In order to determine ERK1/2 phosphorylation in exogenously expressed KISS1R, HEK293 cells were transiently transfected with either FLAG-tagged KISS1R or pLKO GFP plasmid (as negative control) using polyethylenimine (PEI) transfection reagent, in a 2:1 ratio, DNA: PEI in serum free media. After 24 h of transfection, both the KISS1R and pLKO GFP transfected cells were serum starved for 4 h and stimulated with 100 nM KP-10 for 60, 45, 30, 10 and 5 min. An untreated control was also included. ERK1/2 phosphorylation was assessed by Western blotting following the procedure described above.

To generate dose response curves of ERK activation after Kisspeptin stimulation, the cells were starved and then stimulated with increasing concentrations of KP-10, $1 \times 10^{-8}$ to $1 \times 10^{-4}$ M of KP-10, for 5 min and 60 min at 37ºC. Untreated and vehicle (propylene glycol diluted in the same way as the highest concentration of KP-10) controls were included.  After treatment, the cells were lysed on ice. The cells were lysed and analysed by western blotting following the method described above. The experiment was repeated 2 times. Both repeats were done using the Novex 4-15%Tris-Glycine mini-Gels and the Invitrogen gel apparatus. Since it was a stain free gel, after detection of phosphorylated ERK1/2, the membranes were washed 3 times at 10 min interval with PBS Tween and then re-probed with human anti-β-Actin antibody for 1 h. This was followed by incubation with the secondary antibody, horseradish peroxidase conjugated goat anti-mouse, for 1 h. Afterwards, the membrane was washed 3 times at 5 min interval and the bands were visualized as described above.

β-Arrestin expression

Equal amount (12 µg) of BT-20 and MDA-MB-231 lysates were mixed with 4 × loading buffer and resolved on 4-15% Mini-PROTEAN® TGX Stain-free™ protein gels and transferred onto PVDF membranes following method described above in the Western blot protocol. Blocked membranes were incubated overnight at 4ºC with either rabbit anti-β-Arrestin1/2 antibody (1:1000) or anti-β-Arrestin1 and anti-β-Arrestin2 (0.25 µg/ml). The

primary antibodies were prepared in 2.5% BSA in PBS Tween. Subsequently, membranes were processed as described above. β-tubulin was used as a loading control. Therefore, after detection of β-Arrestin1/2 or β-Arrestin1 and β-Arrestin2, the membranes were washed 3 times at 10 min interval with PBS Tween and then re-probed with human anti-β-tubulin antibody for 1 h. This was followed by incubation with the secondary antibody, horseradish peroxidase conjugated goat anti-mouse, for 1 h. Afterwards, the membrane was washed 3 times at 5 min interval and the bands were visualized as described above. The bands were analysed by densitometric analysis using the Image Lab software.

2.3 Immunocytochemistry/ Confocal microscopy

Materials

Table 2.6: List of antibodies used for confocal microscopy.

| Antibody | Species | Supplier | Concentration | Note/ Catalogue number |
|---|---|---|---|---|
| KISS1R, 1213 | Rabbit | Prof R. Millar | Unknown concentration, made a 1:500 dilution of serum | last 10 aa of C-terminal of KISS1R, as shown in Figure 2.1 |
| KISS1R, 1210 | Rabbit | Prof R. Millar | Unknown concentration, made a 1:500 dilution of serum | last 10 aa of KISS1R, as shown in Figure 2.1 |
| Pre-immune, 1 and 2 | Rabbit | Prof R. Millar | Unknown concentration, made a 1:500 | Obtained from the Rabbit used to make 212 and |

| | | | dilution of serum | 1210, before immunization. |
|---|---|---|---|---|
| Goat anti rabbit Alexa Fluor (AF) 488 | Goat | Abcam | 6.7 µg/ml | ab150077 |

N/B: KISS1R, 1212 and KISS1R, 1210 are from different rabbits but they have the same epitope as shown in Figures 1.3 and 2.1.

Table 2.7: Materials used for fixing and staining cells.

| Name | Supplier | Catalogue number |
|---|---|---|
| Glutaraldehyde | Sigma-Aldrich, Missouri, USA | G6257-100ml |
| Crystal violet | Sigma-Aldrich, Missouri, USA | C6158-100G |
| Sodium dodecyl sulphate (SDS) | Sigma-Aldrich, Missouri, USA | L3771-100G |
| Paraformaldehyde | Sigma-Aldrich, Missouri, USA | P6148-100G |
| Triton-X 100 | Sigma-Aldrich, Missouri, USA | X100-100ml |
| Diamond Antifade Mount with DAPI | Invitrogen, California, USA | P36962 |

Methods

Confocal microscopy

BT-20 and MDA-MB-231 cells were seeded at a density of $7 \times 10^4$ cells/ml in 1 ml of media, while HEK293 cells were seeded at a density of 50 000 cells/ml in 1 ml of media, on to 12 mm coverslips in sterile 12 well tissue culture plates and incubated at 37ºC in a humidified incubator with 5% $CO_2$. The following day, the HEK293 cells were transfected with FLAG-tagged-KISS1R, using X-TremeGENE™ transfection reagent, following the manufacturer's protocol and grown overnight at 37ºC in the humidified incubator with 5% $CO_2$. Afterwards, the culture media was aspirated, and the cells were fixed with 2% paraformaldehyde solution in PBS for 15 min. Cells were washed 3 times with 1 ml PBS and permeabilized with 0.2% triton-X in PBS for 5 min. Subsequently, the cells were washed 3 times and incubated with blocking solution (2% bovine serum albumin in 1 × PBS) at room temperature for 1 h. Afterwards, the primary antibodies directed against KISS1R, Antibody 1210 (1:500) for HEK293-FLAG-KISS1R, Antibody 1210 and 1212 (1:500) for BT-20 and MDA-MB-231 cells, as well as pre-immune negative controls (1:500), were added and incubated for 1 h at room temperature. This was followed by a 1 h incubation with secondary anti-rabbit AF488 (6.7 µg/ml) for 1 h. Afterwards, the cells were washed 3 times with 1 × PBS and the coverslips were mounted onto glass slides with mounting fluid. Confocal analysis was performed on a Laser scanning microscope 800 (LSM 800, Zeiss), using the 63x oil objective lens.

2.4 Migration analysis by Scratch assay in serum and serum-free media

The BT-20 and MDA-MB-231 cells were seeded at densities of $4 \times 10^5$ cells/ml and $2 \times 10^5$ cells/ml, respectively, in 12 well tissue culture plates and incubated at 37ºC in a humidified atmosphere with 5% $CO_2$. After overnight incubation, when they were 80-90% confluent, the cell monolayers were scratched with a 200 µl micropipette tip across the centre of the well. Another straight line was scratched perpendicular to the first line to

create a cross on each well. After scratching, the culture media was aspirated and the cells were washed gently with 1 × PBS, to remove detached cells. After washing, the cells were either untreated or treated with either the agonist, 100 nM KP-10, or the antagonist, 100 nM P234, in either serum containing or serum-free media. A vehicle control, 0.02% propylene glycol in either serum or serum-free media was included. The cells were incubated at 37°C in a humidified incubator with 5% $CO_2$. Images of the scratches were taken using the Axiovert inverted microscope (Zeiss, Germany) at 0 and 18 h after treatment, and the width of the scratch was measured at each time point (0 or 18 h) using the ImageJ software. Migration was assessed by measuring the distance between the scraped edges on both sides at 0 h and measuring the distance migrated by the cells at 18 h for each treatment. Migration expressed as the percentage closure of the scratch was calculated by dividing the change in the area of the gap (area at time point 0 – area at time point 18 h) by the area at time point 0 and multiplying by 100. This experiment was performed 3 times independently.

2.5 Spheroids

To generate a non-attachment plate, agarose powder (2 g) in phenol red free medium (100 ml) was autoclaved at 121°C for 30 min. Afterwards, 100 µl was transferred into each well of a 96-well tissue culture plate and allowed to solidify. BT-20 cells in suspension, were seeded at a density of $2 \times 10^4$ cells/well, onto the agarose in the 96 well tissue culture plate and incubated at 37°C in a humidified incubator with 5% $CO_2$, for 4 d to enable them to form spheroids. Afterwards, spheroids were treated with 100 nM KP-10 or with 0.02% propylene glycol as a control. Untreated controls were included. At least 8 spheroids were measured for each condition. Spheroids were incubated for a total of 14 d after treatment. Images of the spheroids before treatment (day 0) and on days, 4, 7, 11 and 14 were taken using the Axiovert Inverted microscope at a 10 × magnification (Zeiss, Germany). The total area of the spheroid under the different treatment conditions was measured using the Image J analysis tool.

2.6 <u>Cell proliferation analysis by crystal violet in serum and serum free media</u>

BT-20 and MDA-MB-231 cells were seeded at densities of $7.5 \times 10^4$ cells/ml and $1.5 \times 10^4$ cells/ml, respectively, in 96-well tissue culture plates and incubated at 37ºC in a humidified incubator with 5% $CO_2$ overnight. The following day, the cells were either untreated or treated with 100 nM or 10 nM KP-10 or 300 nM C15 (a compound that induces cell rounding [99]) or 0.02% propylene glycol (vehicle control), in serum media. For each condition, the cells were treated in quintuplicate for 24, 48 and 72 h at 37ºC in a humidified incubator with 5% $CO_2$. In a separate experiment, the cells were treated with either 100 nM KP-10, 1 µM P234 or 0.02% propylene glycol (vehicle control), in serum free culture conditions, and incubated for 24, 48, 72, 96 and 120 h. After incubation at each time point, the cells were fixed with 100 µl of 1% glutaraldehyde solution for 15 min at room temperature and stained with 100 µl of 0.1% crystal violet for 30 min at room temperature. Subsequently, the cells were rinsed with tap and distilled water and then allowed to air dry. After drying, the cells were lysed in a 1% sodium dodecyl sulphate (SDS) solution and the absorbance of the solution was measured using a Bio-Rad iMark microplate reader at a wavelength of 595 nm. Empty wells without cells were also fixed and stained following the same procedure as the wells with cells. The empty wells were used as controls for nonspecific binding of the crystal violet dye and were the blank controls. The absorbance readings for each treatment were subtracted from the blank controls and the average values were used to plot a graph. This experiment was repeated 4 times, independently.

## 2.7 Endogenous KISS1R sequencing in different cell lines.

## Materials

Table 2.8: List of materials for PCR, gel electrophoresis and sequencing.

| Name | Supplier | Catalogue number | Note |
|---|---|---|---|
| NucleoSpin tissue extraction kit | Macherey-Nagel, Düren, Germany | 740952.50 | |
| Agarose powder | Bio-Rad, California, USA | 1613102 | |
| 2 × PCR master mix | Thermo Fisher Scientific, Massachusetts, USA | K0171 | 0.05 U/μl Taq DNA Pol, reaction buffer, 4 mM $MgCl_2$, 0.4 mM each dNTP |
| Nuclease free water | Thermo Fisher Scientific, Massachusetts, USA | R0581 | |
| GelRed® Nucleic Acid Gel Stain | Biotium, California, USA | 41003 | |
| Gel loading dye (6×), no SDS | NEB, Massachusetts, USA | B7025S | |
| Quick-Load® 1 Kb DNA ladder | NEB, Massachusetts, USA | N3232S | |
| BigDye™ Terminator v.1 Cycle Sequencing reaction kit | Thermo Fisher Scientific, Massachusetts, USA | 4337456 | |

<u>Methods</u>

<u>Genomic DNA Extraction</u>

BT-20 and MDA-MB-231 cells were collected by centrifugation at 300 ×g for 3 min. Genomic DNA extraction was performed using the Macherey-Nagel NucleoSpin tissue extraction kit following the manufacturer's protocol. The DNA concentration was determined using a NanoDrop™ spectrophotometer ND-1000 (Thermo Scientific). In order to assess the purity of the DNA, absorbance measurements were taken at wavelengths of 260 nm and 280 nm. A ratio of approximately 1.8 was considered pure DNA.


<u>Primer Design</u>

To determine the sequence of the last exon, exon 5, a forward oligonucleotide primer in the intron upstream of exon 5 was designed (5'- CCTTTCGTCTAACCACCT-3') in combination with a reverse primer that targeted the 3' untranslated region (UTR) (5'-TCACAACGAAACTGCACC-3') as shown in Figure 2.2. The primers were designed using the CLC Main Workbench version 8.1 (QIAGEN, Aarhus, Denmark). The parameters for the design were: GC content of 40-60%, primer length between 18 to 24 base pairs, and primer melting temperature between 48-58ºC. The designed primers were checked on the NCBI human genome database BLAST, to ensure that they did not bind to any other gene.
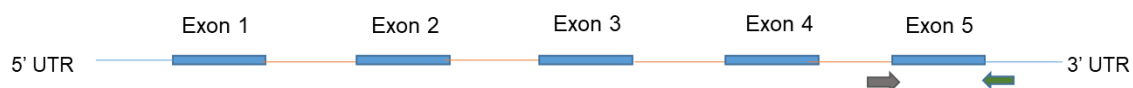


Figure 2.3: KISS1R primers designed to amplify the last exon of the gene.

Grey arrow = forward oligonucleotide primer flanking intron 4, Green arrow = reverse oligonucleotide primer flanking the 3' untranslated region (UTR).

Polymerase chain reaction (PCR)

The PCR was set up on ice using micropipette tips with filters. The genomic DNA was diluted to 250 ng/µl and 1 µl was used for PCR amplification using Thermo Fisher Scientific 2× Taq polymerase mastermix with 1 µM final concentration of the forward and reverse oligonucleotide primers, respectively. The reaction was made up to 50 µl using nuclease free water. The PCR cycling conditions were as follows: initial denaturation at 95ºC for 3 min, and 35 cycles of denaturation at 95ºC for 30 s, annealing at 47ºC for 30 s and extension at 68ºC for 30 s. A final extension was done at 68ºC for 5 min and a 4ºC hold for infinity was included. The PCR and sequencing reaction (described below) were performed on a thermocycler (Applied Biosystems, Foster city, CA, USA). After amplification, the PCR products were purified to remove the excess primers and remaining reagents, using the Macherey-Nagel NucleoSpin Gel and PCR clean-up kit, following the manufacturer's protocol.

Agarose gel electrophoresis

The purified PCR products were analysed by agarose gel electrophoresis. The agarose gel was prepared at a concentration of 1% (w/v) agarose by dissolving the agarose powder in 1 × TAE buffer, in a microwave for 2 min with gentle swirling at 20 s intervals. The gel was allowed to cool to RT and then Gel Red® was added at a 1/10 000 dilution. It was poured onto a casting tray and allowed to set for at least 20 min. A 6× gel dye loading buffer was added to the PCR product to a final concentration of 1× and the gel was ran at 120 V for 30 min in a Bio-Rad gel electrophoresis tank in 1xTAE buffer. The DNA was visualized under a UV Transilluminator using the Bio-Rad imaging system and the band sizes were estimated using the NEB 1 Kb ladder.

Sanger Sequencing

The purified PCR products were quantified using the NanoDrop 1000™ spectrophotometer to determine the concentration of the purified PCR product. A total of

100 ng of the purified PCR product was used for DNA sequencing using the same primers that were used for PCR (the forward or reverse primer). The sequencing was performed using the BigDye$^{TM}$ Terminator V3.1 cycle sequencing kit following the manufacturer's protocol. Briefly, 100 ng of the purified PCR product was mixed with 3.2 pM of either the forward or the reverse primer, and 1× BigDye$^{TM}$ sequencing buffer and 1× BigDye$^{TM}$. The cycling conditions were as follows: Incubation at $96^0$C for 1 min, and 25 cycles of denaturation at 96ºC for 10 s, annealing at 49ºC for 5 s and extension at 60ºC for 6 min and a hold at 4ºC for infinity. After the sequencing reaction was completed, unincorporated labelled ddNTPs and other reagents from the BigDye v3.1 sequencing reaction were removed, and the DNA was precipitated using the sodium acetate and ethanol precipitation technique. Firstly, the sequencing reaction products were transferred to 0.6 ml tubes and then 1.5 µl of 3 M sodium acetate (pH 4.6), 31.3 µl of 99% molecular grade ethanol (Sigma-Aldrich) and 7.25 µl of ultrapure water were added. This mixture was incubated on ice for 15 min. Subsequently, the DNA was pelleted by centrifugation at 16 602 ×g (Sigma 1-14K centrifuge, Sigma Laborzentrifuge, Osterode) for 20 min at 4ºC. The supernatant was aspirated, and the pellet was washed twice with 250 µl of 70% ethanol and centrifuged at maximum speed for 5 min at 4ºC. After the second wash step, the supernatant was removed and the pelleted DNA was dried in an incubator at 37ºC, to remove any residual ethanol. The DNA was sequenced by capillary electrophoresis on the ABI3500xl genetic Analyser instrument (Applied Biosystems) at the African Centre for Gene Technologies (ACGT) located at University of Pretoria's Forestry and Agricultural Biotechnology Institute (FABI) square. The Sanger sequencing results were analysed using CLC Main Workbench version 8.1 (QIAGEN, Aarhus, Denmark). The contigs from the Sanger sequencing were assembled to create a consensus sequence which was aligned to the human *KISS1R* gene (Accession number: NG_008277.1).

## 2.8 Statistical Analysis

All analyses were performed using GraphPad Prism 5.0. A student's unpaired t-test was used to assess the statistical significance of the differences between 2 groups. While a

one-way analysis of variance (One-way ANOVA) was used to assess the statistical significance of the differences between 3 groups. Statistical significance was set at *P < 0.05.*

# Chapter 3 RESULTS

## 3.1 <u>KISS1R is highly expressed in the non-metastatic cell line, BT-20, relative to the migratory cell lines, MCF7 and MDA-MB-231.</u>

Previous studies have shown that there is an inverse association between the stage of tumours and kisspeptin expression and in some cases KISS1R expression.[97,100] We sought to determine if it was also true that KISS1R expression and metastatic potential were correlated in breast cancer. To determine whether there was a correlation between cell migratory behaviour and KISS1R expression, we first assessed the expression of endogenous KISS1R protein in the migratory breast cancer cell lines, MCF7 and MDA-MB-231, and in the non-metastatic breast cancer cell line, BT-20, by western blotting. Protein extraction was performed by lysing the cells with RIPA lysis buffer and clearing by centrifugation. The proteins were resolved by electrophoresis on SDS-PAGE (4-20%) gels and transferred to PVDF membranes. After blocking, the membranes were probed with rabbit polyclonal KISS1R antibody 1213, whose epitope is shown in Figure 1.3 and in Figure 2.1. This antibody was the same antibody used in the study by Matjila *et al*. 2013.[101] Afterwards, the membranes were incubated with secondary Goat anti-rabbit Horseradish peroxidase (HRP)-conjugated antibody and protein bands were visualized by chemiluminescence. All band intensities were normalised to total protein.

The antibody detected several protein bands of differing molecular weights in the three cell lines (Figure 3.1). They include 47, 73 and 100 kD bands, which were detected in the 3 cell lines, while a 120 kD (a) band was only detected in the BT-20 cell line. The 47 kD band (b) is closer to the predicted size of the KISS1R protein (43 kD) and a band at this size was detected in the 3 breast cancer cell lines albeit at different expression levels. KISS1R protein expression was about 10-fold higher in the non-metastatic, triple negative breast cancer cell line, BT-20 (mean = 0.899), compared to the metastatic cell lines, MDA-MB-231 (mean = 0.05) and MCF7 (mean = 0.05) (Figure 3.2). The 73 and 100 kD bands are either other isoform of KISS1R, post-translationally modified versions of KISS1R, or non-specific bands.

To determine the specificity of the bands seen in the western blot of the breast cancer cell lines, we assessed the expression of exogenous KISS1R in HEK293 cells transfected

with either FLAG-KISS1R or empty vector by western blotting. The antibody detected a faint 47 kD band in both the FLAG-KISS1R and empty vector transfected HEK293 cells (Figure 3.1). However, a more prominent band was visible at approximately 43 kD (c) in the FLAG-KISS1R expressing cell lysate. The 73 and 100 kD bands seen in the cancer cell lysates were also present in both the empty vector control and the FLAG-KISS1R expressing lysates suggesting that these may be non-specific bands. As it is known that HEK293 cells express endogenous KISS1R, we suggest that the 47 kD band seen in both lysates may represent the endogenous KISS1R while the 43 kD band represent the exogenously expressed KISS1R.

Thus, an endogenous expressed band resolved at 47 kD is present at high expression levels in BT-20 cells while this protein is expressed at low levels in the migratory breast cancer cell lines MCF-7 and MDA-MB-231. Exogenously expressed KISS1R in the HEK293 cells was slightly different in molecular size to the endogenously expressed KISS1R. This difference could be due to posttranslational modification, such as glycosylation of the endogenous protein compared to the exogenous protein.
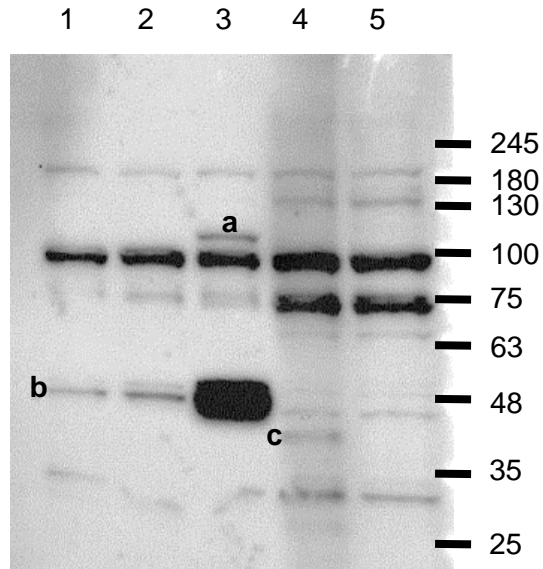
Figure 3.1: A protein corresponding to the predicted MW of KISS1R is highly expressed in the BT-20 cell line compared to the MCF7 and MDA-MB-231 cell lines.

Western blot analysis using a KISS1R antibody against protein lysates prepared from the breast cancer cell lines, MCF7 (Lane 1), MDA-MB-231 (Lane 2) and BT-20 (Lane 3), and exogenous KISS1R overexpressing FLAG-KISS1R HEK293 cells (Lane 4) and control empty vector HEK293 cells (Lane 5). Primary antibody was used at 1:1000. Band marked (a) is approximately 120 kD (b) is approximately 47 kD and (c) is approximately 43 kD. Protein ladder indicated in kD.
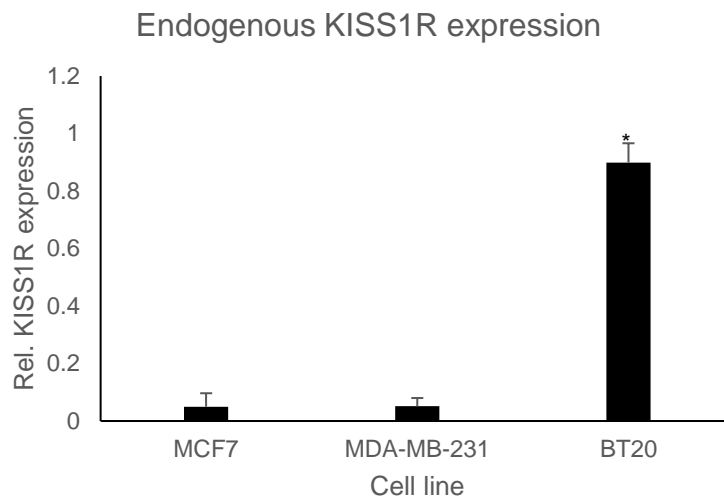
Figure 3.2: Densitometric analysis of the 47 kD band by normalizing band intensity to total protein.

Data are expressed as mean ± SEM of 3 independent repeats. An unpaired student's T-test was performed to compare the KISS1R protein expression in the MCF7, MDA-MB-231 and BT-20 cell lines. *P value <0.05.

3.2 Endogenous KISS1R is expressed in the 3 breast cancer cell lines and the human hepatocellular cancer cell line, HepG2, but not in the mouse neuronal cell line, GT1-7.

To further confirm that the 47 kD band that was detected in the breast cancer cell lines by our KISS1R antibody was KISS1R, we assessed the expression of endogenous KISS1R in the human hepatocellular cancer cell line, HepG2. This cell line is used as a positive control for endogenous KISS1R for most commercially available KISS1R antibodies. The murine GnRH neuronal cell line, GT1-7, was also tested to determine if it expressed KISS1R. Protein extraction was performed by lysing the cells with RIPA lysis buffer and clearing by centrifugation. The proteins were resolved by electrophoresis on an SDS-PAGE (4-12%) gel and transferred to a PVDF membrane. After blocking, the

membrane was probed with the same rabbit polyclonal KISS1R antibody used above. Afterwards, the membrane was incubated with secondary Goat anti-rabbit HRP conjugated antibody and protein bands were visualized by chemiluminescence. After detecting KISS1R the membrane was re-probed with a human tubulin antibody.

As shown in Figure 3.3A (top panel), the antibody detected series of bands of different mobilities. The western blot showed the presence of a 47 kD protein in the MCF7 (lane 1), MDA-MB-231 (lane 2), BT-20 (lane 3) and HepG2 (lane 5) cell lines but not the GT1-7 (lane 4) cell line. As shown on the graph in Figure 3.3B, BT-20 and HepG2 cells showed the highest expression level of this band, compared to the MCF7 and MDA-MB-231 cells. In contrast, the 120 kD band observed faintly in the BT-20 cells was not present in the HepG2 cells. The 73 kD and 100 kD bands that were seen in the previous blots were detected at similar levels in all the cell lines. There was a unique 180 kD band in only the HepG2 cells.

Thus, the data suggests that the antibody detects a band at 47 kD corresponding to KISS1R in the human HepG2 cell line known to express the protein.
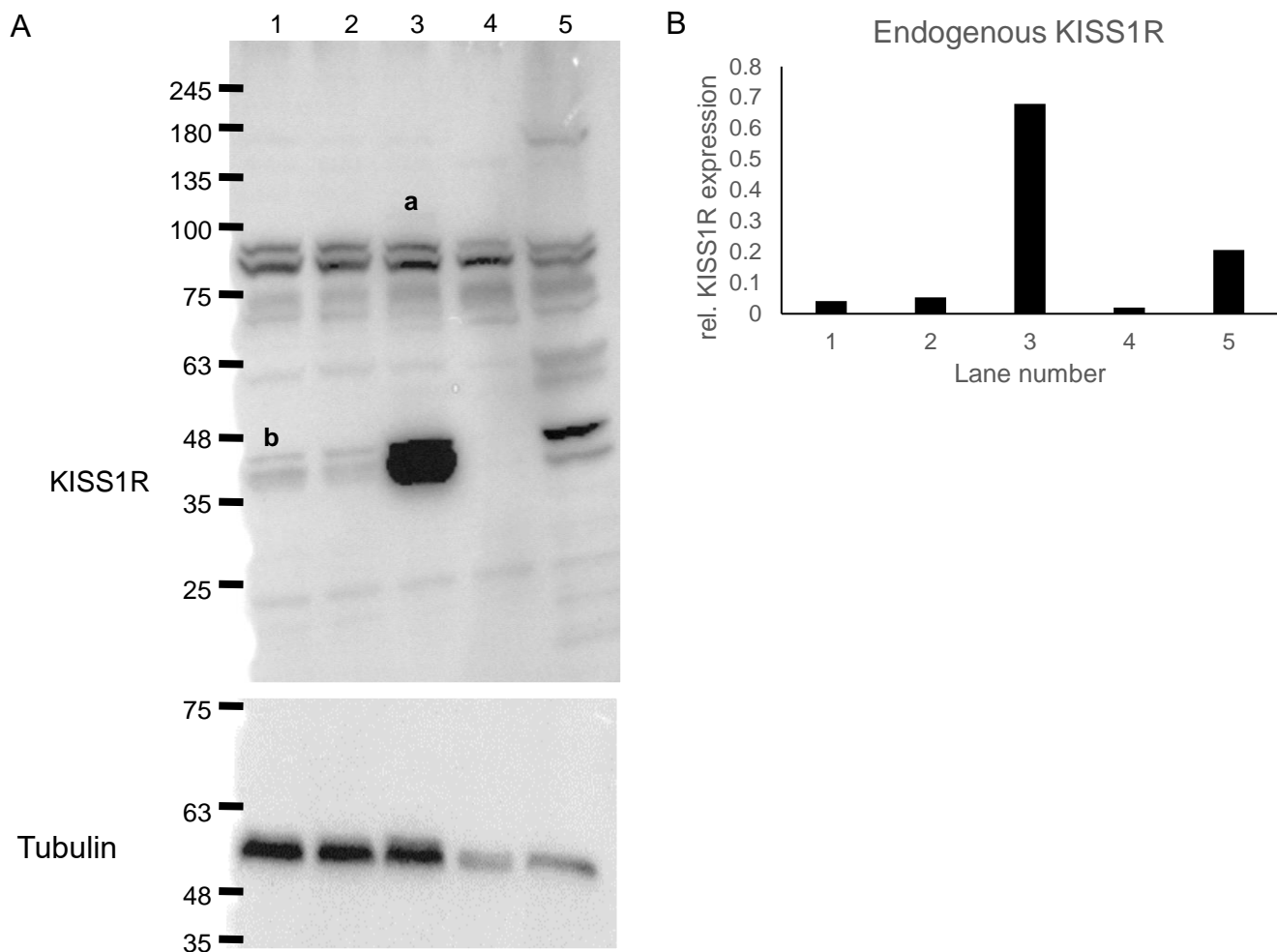
Figure 3.3: KISS1R is differentially expressed in the 3 breast cancer cell lines and HepG2 cell line.

(A) Western blot showing the expression of proteins detected by the KISS1R antibody in the 3 breast cancer cell lines, MCF7 (lane 1), MDA-MB-231 (lane 2), BT-20 (lane 3), and in GT1-7 (lane 4) and HepG2 (lane 5) cell lines. Primary antibody was used at 1:1000. Band marked (a) is approximately 120 kD, the band marked (b) is approximately 47 kD. Tubulin was used as a loading control (lower panel). (B) Densitometric analysis of blot performed by normalizing band intensity to Tubulin. n=1

3.3 <u>KISS1R in the BT-20 cell line is not glycosylated.</u>

Western blot data showed that there was an apparent size difference between the endogenous KISS1R identified with the antibody in the breast cancer cell lines (47 kD) and the exogenously expressed KISS1R in HEK293 cells (43 kD). KISS1R has been shown to have 3 N-linked glycosylation motifs on its extracellular N-terminus, as shown in Figure 1.3. Therefore, we hypothesised that this size difference was due to differences in the glycosylation status between the endogenous and exogenous protein.[79] Furthermore, we were interested to know if the 120 kD band seen only in the BT-20 cells corresponds to a heavily glycosylated protein. To test our hypothesis, BT-20 cells were treated with the antibiotic tunicamycin, which inhibits glycosylation. Alternatively, cell lysates were incubated with the glycosidase Endo H that selectively removes unprocessed high mannose chains or PNGase F which selectively removes N-linked glycosyl chains. BT-20 cells in culture were treated with 5 mg/ml of tunicamycin and incubated at 37ºC in a humidified incubator with 5% $CO_2$ for 16 hours, and then cell lysates were prepared using RIPA lysis buffer. In a separate experiment, BT-20 cells and HEK293 cells overexpressing HA-tagged Neurokinin 3 receptor (NK3R), were lysed using RIPA lysis buffer and cleared by centrifugation. These lysates were split and either treated with 1 unit of PNGase F or Endo H as well as the relevant controls and incubated for 16 hours at 37ºC. All lysates were resolved on SDS-PAGE gel and transferred to membrane before blotting for KISS1R using the antibody as described in the materials and methods. To detect HA-NK3R an anti-HA monoclonal antibody was used. All data were normalized to total protein.

Figure 3.4 shows the result of untreated BT-20 lysates (lane 1) and BT-20 lysates either treated with EndoH (lane 2) or mock control which were lysates incubated with the Endo H buffer but without the enzyme (lane 3). The untreated (lane 1) and the mock treated lysate (lane 3) displayed a similar band pattern with major bands visible with a size of 120 kD (a) and 47 kD (b). When these were compared to the bands present in the Endo H treated cells (lane 2) it was clear that there was no apparent change in the migration of these bands.
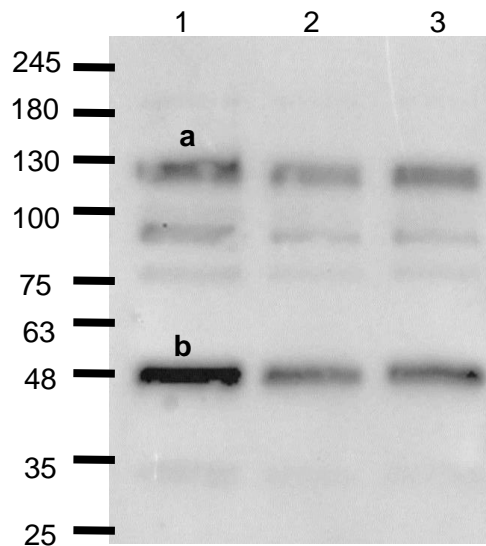
Figure 3.4: KISS1R in BT-20 cells is not glycosylated.

Western blot analysis of BT-20 lysates untreated (lane 1) or treated with Endo H (lane 2) or mock treated (lane 3) with Endo H buffer only. All lanes displayed a similar band pattern with major bands visible at 120 kD (a) and 47 kD (b).

Subsequently, cell lysates were treated with the deglycosylation enzymes, PNGase F or with Endo H to ascertain that the KISS1R in the BT-20 cell line was not glycosylated while a positive control was also included. HEK293 cells expressing NK3R, which is known to be glycosylated (Unpublished data), were analysed. Our result (Figure 3.5, right side of the ladder) showed that the band representing NK3R migrated faster after treatment, showing a calculated size difference of 11 kD from 63 kD to 52 kD, for the Endo H and PNGase F treated cells relative to the mock controls. However, in the BT-20 cells (Figure 3.5, left side of the ladder) there was no visible change in apparent protein size of the 120 kD band or of the 47 kD KISS1R band. This suggests that unlike NK3R, endogenous KISS1R is not glycosylated to any significant extent.
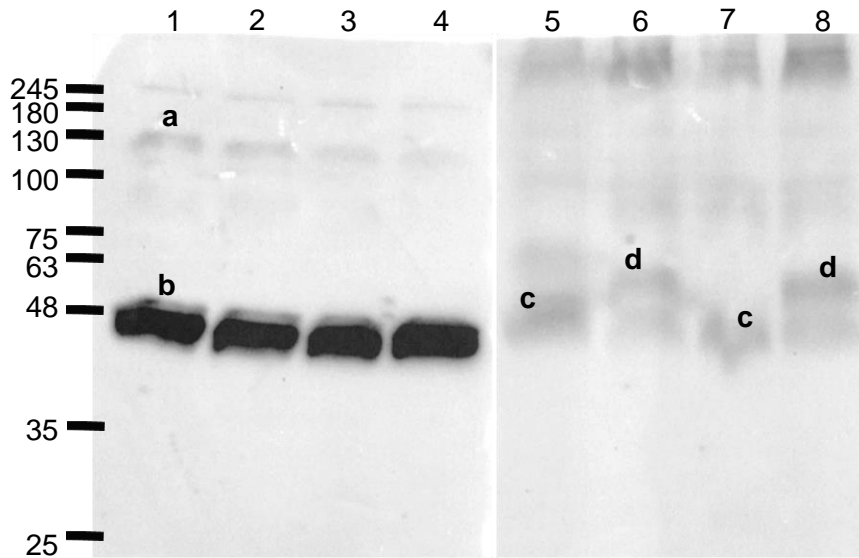
Figure 3.5: Deglycosylation protocols are effective confirming that KISS1R is not extensively glycosylated.

Western blot analysis of KISS1R (left panel) and NK3R (right panel). BT-20 cell lysates were treated with PNGase F (lane 1), PNGase F mock control (lane 2), Endo H (lane 3), Endo H mock control (lane 4). NK3R expression was visualised with a HA antibody (right panel) of cells treated with PNGase F (lane 5), PNGase F mock control (lane 6), Endo H (lane 7) and Endo H mock control (lane 8). The KISS1R antibody was used at 1:1000 while the HA-tag antibody was used at 0.5 µg/ml. Band marked (a) is approximately 120 kD  and (b) is 47 kD. Bands marked (c) and (d) are approximately 52 kD  and  63 kD .

3.4 <u>KISS1R is localized to the plasma membrane and the cytoplasm in cells expressing KISS1R.</u>

KISS1R is a 7 transmembrane receptor (GPCR) and most GPCRs are known to be localised to the plasma membrane in the absence of an agonist. Our data so far has shown that KISS1R is present in HEK293 cells transfected with FLAG-KISS1R and is endogenously expressed in the BT-20 and MDA-MB-231 cell lines. Therefore, we sought to determine the localization of exogenous KISS1R in HEK293 cells transfected with FLAG-KISS1R, and endogenous KISS1R in the BT-20 and MDA-MB-231 cells, using confocal microscopy. Firstly, HEK293 cells transfected with FLAG-KISS1R were fixed and permeabilised with 2% paraformaldehyde and 0.2% triton-X, respectively. Subsequently, the cells were blocked for non-specific binding with 2% bovine serum albumin, and then incubated with rabbit anti-KISS1R followed by Alexa Flour 488 conjugated anti-rabbit antibody and counterstained with DAPI to detect the nucleus and mounted on a microscope slide.

Our result showed that in the HEK293 cells with exogenously expressed KISS1R (Figure 3.6), the KISS1R antibody detected KISS1R on the plasma membrane and in the cytoplasm. Therefore, our data suggests that in HEK293 cells with overexpressed KISS1R, KISS1R is localised to the plasma membrane and cytoplasm in the absence of an agonist.
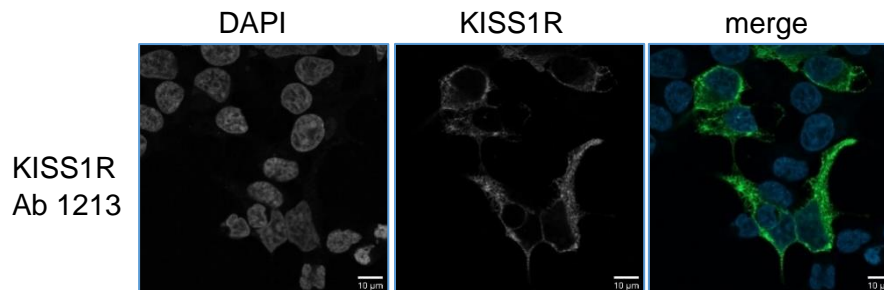
Figure 3.6: Localisation of exogenous KISS1R in HEK293 cells.

HEK293 cells transfected with FLAG-KISS1R were fixed. Anti-KISS1R antibody 1213 was used together with a goat polyclonal anti-rabbit Alexa Fluor 488 Ab to visualise KISS1R localisation. Nuclei were stained with DAPI. Scale bar, 10 μm. Alexa Fluor 488 is green. DAPI is blue.

In order to determine the subcellular localisation of endogenous KISS1R, BT-20 and MDA-MB-231 cells were fixed and permeabilised with 2% paraformaldehyde and 0.2% triton-X, respectively. Subsequently, the cells were stained with rabbit KISS1R antibodies, Ab 1210 and Ab 1213 (1:500) which were obtained from different rabbits but with the same epitope (the last 10 amino acid sequence of human KISS1R), and as a negative each rabbit's control pre-immune serum (1:500).  Thereafter, the cells were stained with the secondary antibody, Alexa Flour 488 conjugated anti-rabbit (6.7 μg/ml), counterstained with DAPI to detect the nucleus and mounted on a microscope slide.

The data showed that in the BT-20 (Figure 3.7) and MDA-MB-231 (Figure 3.8) cells, the KISS1R antibodies (Ab 1210 and Ab 1213), were unable to detect a specific signal. The distribution of signal in the pre-immune and antibody treated cells was similar and although the antibody 1210 generated a stronger signal, no specific localisation was observed.

Therefore, both antibodies seem incapable of detecting the endogenous KISS1R even though antibody 1210 was able to detect a specific signal relating to exogenous expressed KISS1R in HEK293 cells.

Figure 3.7: KISS1R localisation in BT-20 cells.

KISS1R was detected using rabbit polyclonal KISS1R Abs 1210 and 1213. Pre-immune serum P1 and P2 were used as respective negative controls for each antibody. DAPI was used as nuclear stain. Scale bar 10 μm.
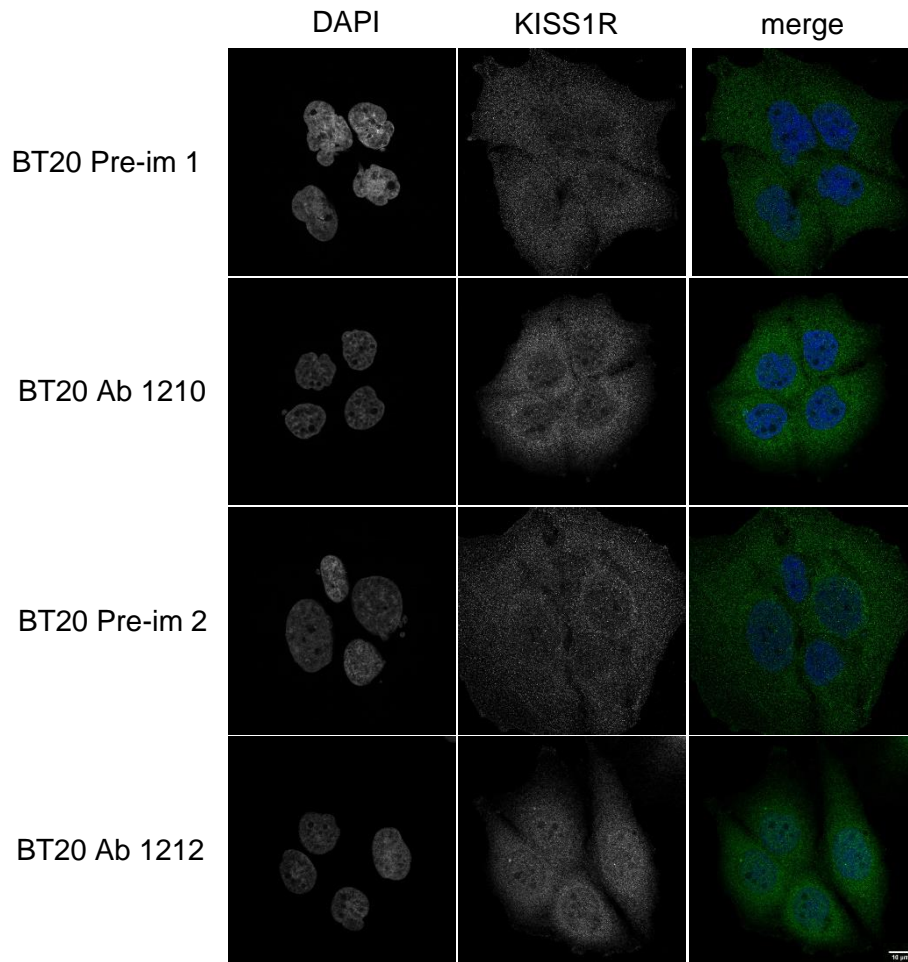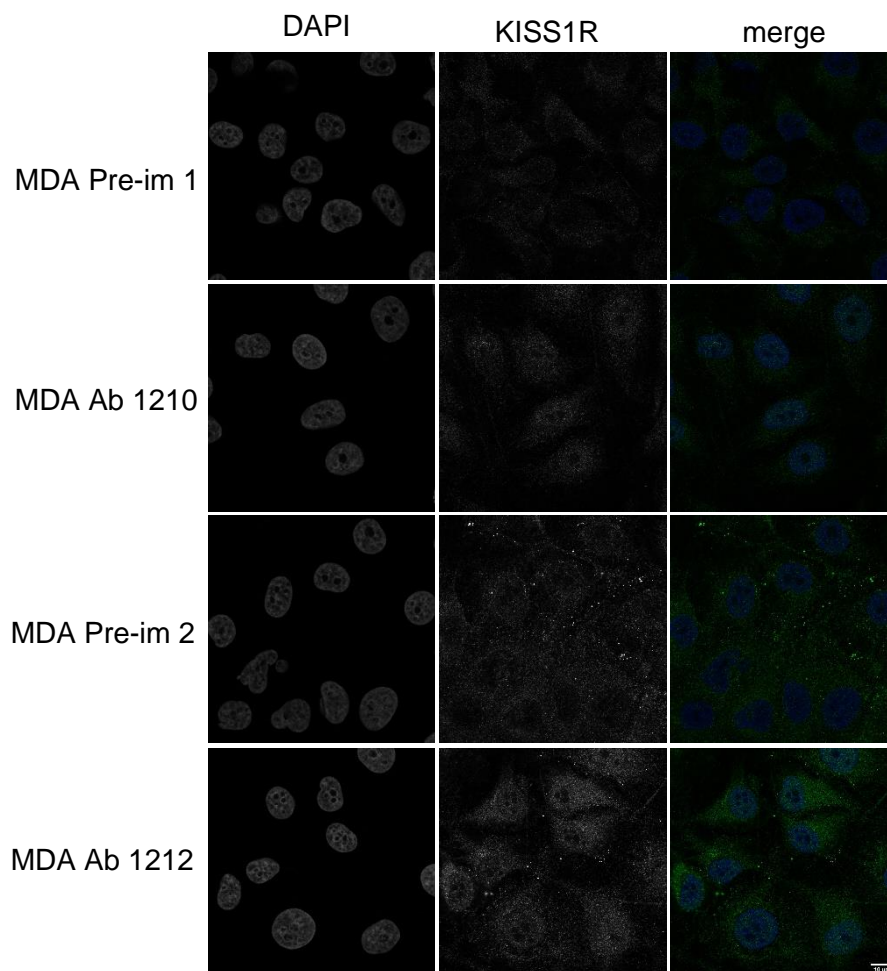
Figure 3.8: KISS1R localisation in MDA-MB-231 cells.

KISS1R was detected using rabbit polyclonal KISS1R Abs 1210 and 1213. Pre-immune serum P1 and P2 were used as respective negative controls for each antibody. DAPI was used as nuclear stain. Scale bar 10 µm.

## 3.5 ERK1/2 is activated in BT-20 and MDA-MB-231 cell lines stimulated with 10% serum media.

As a $G\alpha_{q/11}$ coupled GPCR, KISS1R is likely to be able to activate the ERK1/2 signalling pathway after kisspeptin stimulation.[102] We first wanted to determine if the ERK1/2 pathway was present and functional in the cell lines we were assessing. Thus, we stimulated BT-20 and MDA-MB-231 cells with serum containing medium after a 4 hour serum starvation. Cells were collected 0, 5, 10, 30, 45, 60, and 120 min after stimulation. The cells were lysed using RIPA lysis buffer, resolved on 4-20% SDS-PAGE gels and blotted onto PVDF membranes. ERK1/2 phosphorylation was detected using an anti-phospho-ERK1/2 antibody followed by incubation with secondary antibody conjugated to HRP. The band intensities were detected by chemiluminescence. After detecting phosphorylated ERK1/2 the membranes were re-probed with a human anti-tubulin antibody to act as protein loading control. Western blot data showed that in BT-20 cells, the phospho-ERK1/2 antibody detected bands that were approximately 42 kD and 44 kD, in size representative of ERK 2 and 1 respectively (Figure 3.9A, Top panel). ERK1/2 phosphorylation increased rapidly after serum addition with the highest level of phosphorylation observed at 5 min after serum addition. Phosphorylation slowly decreased after 5 min but remained elevated over control up to 45 min, after which phosphorylation levels were similar to pre-stimulation levels. In MDA-MB-231 cells (Figure 3.9B, Top panel), a similar increase in ERK1/2 phosphorylation level was measured after 5 min with a gradual decline in signal so that by 30 min ERK1/2 phosphorylation was similar to pre-stimulation levels. Therefore, our data show that ERK1/2 can be activated by the growth factors in serum containing media in both cell lines, with maximal activation at 5 min.

A



B
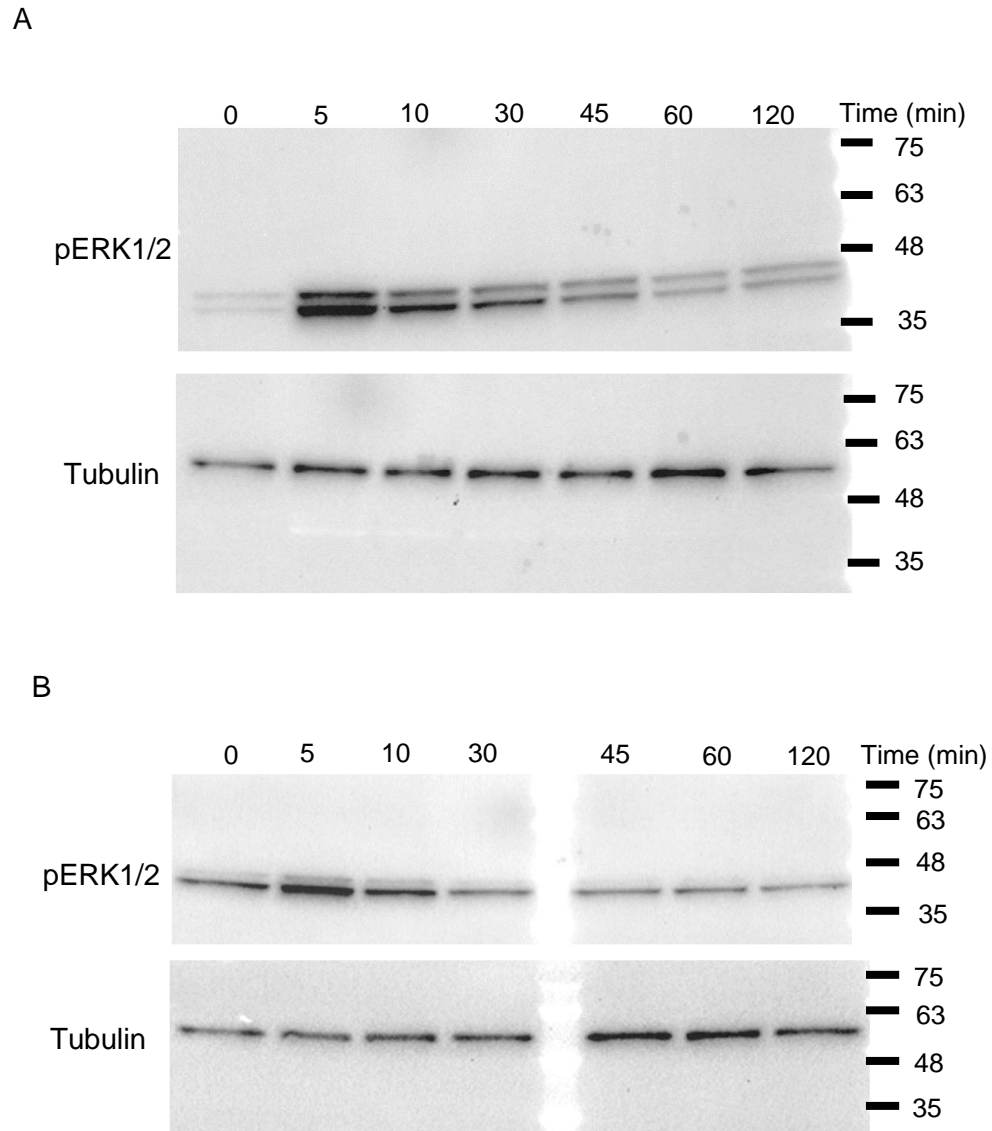


Figure 3.9: ERK1/2 is phosphorylated in BT-20 and MDA-MB-231 cells stimulated with serum media.

Western blots showing the expression of phosphorylated ERK1/2 (pERK1/2), in BT-20 (A) and MDA-MB-231 (B) cells after stimulation with 10% serum media for 0, 5, 10, 30, 45, 60 and 120 min. Afterwards, the cells were harvested and ERK phosphorylation levels were measured through western blotting using the phospho-ERK1/2 antibody (0.25 µg/ml). Tubulin was used a loading control (bottom panel).

### 3.6 Exogenous KISS1R in HEK293 cells activates ERK1/2 phosphorylation.

KISS1R is a G-protein coupled receptor that has been reported to couple to $G\alpha_{q/11}$ G-protein leading to ERK1/2 phosphorylation.[102] Therefore, we sought to determine whether KISS1R expressed in HEK293 cells could trigger ERK1/2 phosphorylation after binding to the ligand, kisspeptin (KP-10). HEK293 cells transfected with either FLAG-KISS1R or pLKO.1 GFP (negative control), were stimulated with 100 nM KP-10 for 5, 30 and 60 min. The concentration of KP-10, 100 nM, was chosen because most studies have shown that ERK1/2 can be activated with 100 nM KP-10.[102–104] Unstimulated controls were also included. After stimulation, cells were lysed in RIPA lysis buffer supplemented with protease and phosphatase inhibitors and cleared by centrifugation. Lysates were resolved by electrophoresis on a 4-12% SDS-PAGE gel and the proteins were transferred onto a PVDF membrane. The membrane was probed by overnight incubation at 4ºC with rabbit anti-phospho-ERK1/2 antibody and HRP conjugated goat anti-rabbit antibody. Proteins were detected by chemiluminescence. After detecting phosphorylated ERK1/2 the membrane was re-probed with a human Actin antibody to correct for protein loading.

Figure 3.10A (top panel) shows the membrane probed for phosphorylated ERK1/2. There were no visible bands in the control transfected HEK293 cells (left side of blot) even after stimulation with KP-10. In contrast, cells transfected with KISS1R responded to KP-10 stimulation with ERK1/2 phosphorylation increasing 5 min after KP-10 addition with ERK1/2  phosphorylation decreasing but remaining higher than unstimulated lysates at 30 min and 60 min. Based on the quantification data (Figure 3.10B) we can conclude that transfection with a KISS1R construct made HEK293 cells sensitive to KP-10 stimulation resulting in the phosphorylation of  ERK1/2. The early stimulation of ERK1/2  at 5 min furthermore suggests that G-protein activation is involved in this stimulation.
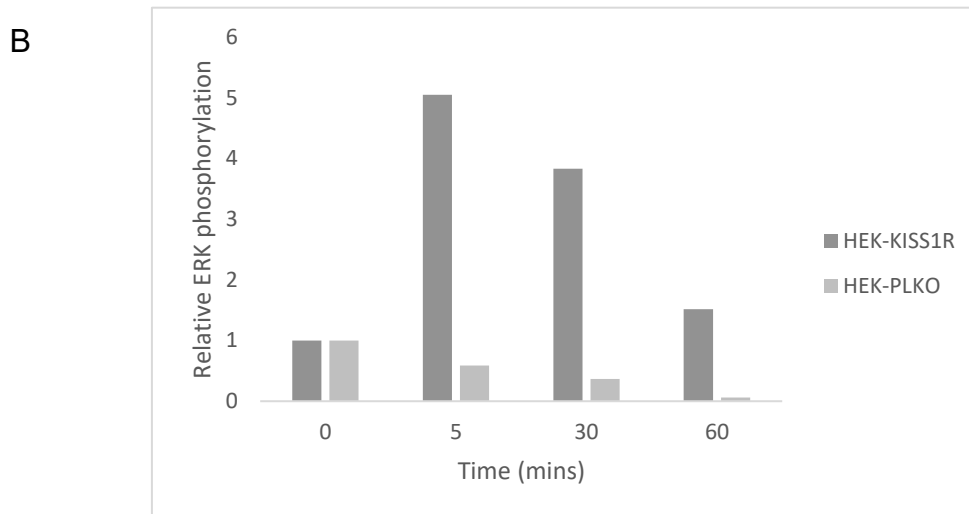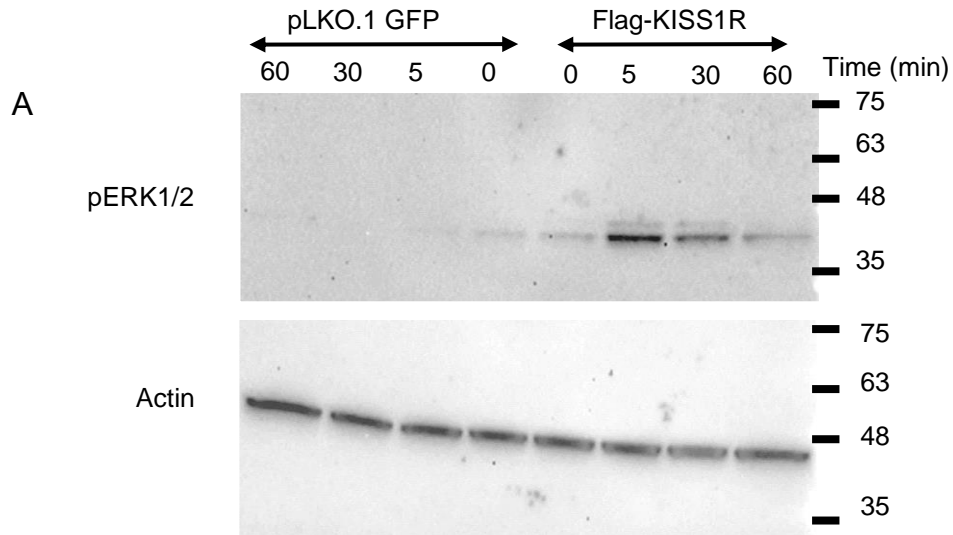
Figure 3.10: KISS1R activates the ERK1/2 pathway when stimulated with KP-10.

(A) HEK293 cells transfected with either flag-tag KISS1R or pLKO.1 GFP (as negative control), were stimulated with 100 nM kisspeptin-10 (KP-10) for 0, 5, 30 and 60 min and then harvested for western blot analysis using rabbit anti-phospho-ERK1/2 antibody (0.25 µg/ml). Actin (bottom panel) was used a loading control. (B) Densitometric analysis of the blot was performed by normalizing band intensity to Actin. n=1

## 3.7 BT-20 cells, but not MDA-MB-231 cells, respond to KP-10 stimulation by increasing ERK1/2 phosphorylation.

Our previous data showed that BT-20 and MDA-MB-231 cells can activate ERK1/2 when stimulated with serum media containing growth factors, with maximal activation at 5 min. Also, we showed that KISS1R overexpression in HEK293 cells sensitizes them to KP-10 stimulation resulting in ERK1/2 phosphorylation. Therefore, we sought to determine whether the endogenous KISS1R expressed in the BT-20 and MDA-MB-231 cells could be stimulated by KP-10 to induce ERK1/2 phosphorylation. BT-20 and MDA-MB-231 cells were stimulated after a serum starvation with 100 nM KP-10 or as vehicle control 0.02% propylene glycol for 5, 10, 30, 45, or 60 min. Unstimulated controls (0 min) were included. After stimulation, the cells were lysed with RIPA lysis buffer and cleared by centrifugation. The lysates were resolved on SDS-PAGE gels and blotted unto PVDF membranes. The phosphorylated ERK1/2 was detected using rabbit anti-phospho-ERK1/2 antibody and appropriate secondary antibody conjugated to HRP. The ERK1/2 bands were visualized by chemiluminescence. All band intensities were normalised to total protein and for each time point KP-10 treatment was divided by the vehicle/PG treatment. The experiment was repeated at least 3 times independently.

Western blot data showed that in BT-20 cells, the phospho-ERK1/2 antibody detected bands that were approximately 42 kD and 44 kD in size, representing ERK2 and ERK1 (Figure 3.11A, Top panel). Analysis of average ERK1/2 phosphorylation shown in Figure 3.11B showed that 5 and 10 minutes after KP-10 stimulation a small increase in ERK phosphorylation was measured with only the increase at 5 min at statistically significant levels. However, at 45 and 60 min, a robust increase in phosphorylation of 1.5 and 2-fold, respectively over control was measured. The vehicle control (PG) was also quantified by normalizing to total protein. The result, Figure 3.11C, showed that PG had no significant effect on ERK1/2 phosphorylation. Therefore, we can conclude that the increase in ERK1/2 phosphorylation was not due to PG. In contrast, MDA-MB-231 cells stimulated with KP-10 did not show any increase in ERK1/2 phosphorylation, (Figure 3.12A, Top panel) and no significant differences were measured after quantification of three

independent experiments (Figure 3.12B). The result, Figure 3.12C, showed that PG had no significant effect on ERK1/2 phosphorylation.

Therefore, endogenous KISS1R in the BT-20 cells responds to stimulation with the agonist KP-10 by increasing ERK1/2 phosphorylation minimally at early time points but a more robust increase is seen after 45 and 60 min unlike MDA-MB-231 cells where no increase is observed at any time after stimulation. ERK1/2 phosphorylation at such later times after stimulation can be associated with β-arrestin1/2 engagement by the receptor.[105]
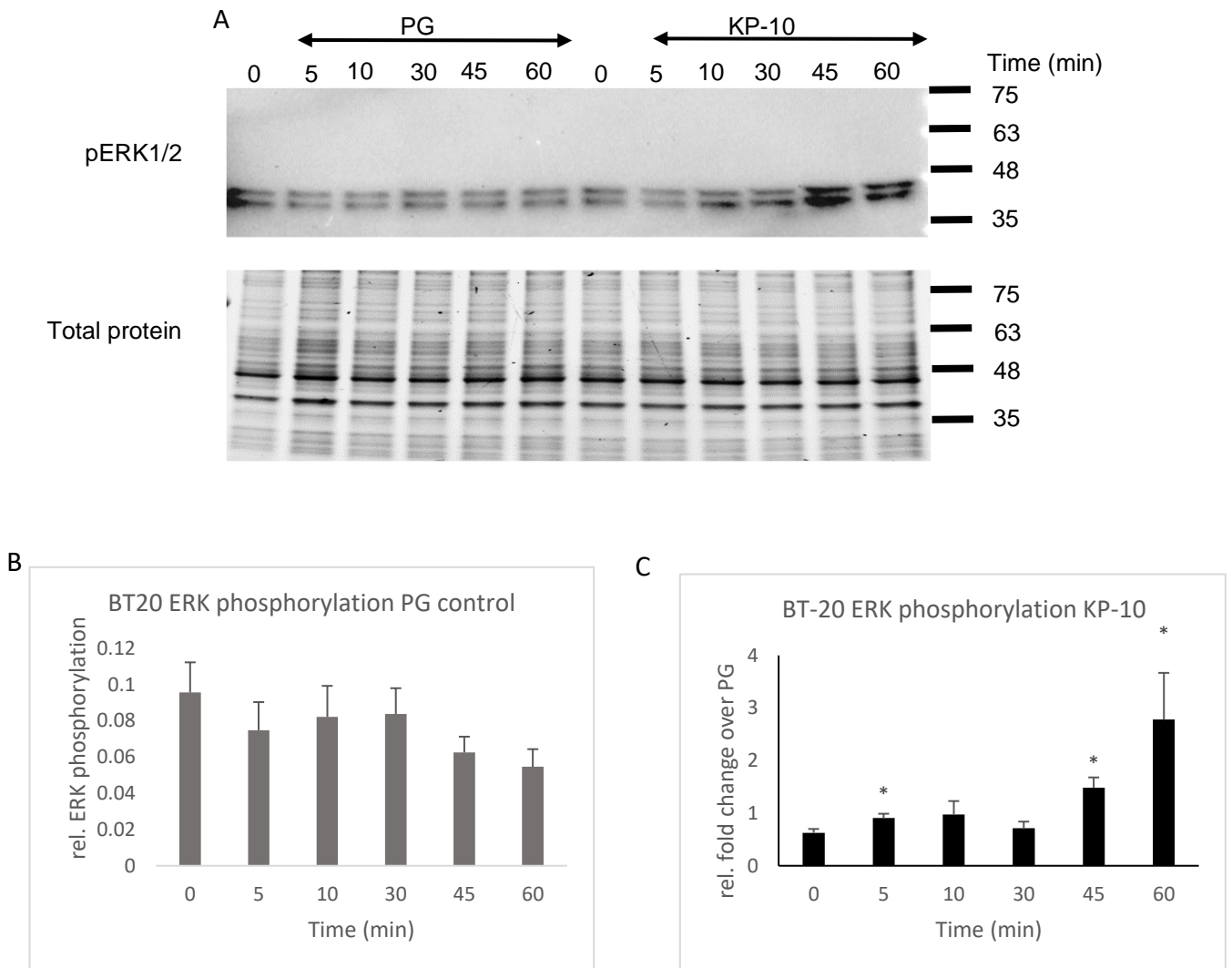
Figure 3.11: KISS1R activates ERK1/2 phosphorylation a β-arrestin dependent manner in BT20 cells stimulated with KP-10.

(A) BT20 cells were stimulated with either 0.02% propylene glycol (PG) as the vehicle control or 100 nM KP-10 for 5, 10, 30, 45 or 60 min. Unstimulated (0) controls were included. After stimulation, the cells were harvested for western blot analysis using rabbit anti-phospho-ERK1/2 antibody. The phospho-ERK1/2 antibody was used at 0.25 µg/ml. (B) Densitometric analysis of the vehicle control (PG) showing that PG had no significant impact on ERK1/2 phosphorylation. (C) Densitometric analysis of the blot was performed by normalizing band intensity to total protein. Relative fold change was determined for each timepoint by dividing KP-10 treated data by PG vehicle treated data. Data are expressed as mean ± SEM of 5 independent repeats. Significance determined by student's T-test between untreated control and each time point. *P value < 0.05.
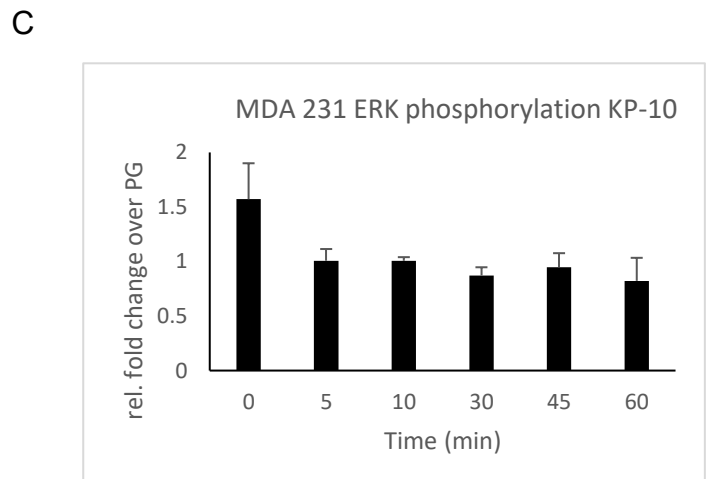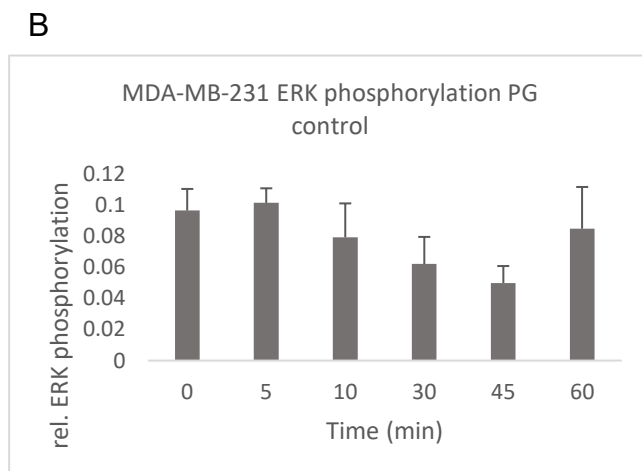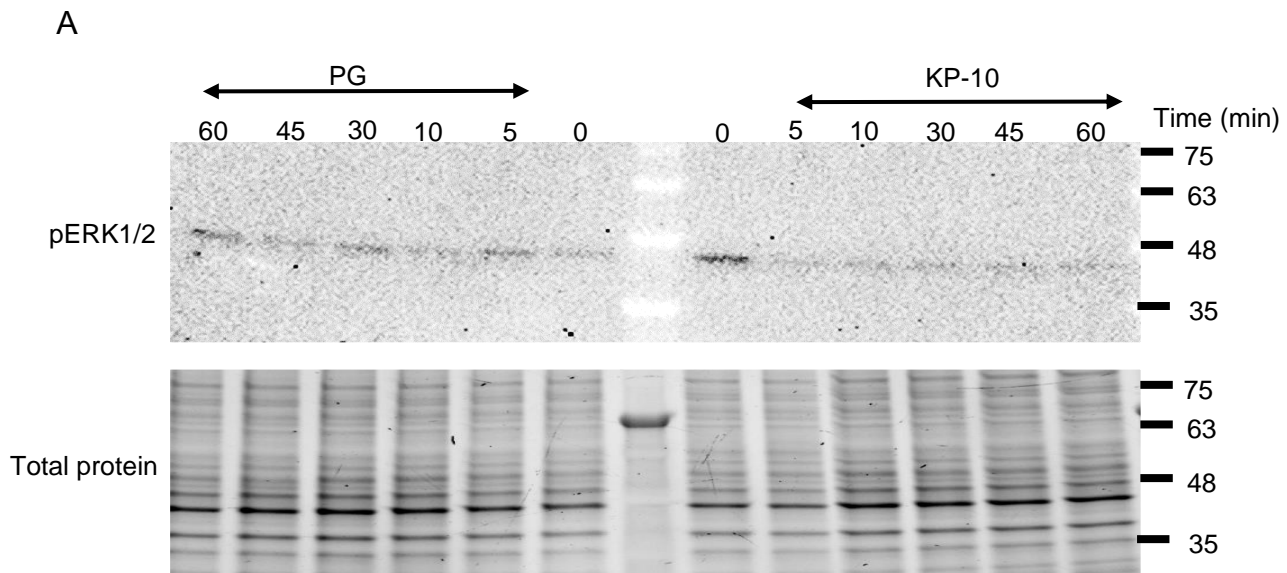
Figure 3.12: KISS1R does not activate ERK1/2 phosphorylation in MDA-MB-231 cells stimulated with KP-10.

 (A) MDA-MB-231 cells were stimulated with either 0.02% propylene glycol (PG) as the vehicle control or 100 nM KP-10 for 5, 10, 30, 45 or 60 min. Unstimulated (0) controls were included. After stimulation, the cells were harvested for western blot analysis using rabbit anti-phospho-ERK1/2 antibody. The phospho-ERK antibody was used at 1:1000. (B) Densitometric analysis of the vehicle control (PG) showing that PG had no significant impact on ERK1/2 phosphorylation. (C) Densitometric analysis of the blot was performed by normalizing band intensity to total protein. Relative fold change was determined for each timepoint by dividing KP-10 treated data by PG vehicle treated data. Data are expressed as mean ± SEM of 3 independent repeats. Significance determined by student's T-test between untreated control and each time point. not significant, $p > 0.05$.

## 3.8 BT-20 cells express endogenous β-arrestin1/2.

Since β-arrestin1/2 proteins have been shown to act as scaffolds for the recruitment and activation of ERK1/2 [102,105], we assessed the expression of endogenous β-arrestin1/2 proteins in the BT-20 and MDA-MB-231 cell lines to determine if the ERK1/2 phosphorylation seen after KP-10 stimulation in BT-20 cells could be mediated by β-arrestin1/2. Protein extraction was performed by lysing the cells with RIPA lysis buffer and clearing by centrifugation. The proteins were resolved by electrophoresis on SDS-PAGE gels and transferred to PVDF membrane. After blocking, the membrane was incubated with a commercially available β-arrestin1/2 antibody (1:1000) from Cell Signalling Technology and secondary Goat anti-rabbit HRP-conjugated antibody. Protein bands were visualized by chemiluminescence. After detecting β-arrestin1/2 the membrane was re-probed with a human anti-tubulin antibody to act as protein loading control. The β-arrestin1/2 expression was normalized to tubulin and average expression was determined from 3 independent experiments.

The western blot data (Figure 3.13A, Top panel) shows the membrane probed for β-arrestin1/2. The antibody detected a single band in the BT-20 (lanes 1, 2, 3) and the MDA-MB-231 (lanes 4, 5, 6) cells, which was approximately 50 kD in size, representing β-arrestin1/2. The quantification data normalised to tubulin (Figure 3.13B), shows that the BT-20 cells expressed 4 times more β-arrestin1/2 compared to MDA-MB-231 cells. Therefore, this data suggests that there is a correlation between late ERK1/2 phosphorylation in BT-20 cells after KP-10 stimulation and β-arrestin1/2 expression.
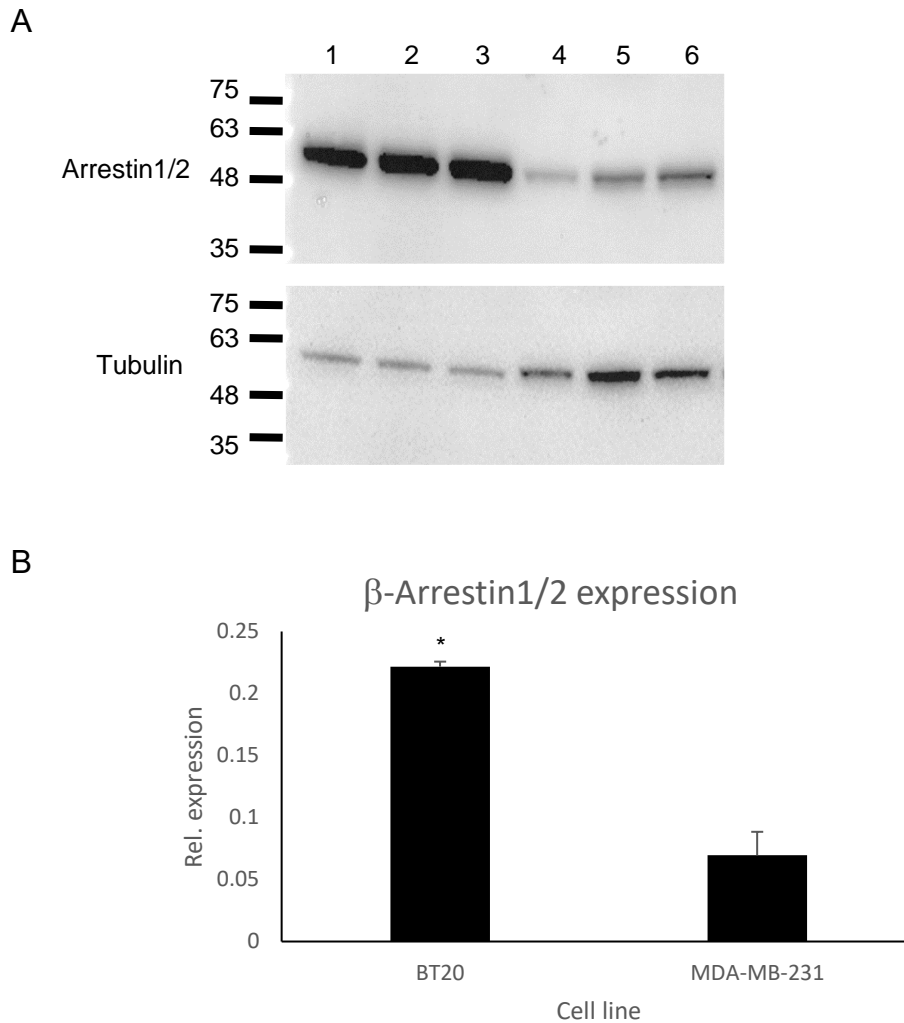
Figure 3.13: β-arrestin1/2 is highly expressed in BT-20 compared to MDA-MB-231.

(A) Western blot showing the expression of endogenous β-arrestin1/2 in BT-20 (lane 1, 2, 3), and MDA-MB-231 (lane 4, 5, 6). Primary antibody was used at 1: 1000. Top panel shows β-arrestin1/2 with an approximate size of 50 kD. The lower panel shows tubulin loading control. (B) Densitometric analysis of blots performed by normalizing band intensity to Tubulin. Data are expressed as mean ± SEM of 3 independent repeats. Unpaired Student's T test was performed to compare the beta arrestin1/2 protein expression in the 2 breast cancer cell lines. ** P value <0.05.

To assess the expression ratio of β-arrestin1 and 2 in BT-20 cells, lysates generated from the cell lines were resolved, blotted and incubated with anti- β-arrestin1 and anti- β-arrestin 2 antibodies (Figure 3.14). After detecting β-arrestin 1 and β-arrestin 2 the membranes were re-probed with an anti-tubulin antibody to act as protein loading control.

The western blot data (Figure 3.14, top panel) shows the membrane probed for β-arrestin1 and β-arrestin2. The β-arrestin1 antibody (left hand side of the blot) detected a strong single band in the BT-20 (lanes 1, 2, 3) and the faint band in the MDA-MB-231 (lanes 4, 5, 6) cells, which was approximately 50 kD in size. Just as observed previously when the cells were probed with β-arrestin1/2 antibody, β-arrestin1 was highly expressed in the BT-20 compared to the MDA-MB-231 cells. On the other hand, our antibody did not detect β-arrestin2 protein (right hand side of the blot) in both BT-20 and MDA-MB-231 cells. Since the tubulin blot (Figure 3.14, lower panel) showed that similar amount of protein was loaded for both β-arrestin1 and β-arrestin2, we conclude that only β-arrestin1 isoform is expressed endogenously in the BT-20.
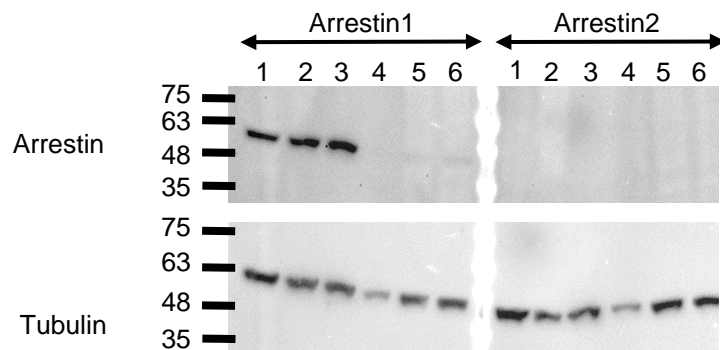


Figure 3.14: β-arrestin 1, but not β-arrestin 2, is highly expressed in the BT-20 cells.

(A) Western blot showing the expression of endogenous β-arrestin 1 (left hand side of the ladder) and β-arrestin 2 (right hand side of the ladder) in BT-20 (lane 1, 2, 3), and MDA-MB-231 cells (lane 4, 5, 6). Primary antibodies were used at 0.25 µg/ml. Top panel is the β-arrestin1 or 2 with an approximately size of 50 kD. The lower panel is the tubulin loading control.

3.9 Endogenous KISS1R in BT-20 and MDA-MB-231 cells does not activate ERK1/2 phosphorylation in a KP-10 dose dependent manner after stimulating for 5 and 60 min.

So far, the results show that when BT-20 and MDA-MB-231 cells were stimulated with 10% serum media, there was an increase in ERK1/2 phosphorylation, with maximal phosphorylation at 5 min. However, when the cells were stimulated with 100 nM KP-10 to activate the endogenous KISS1R in both cell lines, there was no robust increase in ERK1/2 phosphorylation after 5 min of stimulation. Therefore, we speculated that the dose of KP-10 used to activate KISS1R could affect ERK1/2 phosphorylation. In order to test this hypothesis, serum starved BT-20 and MDA-MB-231 cells were stimulated with increasing concentrations (10 nM to 100 μM) of KP-10 for 5 min. After stimulation, the cells were lysed with RIPA lysis buffer supplemented with protease and phosphatase inhibitors. The protein lysates were resolved on SDS-PAGE gels and then transferred to PVDF membranes. The membranes were incubated for 1 hour with 5% blocking solution and then probed overnight at 4ºC with the same phospho-ERK1/2 antibody that was used previously. This was followed by incubation for 1 h with the HRP conjugated goat-anti-rabbit secondary antibody. Band intensities were detected by chemiluminescence. After detecting phosphorylated ERK1/2 the membrane was re-probed with a human Actin antibody to act as protein loading control. The data was quantified by normalising phosphorylated ERK1/2 to Actin and the fold change was determined by dividing KP-10 or PG treated cells by the untreated control.

The western blot data showed that in the BT-20 cells, the phospho-ERK1/2 antibody detected bands that were approximately 42 kD and 44 kD, representing ERK2 and ERK1 (Figure 3.15A, top panel). The quantification data of ERK1/2 phosphorylation normalised to Actin (Figure 3.15B) showed that in BT-20 cells, compared to the vehicle treated cells there was no effect on ERK1/2 phosphorylation as the concentration of KP-10 increased. In the MDA-MB-231 cells (Figure 3.16A), the phospho-ERK1/2 antibody detected a single band that was approximately 42 kD, representing ERK2. The quantification data of ERK1/2 phosphorylation normalised to Actin (Figure 3.16B) showed that in the MDA-MB-231 cells, compared to the vehicle treated cells there was no effect on ERK1/2 phosphorylation as the concentration of KP-10 increased. Therefore, our data suggests

that in the BT-20 and MDA-MB-231 cells, KISS1R does not activate ERK1/2 in a dose dependent manner after 5 min of stimulation with KP-10. This experiment was only repeated 2 times because preliminary data showed that ERK1/2 is not phosphorylated after 5 min of stimulation with KP-10.

A



B



ERK phosphorylation after 5 min

Figure 3.15: Endogenous KISS1R in BT-20 cells does not activate ERK1/2 phosphorylation in a dose dependent manner after 5 minutes of stimulation with KP-10.

(A) BT-20 cells were stimulated with increasing concentrations (10 nM to 100 µM) of KP-10 for 5 min. Unstimulated (UT) and vehicle (PG) controls were included. After stimulation, the cells were harvested for analysis by western blotting using the rabbit phospho-ERK1/2 antibody (0.25 µg/ml). Actin (bottom panel) was used as a loading control. (B) Densitometric analysis of the blots was performed by normalizing band intensity to Actin and dividing the treated cells by unstimulated control. Data are expressed as mean ± SEM of 2 independent repeats.
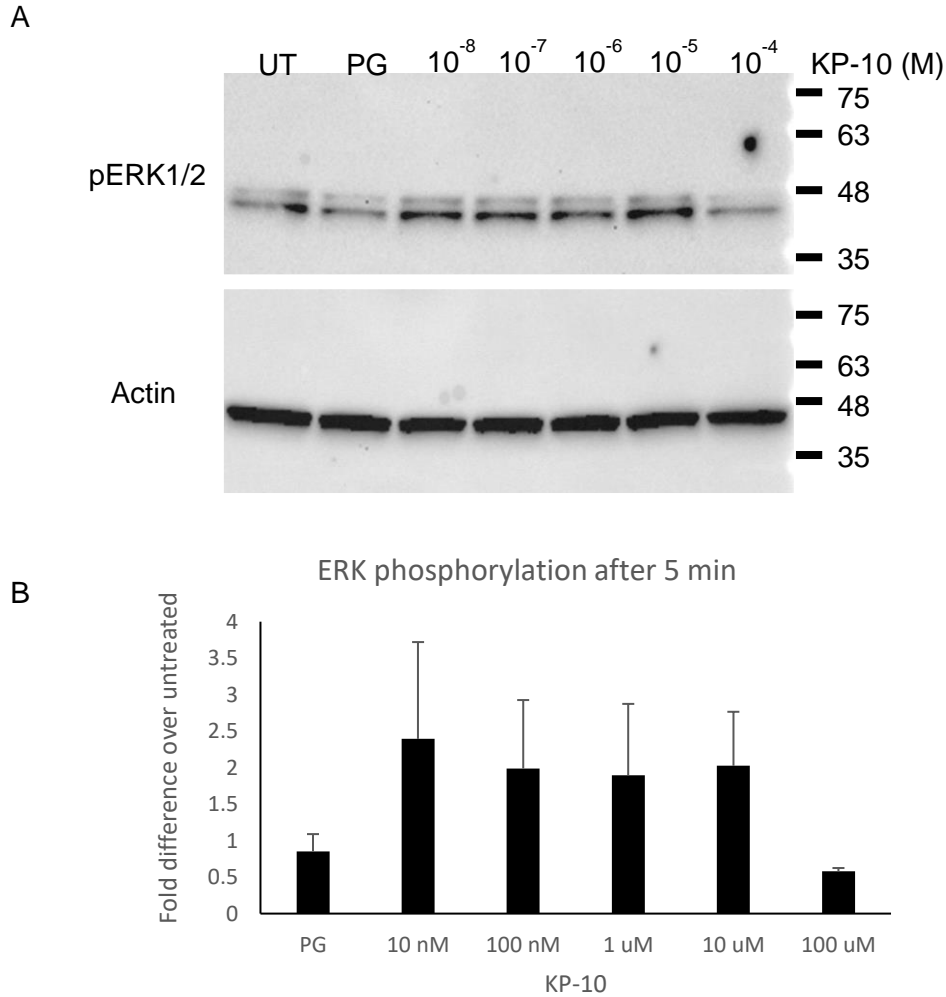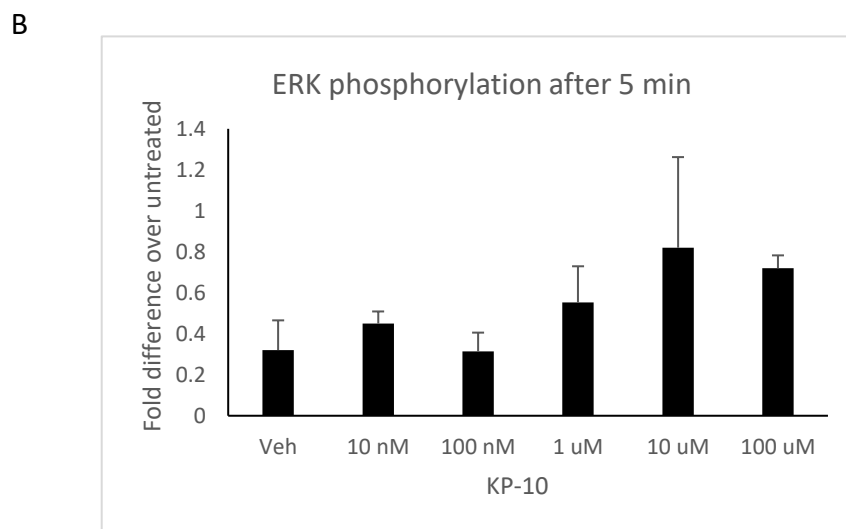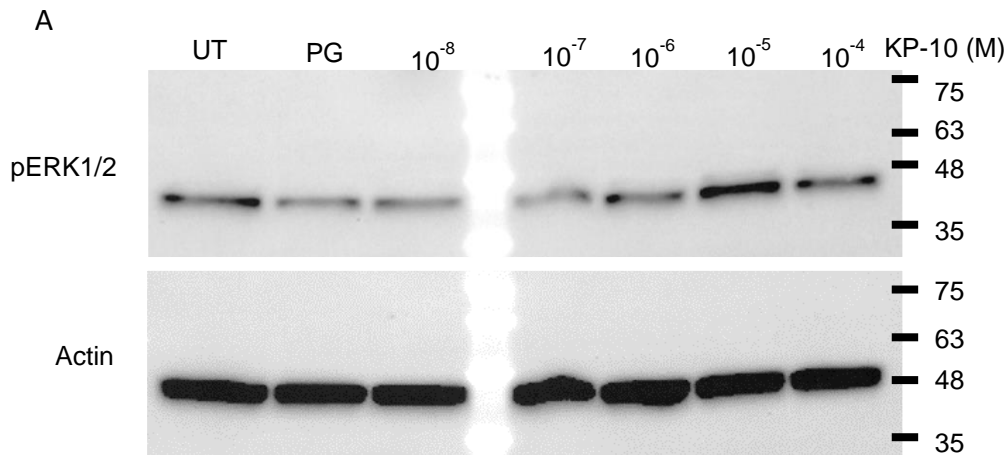
Figure 3.16: Endogenous KISS1R in MDA-MB-231 cells does not activate ERK1/2 phosphorylation in a dose dependent manner after 5 minutes of stimulation with KP-10.

(A) MDA-MB-231 cells were stimulated with increasing concentrations ($10^{-8}$ to $10^{-4}$ M or 10 nM to 100 μM KP-10) of KP-10 for 5 min. Unstimulated (0) and vehicle (PG) controls were included. After stimulation, the cells were harvested for analysis by western blotting using the rabbit phospho-ERK1/2 antibody. Actin (lower panel) was used as a loading control. (B) Densitometric analysis of the blots was performed by normalizing band intensity to Actin and dividing the treated cells by unstimulated control. Data are expressed as mean ± SEM of 2 independent repeats.

Our data was unable to show the optimal concentration of KP-10 that is required by the endogenous KISS1R in the BT-20 and MDA-MB-231 cells to activate ERK1/2 after 5 min of stimulation with KP-10. We decided to stimulate the cells for 60 min since our time course study showed that the endogenous KISS1R in BT20 cells activates ERK1/2 after 60 min stimulation with KP-10. Also, we amended the protocol in order to account for the variation in the final concentration of the vehicle control for each concentration of KP-10. For each KP-10 concentration, we added propylene glycol to ensure that the final concentration of propylene glycol was always 0.02%. Thus, the cells were stimulated for 1 hour at 37ºC with varying concentrations of KP-10, from 1 nM to 1 µM, and a final propylene glycol concentration of 0.02% (v/v). Thereafter, protein extraction was performed using RIPA lysis buffer supplemented with protease and phosphatase inhibitors. The protein lysates were resolved on SDS-PAGE gels and then transferred to PVDF membranes. The membranes were incubated for 1 hour with 5% blocking solution and then probed overnight at 4ºC with the same phospho-ERK1/2 antibody that was used previously. This was followed by incubation for 1 h with the secondary antibody, HRP conjugated goat anti rabbit antibody. Band intensities were detected by chemiluminescence. After detecting phosphorylated ERK1/2 the membrane was re-probed with a human Actin antibody to act as a loading control. To get the relative fold change, the phosphorylated ERK1/2 was normalized to Actin and then KP-10 or PG treated cells were divided by the untreated (UT) control.

The western blot data showed that in the BT-20 cells, the phospho-ERK1/2 antibody detected 2 bands that were approximately 42 kD and 44 kD in size, representing ERK2 and ERK1 (Figure 17A, right hand side of the blot, top panel). Our quantification data of ERK1/2 phosphorylation normalised to Actin (Figure 3.17B), showed that in the BT-20 cell line, relative to the vehicle control (PG), there was an increase in ERK1/2 phosphorylation as the concentration of KP-10 increased from 1 nM to 10 µM. However, none of the increases were statistically significant. In the MDA-MB-231 cells (Figure 3.17A, left hand side of the blot, top panel), the phospho-ERK1/2 antibody detected a single band that was approximately 42 kD representing the ERK2 band. Our quantification data of ERK1/2 phosphorylation normalised to Actin (Figure 3.17C) showed that relative to the vehicle control (PG), there was no increase in ERK phosphorylation in the cells

treated with 1 nM, 10 nM and 1 µM KP-10. However, in the cells treated with 100 nM and 10 µM KP-10, there was a small increase in ERK1/2 phosphorylation, but the increase was not statistically significant ($p > 0.05$). Therefore, this data suggests that in both cell lines, higher concentrations of KP-10 do not result in an increase in ERK1/2 phosphorylation.

A
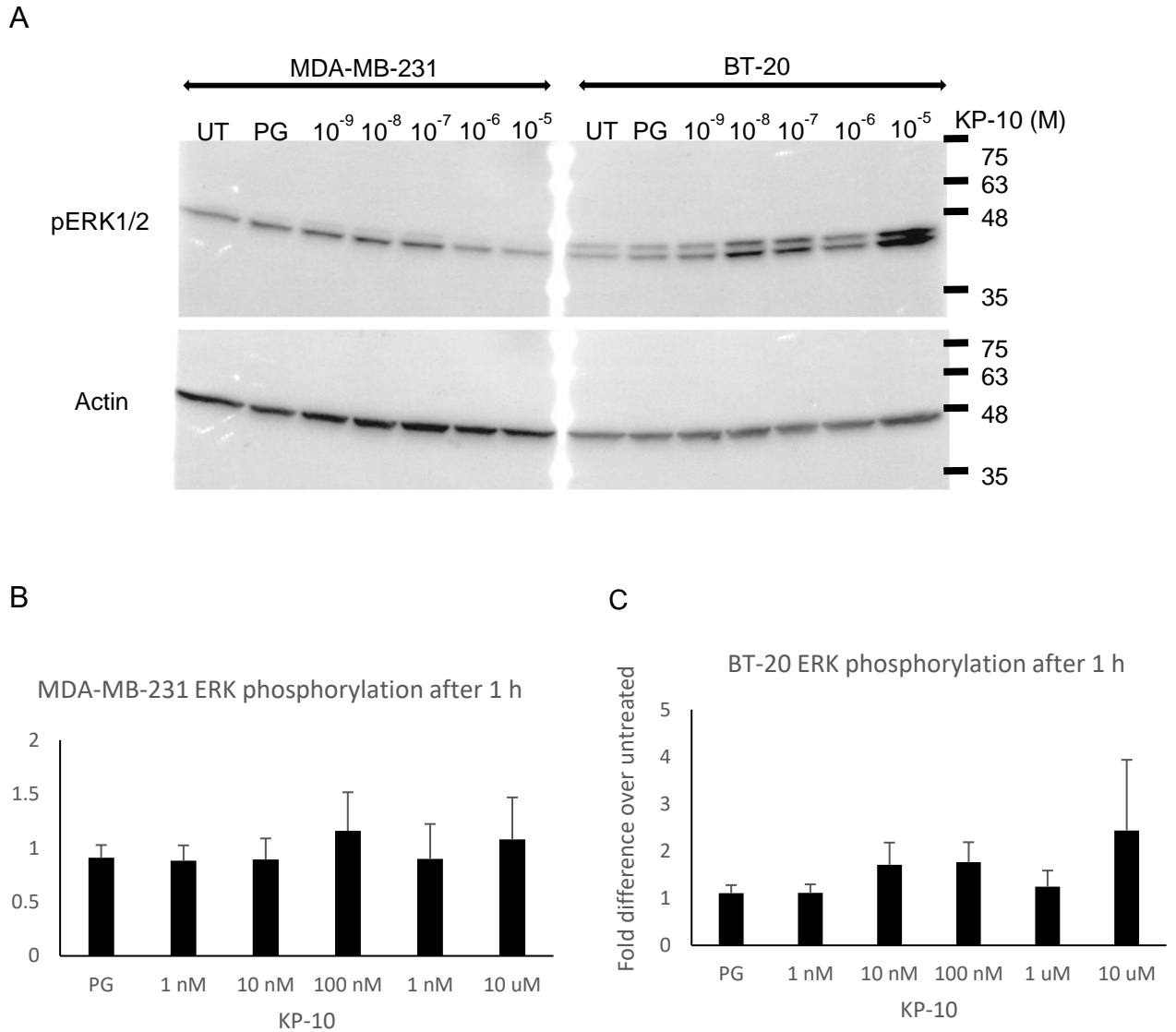


Figure 3.17: Endogenous KISS1R in MDA-MB-231 and BT-20 cells does not significantly activate ERK1/2 phosphorylation in a dose dependent manner after 1 hr stimulation with KP-10.

MDA-MB-231 (left hand side of the ladder) and BT-20 (right hand side of the ladder) cells were stimulated with increasing concentrations (1 nM to 10 µM KP-10) of KP-10 for 1 h. Unstimulated (UT) and vehicle (PG) controls were included. After stimulation, the cells were harvested for analysis by western blotting using the rabbit phospho-ERK1/2 antibody (0.25 µg/ml). Actin (lower panel) was used as a loading control. (B and C) Densitometric analysis of the blots was performed by normalizing band intensity to Actin and dividing the treated cells by unstimulated control. Data are expressed as mean ± SEM of 4 independent repeats. Statistical significance was determined by student's Unpaired T-test between PG control and each concentration, not significant $p > 0.05$. PG represents propylene glycol.

3.10 <u>Cell proliferation is not affected by KISS1R activation.</u>

To determine if the KISS1R dependent effect on ERK1/2 phosphorylation regulates cell proliferation, the proliferation rate of BT-20 and MDA-MB-231 cells stimulated with KP-10 was analysed using the crystal violet assay. BT-20 and MDA-MB-231 cells were seeded in quintuplicate under normal culture conditions (10% serum media) in 96 well plates and incubated overnight. The following day, they were treated with normal medium containing either 100 nM KP-10, 10 nM KP-10, 0.02% propylene glycol (vehicle control), or 300 nM C15 (negative growth control). Plate was incubated for 24, 48 and 72 h. Untreated controls, which were cells with media only, were included. At the end of each time point, the cells were fixed and stained with 1% glutaraldehyde and 0.1% crystal violet, respectively (Figure 3.18A). The stained crystal violet was extracted using 1% SDS and the absorbance determined using a microplate reader at a wavelength of 570 nm.

Our data showed that under normal cell culture condition (10% serum media), KP-10 did not affect cell proliferation of the BT-20 cells (Figure 3.18B) or the MDA-MB-231 cells (Figure 3.18C) compared to the untreated or vehicle control. The negative control, which were cells treated with C15, showed a decreased cell proliferation rate. In the MDA-MB-231. Student's unpaired t-test showed that the decrease was statistically significant.

Next, the effect of KP-10 on cell proliferation under serum free culture conditions was assessed. BT-20 and MDA-MB-231 cells were seeded as before in serum containing media and incubated overnight. The following day, the serum media was replaced with serum free media and the cells were treated with either 100 nM KP-10, 1 µM P234 (KISS1R antagonist), or 0.02% propylene glycol (vehicle control) for 24, 48, 72, 96 and 120 h in serum free media. The longer time points were included because of the reduced proliferation rate observed in serum free medium. At the end of each time point, the cells were fixed and stained with 1% glutaraldehyde and 0.1% crystal violet, respectively (Figure 3.18A). The stained crystal violet was extracted using 1% SDS and the absorbance determined using a microplate reader at a wavelength of 570 nm.

Our data (Figure 3.19) showed that under serum free culture conditions the overall proliferation rate of both cell lines was slower than in serum containing medium as

expected. Interestingly, there was no effect of KP-10 on cell proliferation under serum free culture conditions in both BT-20 (Figure 3.19A) and MDA-MB-231 (Figure 3.19B) cells.

Therefore, based on these data we conclude that KISS1R activation by KP-10 has no significant impact on the growth of BT-20 and MDA-MB-231 cells, both in the presence and absence of serum in the media.
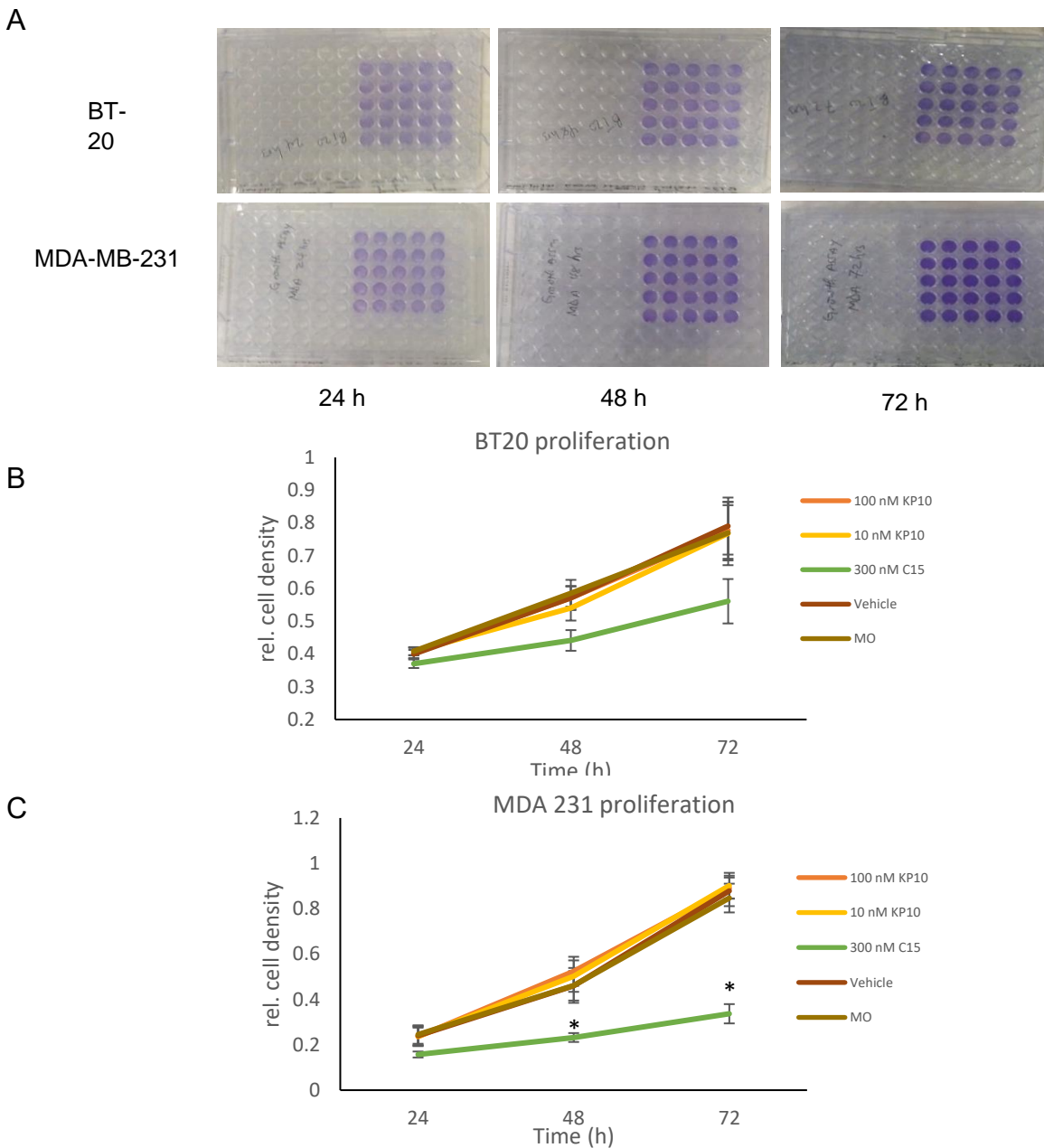
Figure 3.18: KP-10 does not affect BT-20 and MDA-MB-231 cell proliferation in the presence of serum.

(A) BT-20 and MDA-MB231 were left untreated (media only) or were treated with 10 nM KP-10, 100 nM KP-10, 300 nM C15 or vehicle in serum media for 24, 48 and 72 h before cell density was determined using crystal violet. (B) Average proliferation of BT-20 cells over 72 h and (C) average proliferation of MDA-MB-231 cells over 72 h under the indicated conditions. Data shown is the average value of 4 independent repeats with error bars representing SEM. Statistical significance was determined by student's Unpaired T-test between media only control and each treatment. * $p \leq 0.05$. MO, media only.

A

**MDA-MB-231 Proliferation**

B
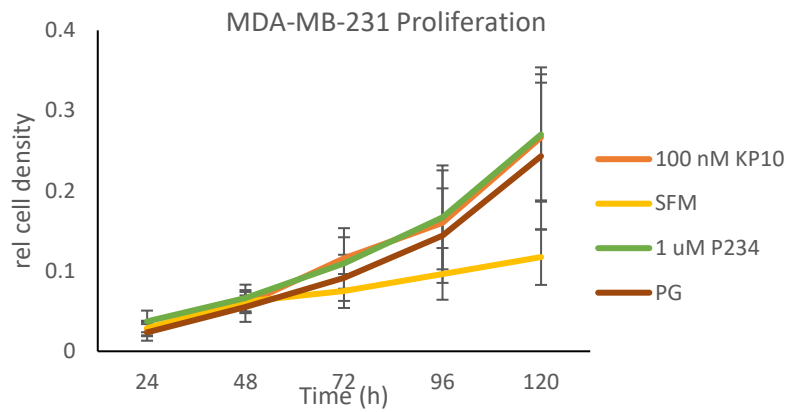
**BT-20 Proliferation**
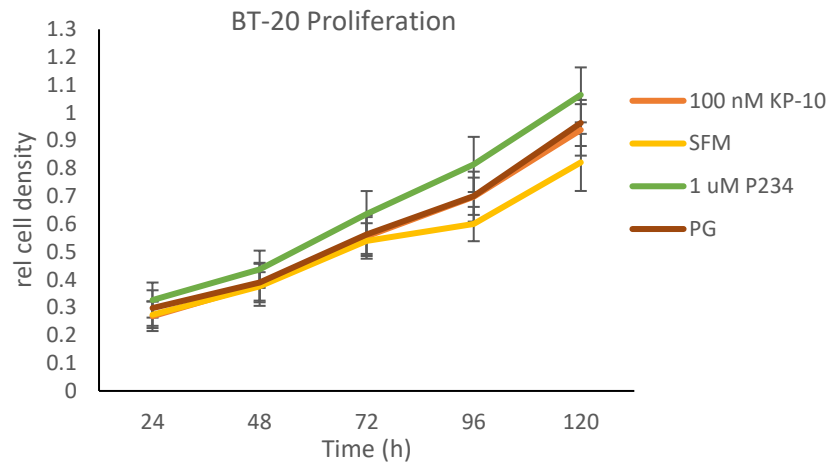
Figure 3.19: KP-10 has no effect on proliferation of BT-20 and MDA-MB-231 cells under serum free culture conditions.

BT-20 and MDA-MB-231 were either untreated (serum free media only) or treated with 100 nM KP-10 or 1 μM P234 (KISS1R antagonist), or vehicle (PG), in serum free media, for 24, 48, 72, 96 and 120 h. At the end of each time point, growth was determined by crystal violet assay. (A and B) Growth curves showing the average cell density at the indicated time points. (PG) propylene glycol. (SFM) serum free media. The data shown is the mean value of 4 independent repeats, Error bars represent SEM. Statistical significance was determined by student's Unpaired T-test between media only control and each treatment. $p \geq 0.05$.

### 3.11 Cell migration under serum free conditions is affected by kisspeptin in MDA-MB-231 cells, but not in BT-20 cells.

Since cell migration is an important part of metastasis and cell invasion, we sought to determine if KISS1R activation by KP-10 will promote or inhibit migration in the BT-20 and MDA-MB-231 cells by scratch assay. The cells were grown to confluence in 12-well tissue culture plates. A gap was created with a 200 μl micropipette tip. The cells were untreated or treated with either 0.02% propylene glycol (vehicle control) or 100 nM KP-10 in 10% serum media. Photographs of the scratches were taken at 0 h and 18 h after treatment using the Zeiss Axiovert microscope (Figures 3.20A and 20B). The experiment was performed for 18 h instead of 24 h because we observed that after 24 h, the scratch created in the MDA-MB-231 cells was closed completely. Migration was evaluated by measuring the area of the scratch at 0 and 18 h using ImageJ software. Migration was expressed as the percentage of the difference between the area migrated at 0 h and 18 h divided by the area at 0 h.

Our data showed that in the BT-20 and MDA-MB-231 cells (Figure 3.20C), under normal culture condition (10% serum), there was no significant effect on the migration of the cells treated with KP-10 compared with the untreated (media only) and vehicle (PG) controls after 18 h. However, the result showed that there was a difference in the migratory potential of both cell lines. The MDA-MB-231 cells was migratory while the BT-20 cells was almost completely non-migratory compared with the MDA-MB-231 cells.

Therefore, we conclude that KP-10 has no effect on the migration of BT-20 and MDA-MB-231 cells in the presence of serum in the media.
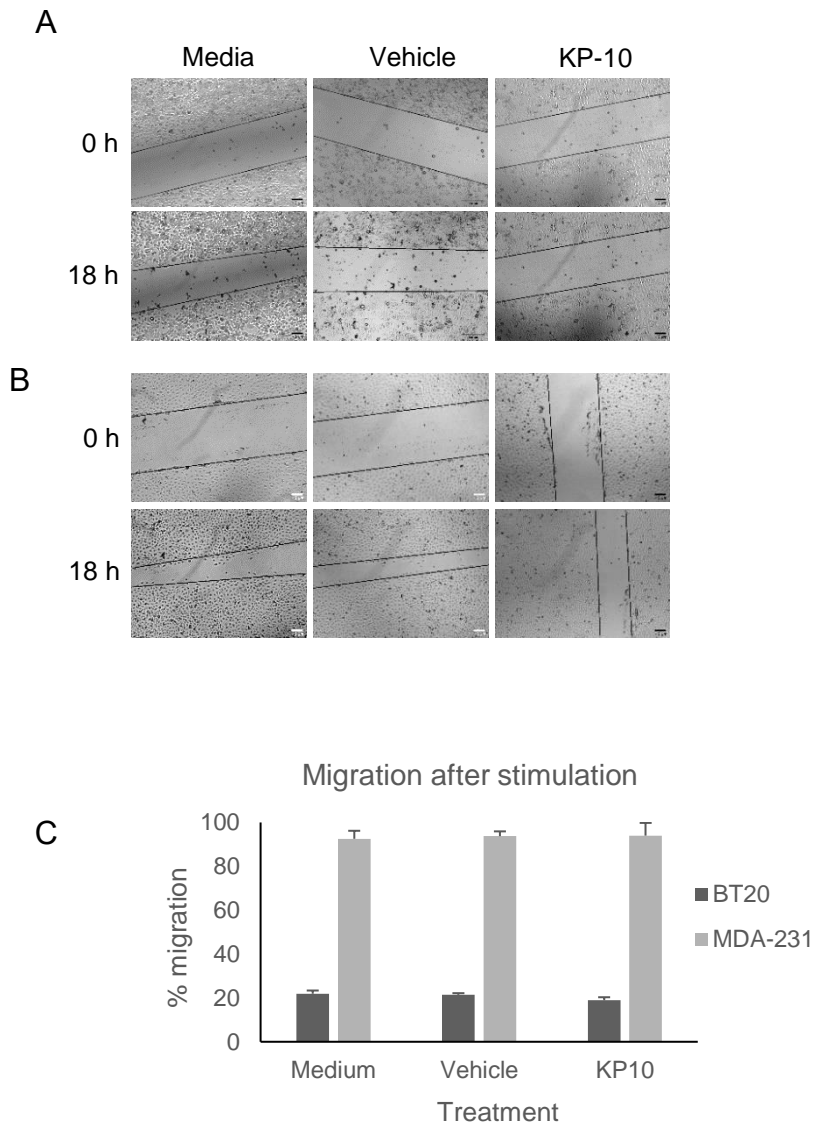
Figure 3.20: KP-10 has no significant effect of the migration of BT-20 and MDA-MB-231 cells expressing endogenous KISS1R under normal culture condition.

(A and B) Images of scratches were taken on BT-20 (A) and MDA-MB-231(B) cells after treating for 18 h with either 0.02% vehicle control (propylene glycol) or 100 nM KP-10.  Media only control was included. The images were taken on the day of treatment (day 0) and 18 h after treatment using the Zeiss Axiovert inverted microscope. (C) Quantification of the relative migration of BT-20 and MDA-MB-231 cells either untreated (media only) or treated with vehicle control (PG) or 100 nM KP-10 under serum culture conditions. Data represents mean of the percentage migration for 3 independent repeats and the error bars are ± SEM. Statistical significance was determined by student's Unpaired T-test between media only control and each treatment. $p \geq 0.05$.

In a subsequent experiment, we assessed the effect of kisspeptin on cell migration under serum free culture conditions. The BT-20 and MDA-MB-231 cells were grown overnight in serum containing media. The following day, scratches were created, and the serum media was aspirated and replaced with serum free media containing either 100 nM KP-10 or 0.2% propylene glycol (PG). A serum free media only (SFM) control was included. Photographs of the scratches were taken at 0 h and 18 h after treatment using the Zeiss Axiovert microscope. Migration was evaluated by measuring the area of the scratch at 0 and 18 h using ImageJ software. Migration was expressed as the percentage of the difference between the area migrated at 0 h and 18 h divided by the area at 0 h.

Overall, the data (Figure 3.21) showed that under serum free culture conditions, the migration rate of both cell lines was slower than in serum media. In the BT-20 cells KP-10 had no effect on migration. In the MDA-MB-231 cells, there was a 12% increase in the migration of KP-10 treated cells compared to the serum free media only control, and the increase was statistically significant ($P<0.05$). Our previous data on the proliferation of MDA-MB-231 cells under serum free conditions showed that KP-10 had no effect on cell proliferation. This implies that the increase in migration was not caused by an increase in proliferation.

Therefore, based on this data, we conclude that KP-10 increases migration in MDA-MB-231 cells but not BT-20, in the absence of serum in the media.
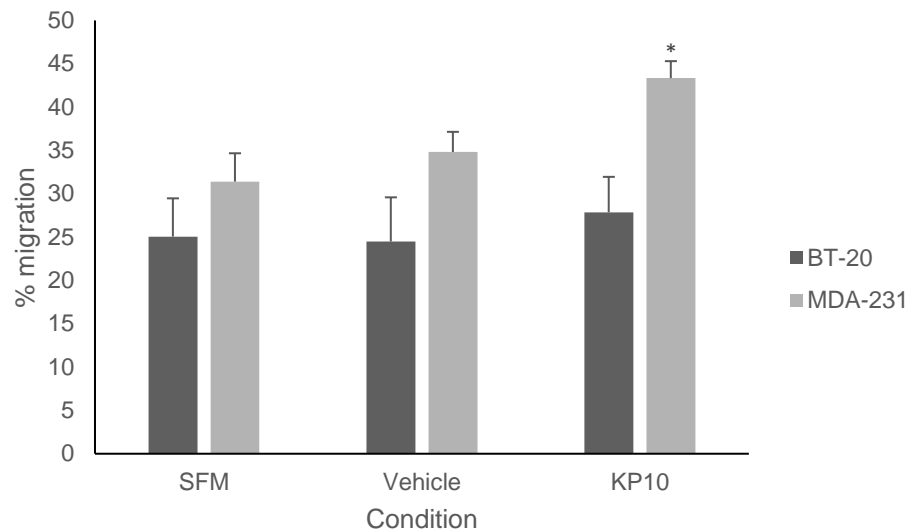
Figure 3.21: KP-10 increases the migration of MDA-MB-231 but not BT-20 cells under serum free culture condition.

Scratches were created on BT-20 and MDA-MB-231 cells grown to confluence and either untreated (serum free media only) or treated for 18 h with vehicle control (PG) or 100 nM KP-10 under serum free culture conditions. Images of the scratches were taken on the day of treatment (day 0) and 18 h after treatment using the Zeiss Axiovert inverted microscope.  Quantification of the relative migration of BT-20 and MDA-MB-231 cells either untreated (serum free media only) or treated with vehicle control (PG) or 100 nM KP-10 serum free (SF) culture conditions. Data represents mean of the percentage migration for 3 independent repeats and the error bars are ± SEM.  Statistical significance was determined by student's Unpaired T-test between media only control and each treatment. *p value ≤ 0.05.

3.12 <u>Endogenous KISS1R activated by Kisspeptin-10 has no significant impact on the growth of BT-20 cells in 3D culture.</u>

In order to determine the ability of the endogenous KISS1R in BT-20 cells activated by kisspeptin (KP-10) to promote or inhibit cancer growth, we examined the effect of KP-10 on the growth of BT-20 cells cultured in 3D as spheroids. BT-20 cells were grown in 3D culture as spheroids and were treated with either 100 nM KP-10 or propylene glycol. BT-20 cells in suspension were seeded at a density of 20 000 cells/well onto agarose in 96 well tissue culture plates and incubated at $37^0C$ in a humidified incubator with 5% $CO_2$ for 7 days to enable them form aggregates or spheroids. Afterwards, they were treated with either 100 nM KP-10 or 0.2% propylene glycol. Untreated or media only controls were included. The experiment was repeated 3 times independently and each repeat had at least 8 replicates per treatment. The spheroids were incubated for a total of 14 days. Images of the spheroids on the day of treatment (day 0) and on days, 4, 7, 11 and 14 after treatment were taken using the Axiovert Inverted microscope (Zeiss, Germany), as shown in Figure 3.22A. The area of the spheroid was measured using ImageJ software and the average of each treatment condition was used to plot a growth curve (Figure 3.22B). Our result (Figure 3.22B) showed that after 7 days of treatment, there was a slight increase in size of the spheroids treated with KP-10, compared with the untreated and vehicle treated controls. However, the increase was not statistically significant ($p > 0.05$). Based on this data, we conclude that KP-10 has no effect on the proliferation of BT-20 cells grown in 3D as spheroids.

A

|  | Medium | Vehicle | KP-10 |
|---|---|---|---|
| 0 d | | | |
| 4 d | | | |
| 7 d | | | |
| 11 d | | | |
| 14 d | | | |

B

BT20 spheroid growth
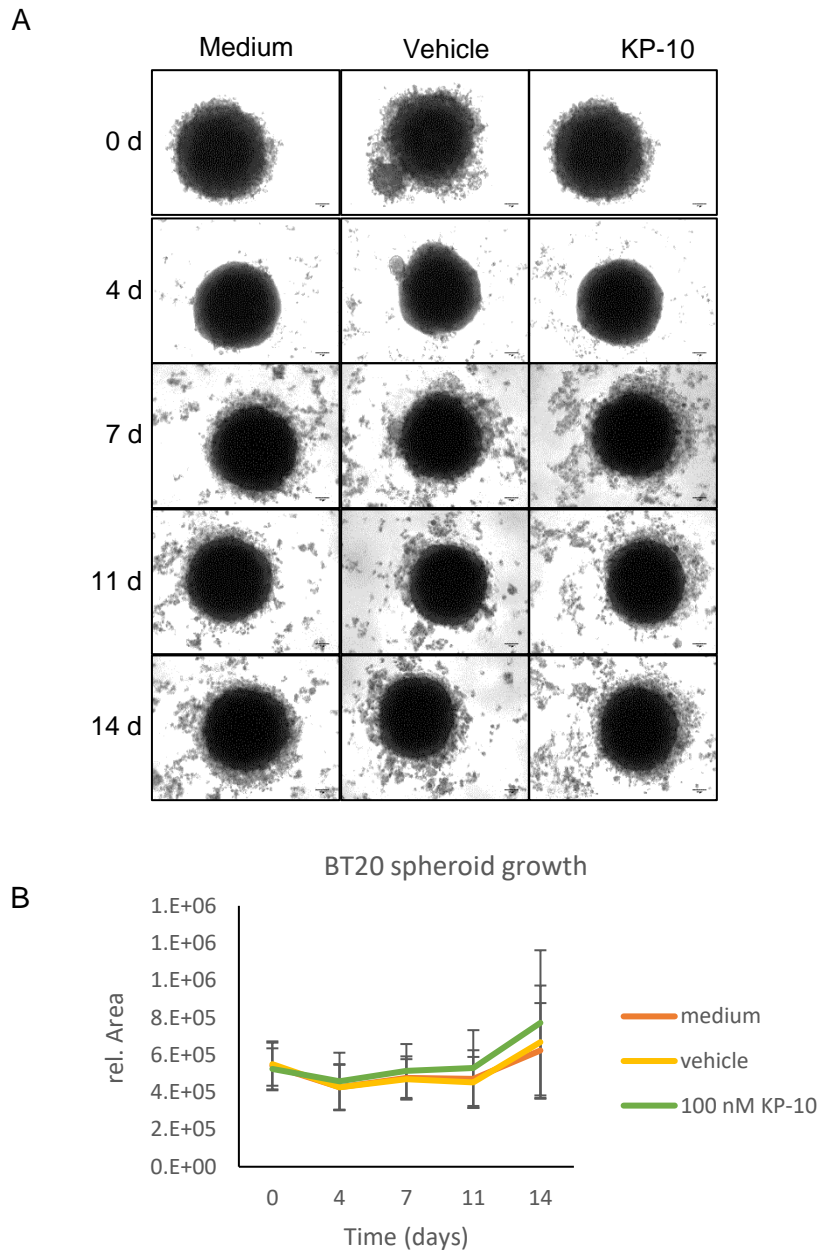


Figure 3.22: KP-10 has no significant effect on the growth of BT-20 cells in 3 D culture.

(A) Representative Differential Interference Contrast (DIC) microscopy Images of the spheroids taken on the day of treatment (day 0) and on days 4, 7, 11, and 14, post treatment with either KP-10 or the vehicle control (PG) using the Axiovert inverted microscope (Zeiss, Germany). (B) Growth curve showing the total area of spheroids that were untreated or treated with either 100 nM KP-10 or the vehicle control (propylene glycol). Statistical significance was determined by performing an Unpaired Student's T test to compare the media only and KP-10 treated cells. $p > 0.05$ Data show the mean of 3 independent repeats and the Error bars represent SEM. Scale = 100 μm.

3.13 <u>A non-synonymous mutation was found in the endogenous *KISS1R* in BT-20 and MDA-MB-231 cell lines.</u>

Our previous data showed that KISS1R activation by KP-10 results in late ERK1/2 response in the BT-20 cells. Whereas in the MDA-MB-231 cells, KISS1R activation by KP-10 does not cause an ERK response. Therefore, we decided to assess the *KISS1R* gene in both cell lines to check for possible mutations that might be responsible for the late ERK1/2 response in BT-20 and lack of ERK1/2 response in MDA-MB-231 cells. We examined the DNA sequence of the last exon of *KISS1R* in the BT-20 and MDA-MB-231 cell lines by Sanger sequencing. We were particularly interested in the last exon, exon 5, because our antibody targets the last 10 amino acids of the KISS1R protein. PCR primers were designed to amplify and sequence the last exon of the KISS1R gene in both cell lines. A forward primer flanking intron 4 and a reverse primer targeting the 3' untranslated region (UTR) were used. Genomic DNA was extracted from both cell lines and conventional polymerase chain reaction (PCR) amplification was performed using these primers. The amplified PCR fragments were examined by electrophoresis on a 1% agarose gel. The gel image is shown in Figure 23. The PCR product length was about 645 base pairs (bp). The PCR products were purified using a PCR clean-up kit, following the manufacturer's protocol. The purified PCR fragments were sequenced directly using the BigDye Terminator V3.1 cycle sequencing kit (Applied Biosystems, Foster city, CA, USA), following the manufacturers protocol. Sanger sequencing was performed using both the forward and the reverse primers with the ABI3500xl genetic Analyzer instrument (Applied Biosystems). The Sanger sequencing results were analysed using CLC Main Workbench version 8.1 (QIAGEN, Aarhus, Denmark). The contigs from the Sanger sequencing were assembled to create consensus sequences for BT-20 (Figure 24A) and MDA-MB-231 (Figure 25A). The consensus sequences were aligned to the last exon of the *KISS1R* gene (Figure 24B and 25B). In both cell lines, a *KISS1R* variant was identified which was characterized by a c.1091T>A in exon 5, resulting in the substitution of leucine to histidine (p.L364H) in the C-terminus or cytoplasmic tail of the receptor (Figure 26).

Therefore, our data shows that the same mutation is present in the cytoplasmic tail of both cell lines. This suggests that the difference in ERK1/2 response between both cell

lines might not be due to a mutation found in one cell line that is not found in the other. However, the other 4 exons require sequencing in order to make a firm conclusion.
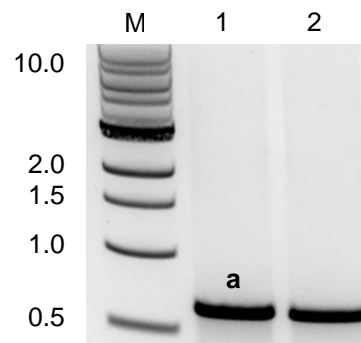


Figure 3.23: Agarose gel electrophoresis of PCR reaction product.

The PCR products were purified using a PCR clean-up kit and analysed by electrophoresis on a 1% agarose gel. The band marked "a" is 645 bp in length. Lane M is the DNA Molecular ladder in Kb, Lane 1 is BT-20, Lane 2 is MDA-MB-231.
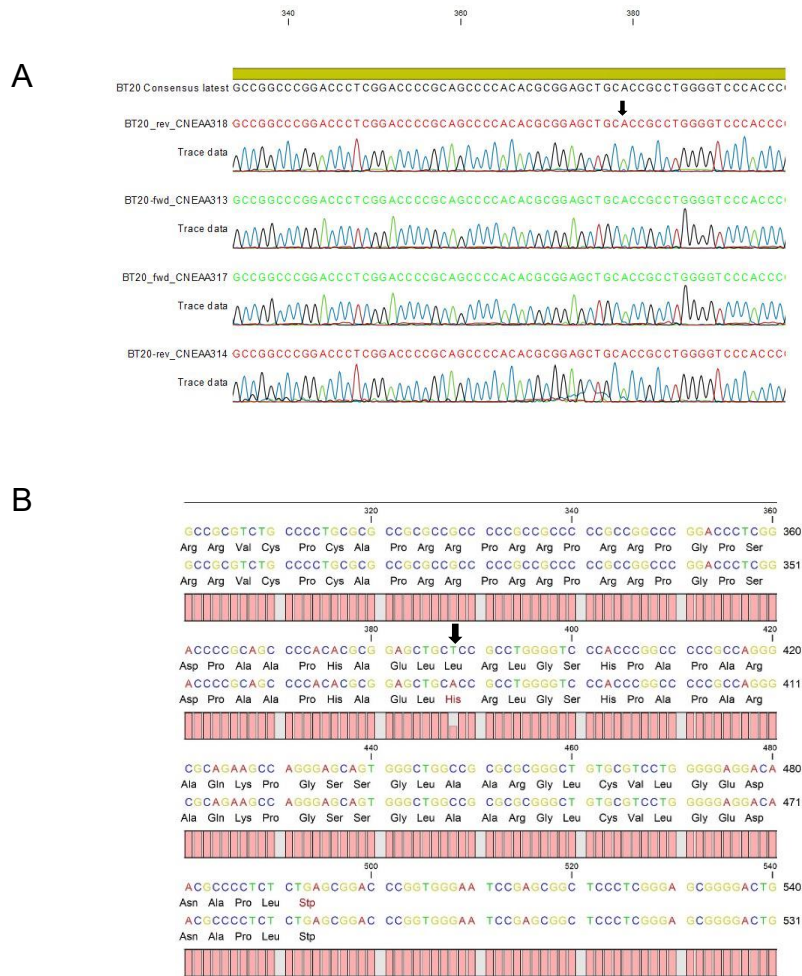
Figure 3.24: A non-synonymous mutation was detected in BT-20 cell line, which led to an amino acid change from leucine to histidine.

The BT-20 PCR product was sequenced using the forward and reverse primers used for PCR. (A) BT-20 contigs assembled to create a consensus sequence. (B) BT-20 consensus sequence aligned to the exon 5 region of the Human *KISS1R*.

Figure 3.25: A non-synonymous mutation was detected in MDA-MB-231 cell lines, which led to an amino acid change from leucine to histidine.

The MDA-MB-231 PCR product was sequenced using the forward and reverse primers used for PCR. (A) MDA-MB-231 contigs assembled to create a consensus sequence. (B) MDA-MB-231 consensus sequence aligned to the exon 5 region of the Human *KISS1R*.

L364H
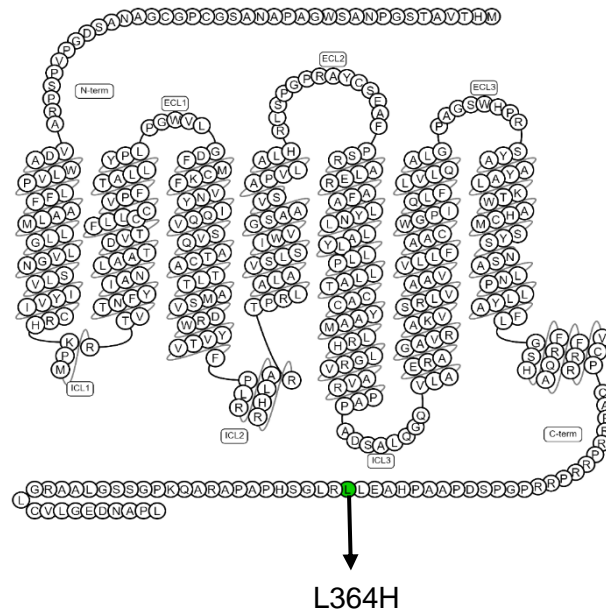
Figure 3.26: The mutation detected on the endogenous *KISS1R* was on the cytoplasmic tail of the receptor.

This mutation was detected in the C-terminal tail of the receptor (highlighted in green) of BT-20 and MDA-MB-231 and it caused an amino acid change from leucine to histidine at position 364. A snake structure of KISS1R showing the 7 transmembrane regions, with the extracellular N-terminus and the intracellular C-terminus. The transmembrane sequence was obtained from the GPCR database (https://gpcrdb.org/protein/kissr_human/). The arrow shows the location of the mutation.

.

# CHAPTER 4 DISCUSSION

KISS1R is the endogenous receptor of the metastasis suppressor gene, *KISS1*. *KISS1* codes for the neuropeptide kisspeptin.[66] *KISS1* expression has been shown to be lost during metastasis in melanoma [73], pancreatic [91], non-small cell lung [106] and gastric cancers.[107] The loss of *KISS1* and *KISS1R* in these cancers have been linked to an increase in migration and invasion. However, in breast cancer many studies [96,97,104] have shown that KISS1 and KISS1R protein expression are elevated compared to normal or non-malignant breast tissues and the high expression levels correlate with an increase in migration and invasion, which are parameters of metastasis. In fact, in a study by Marot *et al* (2007)[100], it was shown that the high expression of *KISS1R* mRNA in oestrogen receptor negative breast cancer patients, correlated with worse prognosis. This insinuates that KISS1R plays a pro-metastatic role in breast cancer, while in other cancers it plays an anti-metastatic role. The reason for the contradictory role of KISS1R in breast cancer has not been fully elucidated. Therefore, this project aimed to give insight into the mechanism through which KISS1R increases or decreases metastasis in breast cancer. Also, in most of the studies where KISS1R was shown to increase breast cancer cell migration and invasion, KISS1R was exogenously expressed. Therefore, we sought to determine if the endogenously expressed receptor will have the same effect as the exogenously expressed receptor.

We began this study by assessing the expression of endogenous KISS1R protein in three breast cancer cell lines: MCF7, MDA-MB-231 and BT-20. These cell lines were chosen based on their unique migratory potential and hormone receptor status. MCF7 is an oestrogen receptor positive and progesterone receptor positive breast cancer cell line that is non-invasive, lowly aggressive and migratory. [108,109] MDA-MB-231 is a triple-negative breast cancer cell line that is aggressive and metastatic.[109] The BT-20 was the first breast cancer cell line to be established in 1958.[110] It is a triple-negative cell line that is non-metastatic.[109,111] Our result showed that endogenous KISS1R protein was differentially expressed in these 3 breast cancer cell lines and the expression levels correlated with the migratory potential of the cells. The non-migratory, non-aggressive triple-negative breast cancer cell line, BT-20, had the highest expression compared to the metastatic, aggressive, triple-negative breast cancer cell line, MDA-MB-231, and oestrogen receptor positive, migratory breast cancer cell line, MCF7, which both expressed relatively low

levels of the receptor. Our data suggests that the high expression of KISS1R is not correlated with enhanced cell migration. Previous studies have shown that MCF7 and MDA-MB-231 express endogenous KISS1R protein.[97,104,112] Our study was the first to show the expression of endogenous KISS1R protein in the BT-20 cell line. However, our result contrasts with the mRNA expression level shown by Marot *et al.* 2007. In a study by Marot *et al.* 2007 [100], it was shown that at mRNA level, MCF7 express *KISS1R* at a low level compared to the placenta while MDA-MB-231 do not express *KISS1R* mRNA. This indicates that there is a contrast between *KISS1R* mRNA and protein expression levels in these 3 cell lines.

In order to determine the specificity of the bands detected in the breast cancer cell lines, we transfected HEK293 cells with either FLAG-KISS1R or empty pcDNA as positive and negative controls, respectively. Our antibody detected a 47 kD KISS1R in both the FLAG-KISS1R and empty pcDNA, but the band intensity was stronger in the FLAG-KISS1R transfected cells compared to the pcDNA transfected cells. Also, apart from the 47 kD band, a 43 kD protein was detected in the FLAG-KISS1R transfected cells. The 43 kD corresponds to the predicted size of the KISS1R protein based on its amino acid sequence. The presence of the 47 kD band in the empty HEK293 cells transfected with empty pcDNA suggests that HEK293 cells could have endogenous KISS1R. A study by Pampillo *et al.* 2009 [113], showed that HEK293 cells express endogenous KISS1R. Therefore, it is possible that the size of the endogenous KISS1R protein is slightly larger than the size of the overexpressed KISS1R protein. It is also possible that the endogenous KISS1R has undergone some post-translational modifications such as glycosylation. Therefore, we tested the glycosylation status of the endogenous KISS1R in the BT-20 cells. We chose the BT-20 cells because the level of endogenous KISS1R expressed in them was higher than the other cell line.

Before testing the glycosylation status of KISS1R in the BT-20 cells, we evaluated other non-breast cancer cell lines that have been previously shown to express endogenous KISS1R. This was to confirm that the 47 kD protein detected in the breast cancer cells was also present in these cell lines. Therefore, we assessed the expression of KISS1R in the 3 breast cancer cell lines, HepG2, which is a human hepatocellular carcinoma cell

line, and GT1-7, which is a mouse GnRH secreting neuronal cell line. Our antibody detected the 47 kD protein in the HepG2 cells as well as in the 3 breast cancer cells. The 47 kD band was detected in the 4 cell lines at different levels, the BT-20 and HepG2 cell lines expressed more KISS1R than the MCF7 and MDA-MB-231 cell lines. The presence of the 47 kD protein in hepatocellular cancer cell line, suggests that the 47 kD band is genuine. Although it was not as visible as the previous result, the 120 kD band was only detected in BT-20 cells. Interestingly, the expression of KISS1R protein in the HepG2 cell line, corresponds to the *KISS1R* mRNA expression in the Cancer Cell Line Encyclopedia, where it was shown that HepG2 express *KISS1R* mRNA with an expression level of 2.2600. In the GT1-7 cell line, no visible 47 kD protein was detected. This result is contrary to the study by Novaira *et al.* 2009 [114], where it was shown that GT1-7 cells express KISS1R protein. One possible explanation for the variation in the expression of KISS1R protein in GT1-7 in our study and theirs could be a difference in our antibody epitope. They may have used a commercially available KISS1R antibody, while we used an in-house KISS1R antibody produced by Professor Millar. Our KISS1R antibody epitope is the last 10 amino acids in the human KISS1R protein, as shown in Figure 2.1. The amino acid sequence of the last 10 amino acids of the human KISS1R protein is; CVLGEDNAPL, while the last 10 amino acid sequence of the mouse KISS1R is CAQSERTASL.[66] They are 60% different from each other. This could be a possible reason why there was no visible 47 kD band detected in the GT1-7 cells. This also confirms that the 72 and 100 kD bands detected on the blot are non-specific since they were also detected in the GT1-7 cell line.

The Human KISS1R protein is 398 amino acids long [79] with a predicted molecular weight of 43 kD, the KISS1R protein that was detected in the breast cancer cell lines as well as the HepG2 cells was about 47 kD. Also, apart from the 47 kD protein, a 120 kD protein was detected in only the BT-20 cell line. This led us to hypothesize that the large protein size and the difference between the predicted and the detected protein was due to post-translational modification. The most common post-translational modification undergone by GPCRs is glycosylation. Glycosylation is necessary for GPCRs to mature and be transported to the plasma membrane. When a cell surface receptor is synthesized in the endoplasmic reticulum, it is converted to the mature protein in the Golgi apparatus.[115]

During this maturation, high mannose glycans such as N-linked oligosacharides and O-linked glycans, containing N-acetylgalactosamine, as well as galactose and sialic acid are added to the receptor. Thereafter, this mature receptor is transported to the plasma membrane.[115] Since KISS1R has been shown to have 3 N-linked glycosylation sites on its N-termini,[79] we evaluated the glycosylation status of the KISS1R in BT-20 cell line using the glycosidase enzymes, endoglycosidase H (Endo H) and Peptide:N-glycosidase F (PNGase F), as well as the antibiotic, Tunicamycin. The reason we used 2 different enzymes is to ensure the complete deglycosylation of the protein since Endo H cleaves only high mannose oligosaccharides, while PNGase F cleaves all types of N-linked glycan oligosaccharides.[115] On the other hand, tunicamycin is an antibiotic that stops the synthesis of N-linked glycoproteins.[116] Our data showed that compared to the non-enzyme treated (mock) and untreated controls, there was no reduction in the size of either the 47 kD or 120 kD protein in BT-20 cells, after treatment with either the antibiotic or the glycosidase enzymes.

In a subsequent experiment, we included a positive control, which was another GPCR that has been shown to be glycosylated. Unpublished data generated in the Centre for Neuroendocrinology have shown that the HA-tagged-NK3 receptor is glycosylated and they have proven that this receptor can be deglycosylated using the glycosidase enzymes, Endo H and PNGase F. Therefore, we overexpressed HA-tagged-NK3R in HEK293 cells and deglycosylated them simultaneously with BT-20 cells expressing endogenous KISS1R. In HEK293 cells with overexpressed HA-tagged-NK3 receptor, the Endo H and PNGase F enzyme treated samples yielded 2 bands that were reduced in molecular size, one of them was 52 kD, representing the predicted molecular size of unglycosylated NK3R and the other one was at 63 kD, representing the part that retained the Endo H and PNGase F resistant carbohydrates that are normally present in the HA tag. However, in the BT-20 cells, there was no difference in the electrophoretic mobility of the enzyme treated lysates when compared to the untreated and mock control. This led us to conclude that the 4 kD difference between the predicted and the observed protein and the 120 kD protein in the BT-20 cells is not due to glycosylation. Apart from having 3 glycosylation sites, KISS1R has also been shown to have 3 possible palmitoylation sites on its carboxyl tail.[79] Therefore, one possible reason for the 5 kD

difference between the observed and predicted protein size and the large protein size in the BT-20 cells could be palmitoylation. This can be proven by performing a depalmitoylation experiment. Another possible explanation for the 120 kD protein detected in only the BT-20 cells could be a complex interaction between KISS1R and another protein. KISS1R has been shown to complex with epidermal growth factor receptor (EGFR), both in the absence and presence of its agonist, kisspeptin.[103] Although this explanation is reasonable it is likely not possible because the gel used was a denaturing gel, so both proteins should have separated during electrophoresis.

The localization of the receptor plays a role in cell signalling. Most GPCRs are localized to the plasma membrane when they are not exposed to their agonists.[117] However, they can also be found in other cellular compartments such as the Golgi apparatus, endosomes and endoplasmic reticulum.[117] Therefore, we assessed the localization of the overexpressed KISS1R in HEK293 cells and endogenous KISS1R in the BT-20 and MDA-MB-231 cells through confocal microscopy. Our data showed that in HEK293 cells transfected with exogenous KISS1R, a sub-population of cells showed no expression. The non-expressing cells were used as control to determine if the antibody only bound to KISS1R expressing cells. The KISS1R staining was only detected in the KISS1R expressing cells, while the non-expressing cells only had the DAPI staining. KISS1R was localized to the plasma membrane and intracellularly. This result is similar to that of Pampillo *et al*. 2009 [113], where they showed that in the absence of the agonist, FLAG-KISS1R expressed in HEK293 cells is localised to the plasma membrane and intracellularly. In future, co-localisation studies with a plasma membrane marker will have to be included in order to ascertain the localization of KISS1R on the plasma membrane. In the BT-20 and MDA-MB-231 cell lines, the antibodies were unable to detect the specific localization of endogenous KISS1R. This was because of the strong non-specific staining in the pre-immune serum negative control. The pre-immune serum is usually collected prior to antibody production, from the same rabbit in which the antibody is produced. One possible reason for the strong background staining in the pre-immune control could have been because maybe the animal used for antibody production had been exposed to another antigen. Sometimes, some antibody production companies reuse their animals if they did not get a good response to a previous immunogen.[118] One of the ways in which

the specificity of the antibody could have been improved is by purifying both the actual antibody and the pre-immune serum with Protein A or Protein G. Another method would be by purifying the pre-immune and the actual antibody by affinity chromatography. The antibody or pre-immune control purified by affinity chromatography is usually highly specific.[118]

Therefore, our antibody was only able to detect specific staining in the exogenous KISS1R in the HEK293 cells, and not the endogenous KISS1R in the BT-20 and MDA-MB-231 cells. It is possible that the difference in staining is because the antibody can only detect the localization of the exogenous KISS1R and not the endogenous one.

We performed a functional assay by assessing ERK1/2 phosphorylation in the BT-20 and MDA-MB-231 cells. ERK1/2 are members of the MAPKs that are activated by different extracellular stimuli such as hormones, growth factors and stress, as well as GPCR agonists.[119] Our serum media contains 10% FBS, which is a growth factor used in cell culture that consist of hormones, growth factors, vitamins and trace elements.[120] These components are necessary for cell proliferation and maintenance.[120] Growth factors activate ERK1/2 through the tyrosine kinase receptor.[121] Therefore, we assessed the mechanism of ERK1/2 phosphorylation in the BT-20 and MDA-MB-231 cell lines by stimulating both cell lines with serum media at different time points. The western blot data showed that ERK1/2 was phosphorylated in both cell lines after 5 min of stimulation with serum media. However, there was a difference in the pattern of ERK1/2 phosphorylation in both cell lines. In the BT-20 cell line, there was maximal ERK1/2 phosphorylation at 5 min, and it levelled off at 45 min and returned to basal level. In the MDA-MB-231 cell line, there was maximal ERK1/2 phosphorylation at 5 min, and it levelled off after 30 min of stimulation and it decreased below basal level from 30 min. Therefore, in both the BT-20 and MDA-MB-231 cells, ERK1/2 is phosphorylated with a maximal activation at 5 min.

As mentioned earlier, ERK1/2 is also activated by some GPCR agonists. When G-protein coupled receptors are activated by their agonists, they activate ERK1/2, either through a G-protein dependent or a β-arrestin dependent pathway. During ERK1/2 activation through the G-protein dependent pathway, molecules such as protein kinase A and C (PKA and PKC) are activated. This leads to the phosphorylation of mitogen activated

protein kinase molecule, Raf-1, which in turn phosphorylates MEK1 and this results in G-protein dependent ERK1/2 phosphorylation.[64,102] The G-protein dependent ERK1/2 activation is rapid and transient and it peaks between 2 to 10 min.[102] While in the β-arrestin dependent pathway, β-arrestin acts as a scaffold for the MAPK molecules; Raf-1 and MEK1, which in turn activate ERK1/2. β-arrestin 1 inhibits ERK while β-arrestin 2 activates ERK.[102] The β-arrestin dependent ERK is slow and persistent and it can last for more than 1 hour.[102] KISS1R is a G-protein coupled receptor and it couples to the $G\alpha_{q/11}$ pathway. Its activation by kisspeptin results in the hydrolysis of PIP2 to IP3 and diacylglycerol, calcium mobilization, and ERK1/2 and p38 MAPK phosphorylation.[102] Therefore, we assessed the ability of exogenous KISS1R to activate ERK in HEK293 cells with overexpressed KISS1R, after stimulating them with KP-10 at different time points. As a negative control, we also transfected some of the cells with pLKO vector instead of KISS1R and stimulated them with KP-10 . In our western blot data, bands were only detected in the KISS1R transfected cells and not the pLKO transfected cells. This means that the bands detected in the KISS1R transfected cells were solely due to the presence of KISS1R in the HEK293 cells. Our data also showed that relative to the untreated control, there was maximal ERK1/2 phosphorylation in the HEK293 cells overexpressing KISS1R after 5 min of stimulation and a decrease at 30 min and 60 min, but it never returned to unstimulated level. This result is similar to the result in a study by Szereszewski *et al* 2010 [102], where it was shown that when wild type KISS1R was exogenously expressed in MEF cell lines, there was maximal ERK phosphorylation at 5 min. Our result shows that in HEK293 cells transiently transfected with FLAG-KISS1R, KISS1R activates ERK1/2 phosphorylation in a G-protein dependent manner. Previous studies [76,102] have shown that kisspeptin/KISS1R signalling activates ERK1/2 in a G-protein dependent and β-arrestin dependent manner.

Since our previous data showed that the ERK1/2 pathway is functional in the BT-20 and MDA-MB-231 cell lines, we assessed the activation of ERK1/2 by the endogenous KISS1R in these cell lines, after stimulation with KP-10 at different time points. Our data showed that in the BT-20 cell line, compared with the unstimulated control, there was a less than 1 fold increase in ERK1/2 phosphorylation at 5 and 10 min and it decreased at 30 min, with a robust increase at 45 and 60 min. The increase at 5, 45 and 60 min were

statistically significant (p<0.05). This suggests that the activation of the endogenous KISS1R in the BT-20 cells results in both acute and prolonged activation of intracellular signalling pathways. This also suggests that KISS1R can activate ERK1/2 in both a G-protein dependent and a G-protein independent or β-arrestin dependent manner, in the BT-20 cell line. This can be proven by knocking down or inhibiting β-arrestin and assessing ERK1/2 phosphorylation thereafter. In contrast, in the MDA-MB-231 cell line, KISS1R did not activate ERK1/2 phosphorylation. Several known and unknown mechanisms could be responsible for the difference in the ERK1/2 activation in both cell lines. One possible explanation for the increase in ERK1/2 phosphorylation in the BT-20 and the no ERK1/2 phosphorylation in MDA-MB-231 cells, could be due to the difference in the level of KISS1R expressed in both cell lines.

A study by Pampillo *et al* 2009 [113], showed that in the MDA-MB-231 cell line, KISS1R can only activate ERK1/2 in MDA-MB-231 cells when β-arrestin 1/2 is present. Therefore, we assessed the expression of endogenous β-arrestin 1/2 proteins in both cell lines.  Our result showed that the BT-20 expressed 4 times more β-arrestin 1/2 than the MDA-MB-231 cells. This suggests that another reason we saw a decrease in ERK1/2 phosphorylation could be due to low levels of β-arrestin 1/2 in the MDA-MB-231 cells. Therefore, the difference in the level of β-arrestin 1/2 expressed in both cell lines could have been one of the reasons why we saw a prolonged ERK1/2 activation in BT-20 cells and no ERK1/2 activation in the MDA-MB-231 cell. β-arrestin1 and 2 regulate the internalization and desensitization of GPCRs, and they act as scaffold proteins for the ERK signalling pathway.[102,113] Also, perhaps the reason we saw a prolonged increase in ERK1/2 activation in the BT-20 cells was because they express β-arrestin 1/2 at high levels. Since β-arrestin 1 has been shown to inhibit ERK1/2 while β-arrestin 2 has been shown to activate ERK1/2[102], we assessed the isoform of  β-arrestin1/2 that is expressed in both cell lines. Our data showed that only β-arrestin 1 was present in both cell lines. Our antibody was unable to detect β-arrestin 2 in both cell lines. This could be a possible explanation as to why ERK1/2 was not activated in the MDA-MB-231 cells, since in a study by Pampillo *et al*. 2009 [113], it was shown that β-arrestin 2 is the isoform that is needed to activate ERK1/2 in MDA-MB-231 cells. This data also suggests that in BT-20, the β-arrestin 1 isoform might be the isoform required to activate ERK1/2. The effect of

β-arrestin 1 and 2 on ERK1/2 phosphorylation can be proven by knocking down the β-arrestin 1/2 in the BT-20 cell line and repeating the time course assay to assess if there will still be ERK1/2 activation after 45 and 60 min of stimulation with KP-10. Alternatively, the β-arrestin 1 and 2 inhibitor, Barbadin, can be used to block β-arrestin 1 and 2 activity.

The only study where ERK1/2 phosphorylation was observed after 60 min of stimulating KISS1R expressing cells with kisspeptin was in a patient with a mutation in the cytoplasmic tail of KISS1R. This mutation was a missense mutation that resulted in an amino acid change from arginine to proline, at amino acid position 386 and it was associated with central precocious puberty.[122] In that study it was shown that the mutated receptor remained on the plasma membrane after a long time of exposure to kisspeptin compared to the wild-type receptor, and it was suggested that the mutation resulted in a decrease in the rate of receptor internalization and degradation.

Our data so far has shown that apart from the difference in the molecular size, there is also a difference in the way the exogenous KISS1R in HEK293 cells and the endogenous KISS1R in the BT-20 cells activate ERK1/2. ERK1/2 activation by the endogenous KISS1R in the BT-20 cells appears to be mediated through both G-protein dependent and G-protein independent pathways, with the G-protein independent pathway being the most robust. Whereas in HEK293 cells with overexpressed KISS1R, ERK1/2 is activated only through the G-protein dependent pathway. This suggests that there might be a bias in the way kisspeptin activates the endogenous and exogenous receptor. We can conclude that there is a tissue bias, as endogenous KISS1R in the BT-20 and MDA-MB-231 cells differ in their ability to activate ERK1/2.

We performed another study to determine the effect of endogenous KISS1R on ERK1/2 phosphorylation in BT-20 and MDA-MB-231 cells stimulated with varying concentrations of KP-10 for 5 min. We chose 5 min because our data showed that when both cell lines were stimulated with serum media, they activated ERK1/2 at 5 min. So, we assumed that the reason we did not see a robust increase in ERK1/2 at 5 min when the cells were stimulated with KP-10 at different time points was because we used 100 nM KP-10. Therefore, we stimulated both cell lines with varying concentrations of KP-10 for 5 min. Our data showed that in the BT-20 cell line, increasing the concentration had no effect on

ERK1/2 phosphorylation. The experiment was repeated 2 times independently. In the MDA-MB-231 cell line, there was no effect in ERK1/2 phosphorylation at the different concentrations. Therefore, we conclude that the ERK1/2 pathway may not be functional in the MDA-MB-231 cells stimulated with KP-10 . Perhaps if 1 or 2 more repeats were included, the data would have been statistically significant.  In a study by Szereszewski et al. 2010 [102], it was shown that with 10 nM kisspeptin, ERK1/2 was activated in MEF cell lines transfected with KISS1R, after stimulating for 10 min. Also, maybe if the cells were stimulated with the different concentrations for 10 min, a significant result could have been obtained at one of the concentrations.

According to the time course assay, there was a significant increase in ERK1/2 in BT-20 cells when they were stimulated with 100 nM KP-10 for 60 min. Therefore, we repeated the experiment to determine the effect of KP-10 concentration on ERK1/2 activation, by stimulating the BT-20 and MDA-MB-231 cells for 60 min with varying concentrations of KP-10. Our result showed that in the BT-20 cell line, there was no increase in ERK1/2 phosphorylation levels with 1 nM kisspeptin. But with 10 nM, 100 nM, 1 μM and 10 μM KP-10 , there was an increase in ERK1/2 phosphorylation levels. However, none of the increase in ERK1/2 phosphorylation were statistically significant. This could have been because after the first repeat, an older batch of kisspeptin peptide was used for the next 2 repeats. Perhaps the ligand was degraded. This can be proven by repeating the same experiment using a new or fresh batch of KP-10. In the MDA-MB-231 cell line, relative to the vehicle treated control, there was no increase in ERK1/2 phosphorylation as the concentration of KP-10 increased. Although there was a slight increase with 100 nM KP-10, but the increase was not statistically significant. In summary, the level of ERK1/2 activation was still higher in the BT-20 cell lines, compared to the MDA-MB-231 cell line.

Our data suggests that the endogenous KISS1R in the MDA-MB-231 cell line may not activate ERK1/2. Apart from ERK1/2 activation, KISS1R activation by kisspeptin also leads to the stimulation of inositol-1,4,5-triphosphate, calcium mobilization and arachidonic acid release.[66,76] Therefore, these other pathways can be tested in the BT-20 and MDA-MB-231 cell lines.

So far, we have established that the 3 breast cancer cell lines used in our study express endogenous KISS1R. Also, the activation of endogenous KISS1R in the BT-20 cell line activates ERK in a G-protein independent or β-arrestin dependent manner, while in the MDA-MB-231 cells, it has no effect on ERK phosphorylation. This means that the endogenous KISS1R in the MDA-MB-231 cell might be either inactive or it might be activating another pathway. We went further to assess the effect of the endogenous KISS1R activated by KP-10 on the proliferation and migration of the BT-20 and MDA-MB-231 cells. We performed our assay with 100 nM because most studies [96,97,102–104] on kisspeptin/KISS1R signalling were performed using 100 nM KP-10.

We performed a proliferation assay on the BT-20 and MDA-MB-231 cell lines, in order to determine how KP-10 affects the proliferation of cells that express endogenous KISS1R. Our data showed that both under normal and serum free culture conditions, KP-10 had no effect on cell proliferation. Our data is similar to that of Ziegler *et al*. 2013 [123], where it was shown that in MDA-MB-231 cells expressing endogenous KISS1R , KP-10 had no effect on proliferation. In that study, it was shown that the anti-proliferative role of KISS1R depends on the status of the receptor. KISS1R decreased proliferation in MDA-MB-231 cells when it was overexpressed in the cell lines. While in the cells with endogenous KISS1R, KP-10 had no effect on proliferation. Perhaps the reason we did not see any effect on cell proliferation was because we were assessing the endogenous receptor.

Cancer cells become metastatic when cells undergo epithelial-to-mesenchymal transition and acquire the ability to migrate and invade surrounding tissues.[96] One of the ways in which kisspeptin has been shown to suppress metastasis in colorectal and other cancers is by inhibiting cell migration.[86,90,106,124] Therefore, we sought to determine if the activation of KISS1R by KP-10 affects BT-20 and MDA-MB-231 cell migration. Our data showed that under normal serum conditions, KP-10 had no effect on the migration of BT-20 and MDA-MB-231 cells that express the endogenous receptor. However, when the cells were treated under serum free culture conditions, there was an increase in the migration of the KP-10 treated MDA-MB-231 cells, compared to the vehicle treated and untreated cells. There was no impact on the migration of BT-20 cells. Our previous data showed that KP-10 had no effect on the proliferation of MDA-MB-231 cells under serum free culture

conditions. Therefore, this excludes the possibility that the increase in migration was due to an increase in proliferation. Our result is contrary to the result from Cvetkovic *et al.* 2013 [104], where it was shown that under normal culture conditions, 10% serum media, there was an increase in the migration of MDA-MB-231 cells treated with either 10 nM or 100 nM KP-10. Their study was performed under normal culture conditions. In our study, we only saw an increase in migration when the serum was removed. A possible explanation for the difference in migration in the presence and absence of serum could be that the serum might have other compounds that could be interfering or competing with kisspeptin. The study was done for 18 h because it was observed that at 24 h, the gaps were completely closed for the MDA-MB-231 cell lines. Therefore, our data show that although the KISS1R in the MDA-MB-231 cells does not activate ERK, when treated with KP-10 under serum free conditions, migration was increased. This suggests that the endogenous KISS1R in the MDA-MB-231 cells does not activate ERK1/2 when stimulated with KP-10 but activates other downstream signalling pathways.

We also assessed the effect of KISS1R activation by KP-10 on the growth of BT-20 cells grown in 3D as spheroids. Spheroids are cells grown as aggregates so that the cells are in close contact with each other, grow in a way that stimulates the synthesis of extracellular matrix proteins and encourage cell-to cell-communication.[125] With this 3D spheroid model, tumour growth mimics the microenvironment of the solid tumours in vivo. Since spheroids are better representatives of what happens in vivo [125], we assessed how the growth of BT-20 cells in 3D spheroids can be affected by KP-10 treatment. Our result showed that there was a slight increase in the growth of the cells treated with KP-10, relative to the vehicle (propylene glycol) treated and untreated controls. However, the increase was not significant. This suggests that KP-10 may not have any significant effect on the growth of breast cancer cells expressing endogenous KISS1R.

Our data on the ERK1/2 phosphorylation time course assay showed that ERK1/2 was phosphorylated for a prolonged period in the BT-20 cells. Whereas in the MDA-MB-231 cells, there was no ERK1/2 phosphorylation. Therefore, we hypothesised that there might be a mutation in one or both cell lines that is causing a difference in ERK1/2 phosphorylation in both cell lines. Therefore, we sequenced the last exon of the *KISS1R*

in the BT-20 and MDA-MB-231, through Sanger sequencing. We chose the last exon because the epitope for the antibody that we used for western blotting is the last 10 amino acids of the receptor, which is on the last exon of the gene. Our data showed that in the exon 5 of both cell lines, there was a single base substitution at position 1091 of the *KISS1R* gene, that led to the substitution of a thymine for adenine (c. 1091T>A) in both cell lines, as well as an amino acid substitution of leucine for histidine at position 364 of the KISS1R protein (p.L364H), which is on the C terminal tail of the receptor. In a study by Teles *et al* (2010) [126], the L364H mutation was one of the mutations that was detected in the *KISS1R* gene of patients with isolated hypogonadotropic hypogonadism (IHH). In that study, IHH was defined as low levels of gonadotropins, sex steroids and the absence of other pituitary hormone deficiencies. It had a prevalence of 34.2% percent.[126] In another study by Semple *et al* 2005 [127], this mutation was also detected in 23% of the patients with hypogonadotropic hypogonadism. So far, no study has reported if this mutation influences the signalling of the receptor. Also, on NCBI, it was described as a benign mutation. Therefore, one possible future study that could be performed will be to introduce this mutation in the wild-type *KISS1R* that we have been overexpressing in the HEK293 cells, by site-directed mutagenesis. Then functional assay such as ERK1/2 phosphorylation and inositol-1, 3,5-triphosphate accumulation assay will be performed, in order to assess how this mutation affects signalling compared to the wild-type. Therefore, we conclude that the difference in ERK1/2 phosphorylation pattern in the BT-20 and MDA-MB-231 cells is not due to different *KISS1R* variants. However, in order to make a firm conclusion, we will need to sequence the remaining 4 exons or the entire gene, to ensure that there are no other nucleotide substitutions that could be affecting receptor activity.

CONCLUSION

In conclusion, our study has shown that KISS1R is expressed in the 3 breast cancer cell lines; BT20, MDA-MB-231 and MCF7, at different levels. The non-metastatic TNBC cell line, BT-20, expressed 10 times more KISS1R than the metastatic TNBC cell line, MDA-MB-231. This data suggests that a high KISS1R expression may not always mean an increase in metastatic behaviour in breast cancer. This can be proven further by analysing the expression of KISS1R protein in a large population of breast cancer patients and assessing how the stage or grade of the tumour correlates with KISS1R expression. Our data also showed that the KISS1R protein expressed in the BT20 cells activates ERK1/2 in a G-protein independent manner when stimulated with the KP-10. In contrast, the KISS1R in the MDA-MB-231 cells did not activate ERK1/2. This suggests that there is a tissue bias between BT20 and MDA-MB-231 cells. We suspect that the ERK1/2 phosphorylation in the BT-20 cells could be due to the high level of β-arrestin1/2 expressed in these cells. This can be proven by knocking down the β-arrestin1/2 and assessing its effect on ERK1/2 phosphorylation. We also propose that in future, other signalling pathways that are shown in Figure 1.3 to be activated by kisspeptin/KISS1R signalling such as phosphoinositide 3-kinase (PI3K)/AKT and focal adhesion kinase pathways, which have also been linked with metastasis, be assessed in these cell lines. Our data was unable to decipher the exact role of the endogenous KISS1R on breast cancer cell migration and proliferation.  Therefore, a possible future study would be to assess the effect of KISS1R on other parameters of metastasis such as anoikis, invasion and cell adherence. In a study by Goertzen *et al*. 2016 [96] it was shown that using shRNA to knockdown KISS1R in the MDA-MB-231 cell line reduced migration without affecting cell viability. Therefore, another possible future study would be to knockdown the KISS1R in the BT-20 cell and MDA-MB-231 cells and evaluating the effect of KISS1R knockdown on cell migration and proliferation. Finally, our data showed the presence of a non-synonymous mutation in the *KISS1R* in BT-20 and MDA-MB-231 cells. This mutation led to an amino acid change from leucine to histidine, in the cytoplasmic tail of the receptor. However, this mutation has not been shown to have any effect on the signalling.

# CHAPTER 5 REFERENCES

1. Ciaramella V, Maria C, Corte D, Ciardiello F. Kisspeptin and Cancer : Molecular interaction , Biological Functions , and Future Perspectives. Front Endocrinol (Lausanne). 2018;9(115):1–5.

2. Szereszewski JM, Pampillo M, Ahow MR, Offermanns S, Shirasaki F, Takata M, et al. Biological and Pharmacological Aspects of the NK1-Receptor. Shukla AK, editor. Nat Rev Cancer [Internet]. 1st ed. 2018;9(6):1–12. Available from: http://advances.nutrition.org/cgi/doi/10.3945/an.116.012211

3. Kunjumoideen K. History of cancer. Cancer Treat Res. 2005;154:19–31.

4. Lukong KE. Understanding breast cancer – The long and winding road. BBA Clin [Internet]. 2017;7:64–77. Available from: http://dx.doi.org/10.1016/j.bbacli.2017.01.001

5. Faguet GB. A brief history of cancer: Age-old milestones underlying our current knowledge database. Int J Cancer. 2015;136(9):2022–36.

6. Sudhakar A. History of Cancer, Ancient and Modern Treatment Methods. J Cancer Sci Ther. 2009;1(2):1–4.

7. Stewart BW WC. World Cancer Report 2014. Int Agency Res Cancer [Internet]. 2014;7(2):1–630. Available from: http://advances.nutrition.org/cgi/doi/10.3945/an.116.012211

8. Wang H, Naghavi M, Allen C, Barber RM, Carter A, Casey DC, et al. Global, regional, and national life expectancy, all-cause mortality, and cause-specific mortality for 249 causes of death, 1980–2015: a systematic analysis for the Global Burden of Disease Study 2015. Lancet. 2016;388(10053):1459–544.

9. Bray, F., Ferlay, J., Soerjomataram, I., Siegel, R. L., Torre, L. A., Jemal A. Global Cancer Statistics 2018: GLOBOCAN Estimates of Incidence and Mortality Worldwide for 36 Cancers in 185 Countries Freddie. CA Cancer J Clin. 2018;68(11):394–424.

10. National Cancer Institute. No Title [Internet]. What is cancer? 2015. Available from: https://www.cancer.gov/about-cancer/understanding/what-is-

cancer?fbclid=/wARO

11.    Vogelstein B, Kinzler KW. Cancer genes and the pathways they control. Nat Med. 2004;10(8):789–99.

12.    Liu X, Jakubowski M, Hunt JL. KRAS gene mutation in colorectal cancer is correlated with increased proliferation and spontaneous apoptosis. Am J Clin Pathol. 2011;135(2):245–52.

13.    Cooper G. The development and causes of Cancer. [Internet]. 2nd editio. Sunderland: Sinauer Associates; 2000. Available from: https://www.ncbi.nlm.nih.gov/books/NBK9963/

14.    Sinha T. Tumors: Benign and Malignant. Canc Ther Oncol Int J. 2018;10(3):1–3.

15.    Moses C, Garcia-bloj B, Harvey AR, Blancafort P. Hallmarks of cancer : The CRISPR generation. Eur J Cancer [Internet]. 2018;93:10–8. Available from: https://doi.org/10.1016/j.ejca.2018.01.002

16.    Hanahan, Douglas, Weinberg, Robert A. The Hallmarks of Cancer. Cell. 2000;100:57–70.

17.    Hanahan D, Robert A W. Biological Hallmarks of cancer. 9th ed. Robert C. Bast Jr., Carlo M. Croce, William N. Hait, Waun Ki Hong, Donald W. Kufe, Martine Piccart-Gebhart, Raphael E. Pollock, Ralph R. Weichselbaum, Hongyang Wang and JFH, editor. Holland-Frei cancer Medicine. John Wiley & Sons Inc.; 2017. 1–10 p.

18.    Polyak K. Heterogeneity in breast cancer. J Clin Invest. 2011;121(10):3786–8.

19.    Rayter Z. History of breast cancer therapy. Cambridge Univ Press.

20.    Koren S, Bentires-Alj M. Breast Tumor Heterogeneity: Source of Fitness, Hurdle for Therapy. Mol Cell [Internet]. 2015;60(4):537–46. Available from: http://dx.doi.org/10.1016/j.molcel.2015.10.031

21.    Redig AJ, Mcallister SS. Breast cancer as a systemic disease : a view of metastasis. J Intern Med. 2013;274:113–26.

22. Mørch LS, Skovlund CW, Hannaford PC, Iversen L, Fielding S, Lidegaard Ø. Contemporary hormonal contraception and the risk of breast cancer. N Engl J Med. 2017;377(23):2228–39.

23. Feng Y, Spezia M, Huang S, Liu B, Lei Y, Du S, et al. ScienceDirect Breast cancer development and progression : Risk factors , cancer stem cells , signaling pathways , genomics , and molecular pathogenesis. Genes Dis [Internet]. 2018;5(2):77–106. Available from: https://doi.org/10.1016/j.gendis.2018.05.001

24. Campa CM, Menéndez JM, González CA, González A, García VÁ, Cos S. What is known about melatonin , chemotherapy and altered gene expression in breast cancer ( Review ). 2017;2003–14.

25. Noonan MM, Dragan M, Mehta MM, Hess DA, Brackstone M, Tuck AB, et al. The matrix protein Fibulin-3 promotes KISS1R induced triple negative breast cancer cell invasion. 2018;9(53):30034–52.

26. Jin X, Mu P. Targeting Breast Cancer Metastasis. Breast Cancer Basic Clin Res. 2015;9(S1):23–34.

27. Eeden, RV, Rapoport B. Triple-negative breast cancer – the past , present and future : recent and emerging trends in immunotherapy. Breast Cancer Manag. 2016;5(1):1–5.

28. Kim S. New and emerging factors in tumorigenesis: An overview. Cancer Manag Res. 2015;7:225–39.

29. Perera RM, Bardeesy N. On oncogenes and tumor suppressor genes in the mammary gland. Cold Spring Harb Perspect Biol. 2012;4(6):1–3.

30. Barrette PH. The Works of Charles Darwin:Vol 16: On the Origin of Species [Internet]. Routlege; 2016. 92 p. Available from: https://books.google.co.za/books?id=1wU3DAAAQBAJ&pg=PA92&lpg=PA92&dq =It+has+been+proven+that+if+a+plot+of+ground+is+sown+with+one+species+of +grass,+and+a+similar+plot+of+ground+is+sown+with+several+distinct+genera+ of+grasses,+a+greater+number+of+plants+an

31.   Hector A, Hooper R. Darwin and the First Ecological Experiment. Science (80- ). 2012;295(2002):639.

32.   Guan X. Cancer metastases : challenges and opportunities. Acta Pharm Sin B. 2015;5(5):402–18.

33.   Seyfried, TN, Huysentruyt L. On the origin of cancer. Crit Rev Oncol Hematol. 2013;18(1–2):43–73.

34.   Su Z, Yang Z, Xu Y, Chen Y, Yu Q. Apoptosis, autophagy, necroptosis, and cancer metastasis. Mol Cancer. 2015;14(1):1–14.

35.   Drukteinis JS, Mooney BP, Flowers CI, Gatenby RA. Beyond mammography: New frontiers in breast cancer screening. Am J Med [Internet]. 2013;126(6):472–9. Available from: http://dx.doi.org/10.1016/j.amjmed.2012.11.025

36.   Patricia S. METASTASIS SUPPRESSORS ALTER THE SIGNAL TRANSDUCTION OF CANCER CELLS. Nat Rev Cancer. 2003;3:55–63.

37.   Langley RR, Fidler IJ. Interactions in Metastasis To Different Organs. Int J Cancer. 2012;128(11):2527–35.

38.   Geiger TR, Peeper DS. Metastasis mechanisms. BBA - Rev Cancer [Internet]. 2009;1796(2):293–308. Available from: http://www.sciencedirect.com/science/article/pii/S0304419X09000535

39.   McSherry EA, Donatello S, Hopkins AM, McDonnell S. Molecular basis of invasion in breast cancer. Cell Mol Life Sci. 2007;64(24):3201–18.

40.   Li DM, Feng YM. Signaling mechanism of cell adhesion molecules in breast cancer metastasis: Potential therapeutic targets. Breast Cancer Res Treat. 2011;128(1):7–21.

41.   Berx G, Cleton-Jansen AM, Nollet F, de Leeuw WJ, van de Vijver M, Cornelisse C, et al. E-cadherin is a tumour/invasion suppressor gene mutated in human lobular breast cancers. EMBO J [Internet]. 1995;14(24):6107–15. Available from: http://doi.wiley.com/10.1002/j.1460-2075.1995.tb00301.x

42.  Yilmaz M, Christofori G. Mechanisms of Motility in Metastasizing Cells. Mol Cancer Res [Internet]. 2010;8(5):629–42. Available from: http://mcr.aacrjournals.org/lookup/doi/10.1158/1541-7786.MCR-10-0139

43.  Kalluri R, Weinberg RA. The basics of epithelial-mesenchymal transition. J Clin Invest. 2009;119(6):1420–8.

44.  Gupta GP, Massagué J. Cancer Metastasis: Building a Framework. Cell. 2006;127(4):679–95.

45.  Samatov TR, Tonevitsky AG, Schumacher U. Epithelial-mesenchymal transition: Focus on metastatic cascade, alternative splicing, non-coding RNAs and modulating compounds. Mol Cancer. 2013;12(107):1–12.

46.  Heldin CH, Vanlandewijck M, Moustakas A. Regulation of EMT by TGFβ in cancer. FEBS Lett. 2012;586(14):1959–70.

47.  Ikushima H, Miyazono K. TGFB 2 signalling: A complex web in cancer progression. Nat Rev Cancer [Internet]. 2010;10(6):415–24. Available from: http://dx.doi.org/10.1038/nrc2853

48.  Hamidi H, Ivaska J. Every step of the way: integrins in cancer progression and metastasis. Nat Rev Cancer [Internet]. 2018;18:533–48. Available from: http://dx.doi.org/10.1038/s41568-018-0038-z

49.  Eccles SA, Welch DR. Metastasis: recent discoveries and novel treatment strategies. Lancet. 2007;369(9574):1742–57.

50.  Krakhmal N V., Zavyalova M V., Denisov E V., Vtorushin S V., Perelmuter VM. Cancer invasion: Patterns and mechanisms. Acta Naturae. 2015;7(2):17–28.

51.  Talkenberger K, Ada Cavalcanti-Adam E, Voss-Böhme A, Deutsch A. Amoeboid-mesenchymal migration plasticity promotes invasion only in complex heterogeneous microenvironments. Sci Rep. 2017;7(1):1–12.

52.  Hanna S, El-Sibai M. Signaling networks of Rho GTPases in cell motility. Cell Signal [Internet]. 2013;25(10):1955–61. Available from:

http://dx.doi.org/10.1016/j.cellsig.2013.04.009

53.   Krakhmal N V, Zavyalova M V, Denisov E V, Vtorushin S V, Perelmuter VM. Cancer Invasion: Patterns and Mechanisms. Acta Naturae [Internet]. 2015;7(2):17–28. Available from: http://www.ncbi.nlm.nih.gov/pubmed/26085941%0Ahttp://www.pubmedcentral.nih .gov/articlerender.fcgi?artid=PMC4463409

54.   Vinay DS, Ryan EP, Pawelec G, Talib WH, Stagg J, Elkord E, et al. Immune evasion in cancer : Mechanistic basis and therapeutic strategies. Semin Cancer Biol [Internet]. 2015;35:S185–98. Available from: http://dx.doi.org/10.1016/j.semcancer.2015.03.004

55.   Strell C, Entschladen F. Extravasation of leukocytes in comparison to tumor cells. Cell Commun Signal. 2008;6:1–13.

56.   Paget S. The Distribution of Secondary Growths in Cancer of the Breast. Lancet. 1889;133(3421):571–3.

57.   Balkwill F, Mantovani A. Inflammation and cancer: Back to Virchow? Lancet. 2001;357(9255):539–45.

58.   Scully, Olivia Jane, Bay, Boon-Huat, Yip, George, Yu Y. Breast Cancer Metastasis. Cancer Genoimics & Proteomics. 2012;9:311–20.

59.   Pachmayr E. Underlying Mechanisms for Distant Metastasis –. 2017;11–20.

60.   de Castro Junior G, Puglisi F, de Azambuja E, El Saghir NS, Awada A. Angiogenesis and cancer: A cross-talk between basic science and clinical trials (the "do ut des" paradigm). Crit Rev Oncol Hematol. 2006;59(1):40–50.

61.   Mohan ML, Vasudevan NT, Gupta MK, Elizabeth E, Prasad SVN, Foundation CC. Balancing Act of Receptor Function. Curr Mol Pharmacol. 2015;

62.   Hanlon CD, Andrew DJ. Outside-in signaling - a brief review of GPCR signaling with a focus on the Drosophila GPCR family. J Cell Sci [Internet]. 2015;128(19):3533–42. Available from:

http://jcs.biologists.org/cgi/doi/10.1242/jcs.175158

63.   Zhang R, Xie X. Tools for GPCR drug discovery. Acta Pharmacol Sin. 2012;33(3):372–84.

64.   Osmond RIW, Sheehan A, Borowicz R, Barnett E, Harvey G, Turner C, et al. GPCR screening via ERK 1/2: A novel platform for screening G protein-coupled receptors. J Biomol Screen. 2005;10(7):730–7.

65.   Lefkowitz R, Kobilka B. Studies of G-Protein Coupled Receptor. R Swedish Acad Sci. 2012;50005:549–57.

66.   Stafford, L. J., Xia, C., Ma, W., Cai, Y and Liu M. Advances in Brief Identification and Characterization of Mouse Metastasis-suppressor KiSS1 and Its G-Protein coupled Receptor. Cancer Res. 2002;62:5399–404.

67.   Wang J, Gareri C, Rockman HA. G-protein-coupled receptors in heart disease. Circ Res. 2018;123(6):716–35.

68.   Tuteja N. Signaling through G protein coupled receptors. plant Signal Behav. 2009;4(10):942–7.

69.   Ashokan A, Aradhyam GK. Measurement of intracellular Ca 2+ mobilization to study GPCR signal transduction. In: Shukla AK, editor. Methods in Cell Biology [Internet]. 2nd ed. Elsevier Inc.; 2017. p. 59–66. Available from: http://dx.doi.org/10.1016/bs.mcb.2017.07.002

70.   Eishingdrelo H, Kongsamut S. Minireview : Targeting GPCR Activated ERK Pathways for Drug Discovery. 2013;9–15.

71.   Ma L, Pei G. β-arrestin signaling and regulation of transcription. J Cell Sci. 2007;120:213–8.

72.   Kochetkova M, Kumar S, McColl SR. Chemokine receptors CXCR4 and CCR7 promote metastasis by preventing anoikis in cancer cells. Cell Death Differ. 2009;16(5):664–73.

73.   Lee J, Miele ME, Hicks DJ, Karen K, Trent J, Weissman B, et al. KiSS-1 , a Novel

Human Malignant Melanoma. 1996;88(23):1731–7.

74. Clarke H, Dhillo WS, Jayasena CN. Comprehensive Review on Kisspeptin and Its Role in Reproductive Disorders. Endocrinol Metab [Internet]. 2015;30(2):124–41. Available from: https://synapse.koreamed.org/DOIx.php?id=10.3803/EnM.2015.30.2.124

75. Roseweir AK, Millar RP. The role of kisspeptin in the control of gonadotrophin secretion. Hum Reprod Update. 2009;15(2):203–12.

76. Kotani M, Detheux M, Vandenbogaerde A, Communi D, Vanderwinden JM, Le Poul E, et al. The Metastasis Suppressor Gene KiSS-1 Encodes Kisspeptins, the Natural Ligands of the Orphan G Protein-coupled Receptor GPR54. J Biol Chem. 2001;276(37):34631–6.

77. Trevisan CM, Montagna E, De Oliveira R, Christofolini DM, Barbosa CP, Crandall KA, et al. Kisspeptin/GPR54 System: What Do We Know about Its Role in Human Reproduction? Cell Physiol Biochem. 2018;49(4):1259–76.

78. Murphy KG. YOUNG INVESTIGATOR PERSPECTIVES Kisspeptins : Regulators of Metastasis and the Hypothalamic- Pituitary-Gonadal Axis. J Neuroendocrinol. 2005;17:519–25.

79. Lee DK, Nguyen T, Neill GPO, Cheng R, Liu Y, Howard AD, et al. Discovery of a receptor related to the galanin receptors. 1999;446:103–7.

80. Hori A, Honda S, Asada M, Ohtaki T, Oda K, Watanabe T, et al. Metastin suppresses the motility and growth of CHO cells transfected with its receptor. Biochem Biophys Res Commun. 2001;286(5):958–63.

81. Muir AI, Chamberlain L, Elshourbagy NA, Michalovich D, Moore DJ, Calamari A, et al. AXOR12, a Novel Human G Protein-coupled Receptor, Activated by the Peptide KiSS-1. J Biol Chem. 2001;276(31):28969–75.

82. GPCRdb. Kisspeptin receptor Human [Internet]. [cited 2020 Nov 9]. Available from: https://gpcrdb.org/protein/kissr_human/

83. Cao Y, Li Z, Jiang W, Ling Y, Kuang H. Reproductive functions of Kisspeptin / KISS1R Systems in the Periphery. Reprod Biol Endocrinol. 2019;17(65):1–9.

84. Fernandois D, Na E, Cuevas F, Cruz G, Lara HE, Paredes AH. Kisspeptin is involved in ovarian follicular development during aging in rats. J Endocrinol. 2016;228(3):161–70.

85. Pinto FM, Cejudo-Román A, Ravina CG, Fernández-Sánchez M, Martín-Lozano D, Illanes M, et al. Characterization of the kisspeptin system in human spermatozoa. Int J Androl. 2012;35(1):63–73.

86. Ji K, Ye L, Ruge F, Hargest R, Mason MD, Jiang WG. Implication of metastasis suppressor gene, Kiss-1 and its receptor Kiss-1R in colorectal cancer. BMC Cancer. 2014;14(1):1–12.

87. Sanchez-carbayo M, Capodieci P, Cordon-cardo C. Tumor Suppressor Role of KiSS-1 in Bladder Cancer Loss of KiSS-1 Expression Is Associated with Bladder Cancer. Am J Med. 2003;162(2):609–17.

88. Ikeguchi M, Hirooka Y, Kaibara N. Quantitative reverse transcriptase polymerase chain reaction analysis for KiSS-1 and orphan G-protein-coupled receptor (hOT7T175) gene expression in hepatocellular carcinoma. J Cancer Res Clin Oncol. 2003;129(9):531–5.

89. Wang H, Jones J, Turner T, He QP, Hardy S, Grizzle WE, et al. Clinical and biological significance of KISS1 expression in prostate cancer. Am J Pathol. 2012;180(3):1170–8.

90. Jiang Y, Berk M, Singh LS, Tan H, Yin L, Powell CT, et al. KiSS1 suppresses metastasis in human ovarian cancer via inhibition of protein kinase C alpha. Clin Exp Metastasis. 2005;22(5):369–76.

91. Masui T, Doi R, Mori T, Toyoda E, Koizumi M, Kami K, et al. Metastin and its variant forms suppress migration of pancreatic cancer cells. Biochem Biophys Res Commun. 2004;315(1):85–92.

92. Makri A, Pissimissis N, Lembessis P, Polychronakos C, Koutsilieris M. The

kisspeptin (KiSS-1)/GPR54 system in cancer biology. Cancer Treat Rev [Internet]. 2008;34(8):682–92. Available from: http://dx.doi.org/10.1016/j.ctrv.2008.05.007

93.  Stark AM, Tongers K, Maass N, Mehdorn HM, Held-Feindt J. Reduced metastasis-suppressor gene mRNA-expression in breast cancer brain metastases. J Cancer Res Clin Oncol. 2005;131(3):191–8.

94.  Martin TA, Watkins G, Jiang WG. KiSS-1 expression in human breast cancer. Clin Exp Metastasis. 2005;22:503–11.

95.  Cvetković D, Babwah A V., Bhattacharya M. Kisspeptin/KISS1R System in Breast Cancer. J Cancer [Internet]. 2013;4(8):653–61. Available from: http://www.jcancer.org/v04p0653.htm

96.  Goertzen CG, Dragan M, Turley E, Babwah A V., Bhattacharya M. KISS1R signaling promotes invadopodia formation in human breast cancer cell via β-arrestin2/ERK. Cell Signal. 2016;

97.  Blake A, Dragan M, Tirona RG, Hardy DB, Brackstone M, Tuck AB, et al. G protein-coupled KISS1 receptor is overexpressed in triple negative breast cancer and promotes drug resistance. Nat Publ Gr [Internet]. 2017;7(46525):1–17. Available from: http://dx.doi.org/10.1038/srep46525

98.  Abcam. Western blot protocol [Internet]. 2020. [cited 2019 Feb 26]. Available from: https://www.abcam.com/protocols/general-western-blot-protocol

99.  Van Vuuren RJ, Botes M, Jurgens T, Joubert AM, Van Den Bout I. Novel sulphamoylated 2-methoxy estradiol derivatives inhibit breast cancer migration by disrupting microtubule turnover and organization 06 Biological Sciences 0601 Biochemistry and Cell Biology. Cancer Cell Int [Internet]. 2019;19(1):1–10. Available from: https://doi.org/10.1186/s12935-018-0719-4

100. Marot D, Bieche I, Aumas C, Kuttenn F, Lidereau R, Roux N De. High tumoral levels of Kiss1 and G-protein- coupled receptor 54 expression are correlated with poor prognosis of estrogen receptor-positive breast tumors. 2007;691–702.

101. Matjila M, Millar R, van der Spuy Z, Katz A. The Differential Expression of Kiss1,

MMP9 and Angiogenic Regulators across the Feto-Maternal Interface of Healthy Human Pregnancies: Implications for Trophoblast Invasion and Vessel Development. PLoS One. 2013;8(5).

102. Szereszewski JM, Pampillo M, Ahow MR, Offermanns S, Babwah A V. GPR54 Regulates ERK1 / 2 Activity and Hypothalamic Gene Expression in a G a q / 11 and b -Arrestin-Dependent Manner. PLoS One. 2010;5(9):1–14.

103. Zajac M, Law J, Cvetkovic DD, Pampillo M, Mccoll L, Pape C, et al. GPR54 ( KISS1R ) Transactivates EGFR to Promote Breast Cancer Cell Invasiveness. 2010;6(6).

104. Cvetković D, Dragan M, Leith SJ, Mir ZM, Leong HS, Pampillo M, et al. KISS1R induces invasiveness of estrogen receptor-negative human mammary epithelial and breast cancer cells. Endocrinology. 2013;154(6):1999–2014.

105. Shenoy SK, Drake MT, Nelson CD, Houtz DA, Xiao K, Madabushi S, et al. Activation by the ☐ 2 Adrenergic Receptor *. J Biol Chem [Internet]. 2006;281(2):1261–73. Available from: http://dx.doi.org/10.1074/jbc.M506576200

106. Sun Y, Xu S. Expression of KISS1 and KISS1R ( GPR54 ) may be used as favorable prognostic markers for patients with non-small cell lung cancer. 2013;521–30.

107. Dhar DK, Naora H, Kubota H, Maruyama R, Yoshimura H, Tonomoto Y, et al. Downregulation of KiSS-1 expression is responsible for tumor invasion and worse prognosis in gastric carcinoma. Int J Cancer. 2004;111(6):868–72.

108. Comşa Ş, Cîmpean AM, Raica M. the Story of Mcf7. 2015;3154:3147–54.

109. Subik. K., Lee, J.F., Baxter, L., Strzepek, T., Costello, D., Crowley, P., Xing, L., Hung, M.C., Bonfiglio, T., Hicks, D., G. and Tang P. Breast Cancer : Basic and Clinical Research The Expression Patterns of ER , PR , HER2 , CK5 / 6 , EGFR , Ki-67 and AR by Immunohistochemical Analysis in Breast Cancer Cell Lines. Basic Cancer Basic Clin Res. 2010;4:35–41.

110. Holliday DL, Speirs V. Choosing correct breast cancer cell line. Breast cancer Res

[Internet]. 2011;13(4):1–7. Available from: http://download.springer.com/static/pdf/110/art%253A10.1186%252Fbcr2889.pdf?originUrl=http%3A%2F%2Fbreast-cancer-research.biomedcentral.com%2Farticle%2F10.1186%2Fbcr2889&token2=exp=1494268443~acl=%2Fstatic%2Fpdf%2F110%2Fart%25253A10.1186%25252Fbcr2889.pdf

111. Ottewell PD, O'Donnell L, Holen I. Molecular alterations that drive breast cancer metastasis to bone. Bonekey Rep. 2015;4(January):1–10.

112. Dragan M, Nguyen M, Guzman S, Goertzen C, Brackstone M, Dhillo WS, et al. G protein-coupled kisspeptin receptor induces metabolic reprograming and tumorigenesis in estrogen receptor-negative breast cancer. 2020;

113. Pampillo M, Camuso N, Taylor JE, Szereszewski JM, Ahow MR, Zajac M, et al. Regulation of GPR54 Signaling by GRK2 and □ -Arrestin. 2009;23(December):1–15.

114. Novaira, H. J., Ng, Y., Wolfe, A. and Radovick S. Kisspeptin increases GnRH mRNA expression and secretion in GnRH secreting neuronal cell lines. Mol Cell Endocrinol. 2009;311:126–34.

115. Peta UE, Hogue M, Walker P, Bouvier M. Export from the Endoplasmic Reticulum Represents the Limiting Step in the Maturation and Cell Surface Expression of the Human □ Opioid Receptor *. 2000;275(18):13727–36.

116. Chen Q, Miller LJ, Dong M. Role of N -linked glycosylation in biosynthesis , trafficking , and function of the human glucagon-like peptide 1 receptor. 2010;(8):62–8.

117. Hislop, J. N., and Zastrow M V. Analysis of GPCR Localization and Trafficking. Methods Mol Biol [Internet]. 2011;746:425–40. Available from: http://link.springer.com/10.1007/978-1-61779-126-0

118. Ivell R, Teerds K, Hoffman GE. Proper Application of Antibodies for Immunohistochemical Detection : Antibody Crimes and How to Prevent Them.

2014;155(March):676–87.

119.  Faure, M., Voyno-Yasenetskaya, T. A., and Bourne HR. cAMP and βγ Subunits of Heterotrimeric G Proteins Stimulate the Mitogen-activated Protein Kinase Pathway in CPS-7 Cells. J Biol Chem. 1994;269(March 18):7851–4.

120.  Valk J Van Der, Bieback K, Buta C, Cochrane B, Dirks WG. Fetal Bovine Serum ( FBS ): Past – Present – Future. ALTEX. 2018;35(1):99–118.

121.  Katz, M., Amit, I., and Yarden Y. Regulation of MAPKs by growth factors and receptor tyrosine kinases. Biochim Biophys Acta. 2007;1773(8):1161–76.

122.  Teles, M. G., Bianco, S. D. C., Brito, V. N., Tratbach, E. B., Kuohung, W., Seminara, S. B., Mendonca, B. B., Kaiser, U. B., and Latronico AC. -Activating Mutation in a Patient with Central Precocious Puberty. N Engl J Med. 2008;358:709–15.

123.  Ziegler E, Olbrich T, Emons G, Gründker C. Antiproliferative effects of kisspeptin - 10 depend on artificial GPR54 ( KISS1R ) expression levels. Oncol Rep. 2013;29:549–54.

124.  Wang CH, Qiao C, Wang RC, Zhou WP. KiSS-1-mediated suppression of the invasive ability of human pancreatic carcinoma cells is not dependent on the level of KiSS-1 receptor GPR54. Mol Med Rep. 2016;13(1):123–9.

125.  Brüningk SC, Ian Rivens CB, Oelfke U, Uwe O, Haar G ter. 3D tumour spheroids for the prediction of the effects of radiation and hyperthermia treatments. Sci Rep. 2020;10:1–13.

126.  Teles MG, Trarbach EB, Noel SD, Guerra G, Jorge A, Beneduzzi D, et al. A novel homozygous splice acceptor site mutation of KISS1R in two siblings with normosmic isolated hypogonadotropic hypogonadism. Eur J Endocrinol. 2010;163(1):29–34.

127.  Semple, R. K., Achermann, J. C., Ellery, J., Farooqi, I. S., Karet, F. E., Stanhope, R. G., O'Rahilly, S, m Aparicio SA. Two Novel Missense Mutations in G Protein-Coupled Receptor 54 in a Patient with Hypogonadotropic. J Clin Endocrinol

Metab. 2005;90(3):1849–55.

128.  UniProt. UniProt_Q91V45 (KISS1R_MOUSE). 2020.
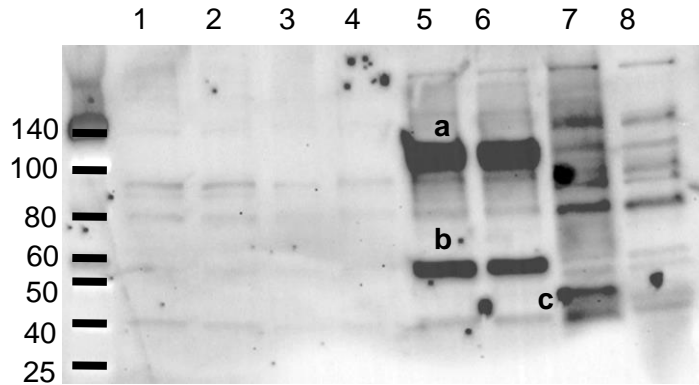
Appendix Figure 1: KISS1R is highly expressed in the BT-20 cell line compared to the MCF7 and MDA-MB-231 cell lines.
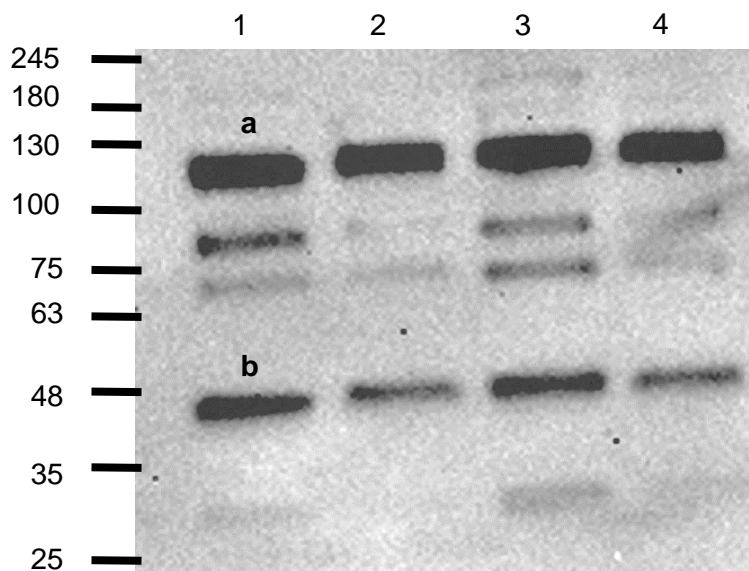
Western blot showing the expression of proteins detected by the KISS1R antibody in the breast cancer cell lines, MCF7 (lane 1, 2), MDA-MB-231 (lane 3, 4) and BT-20 (lane 5, 6), and exogenous KISS1R protein in HEK293-FLAG-KISS1R (lane 7) with HEK293- empty-vector as control (lane 8). Primary antibody was used at 1: 1000. Bands marked (a) are only found in BT-20 cells and have a size of 120 kD, (b) band seen in all samples at 47 kD and (c) 43 kD band only seen in exogenous KISS1R expressing cells. Two independent repeats of Figure 3.1.
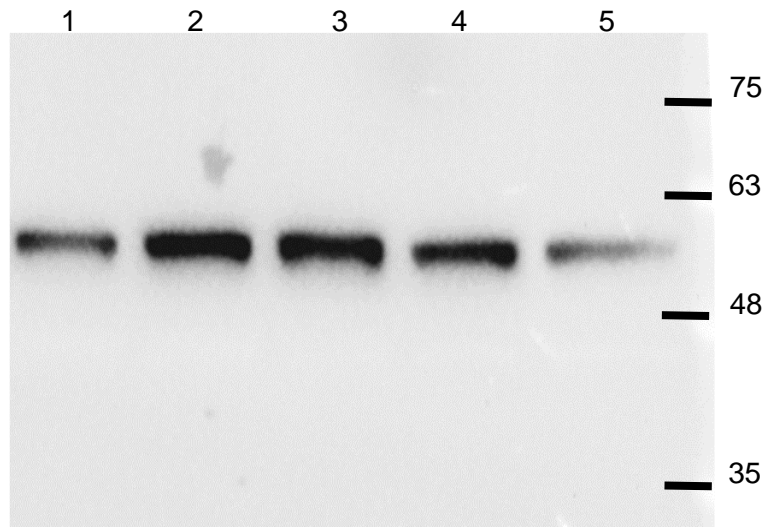


Appendix Figure 2: Western blot showing tubulin expression for Figure 3.1.
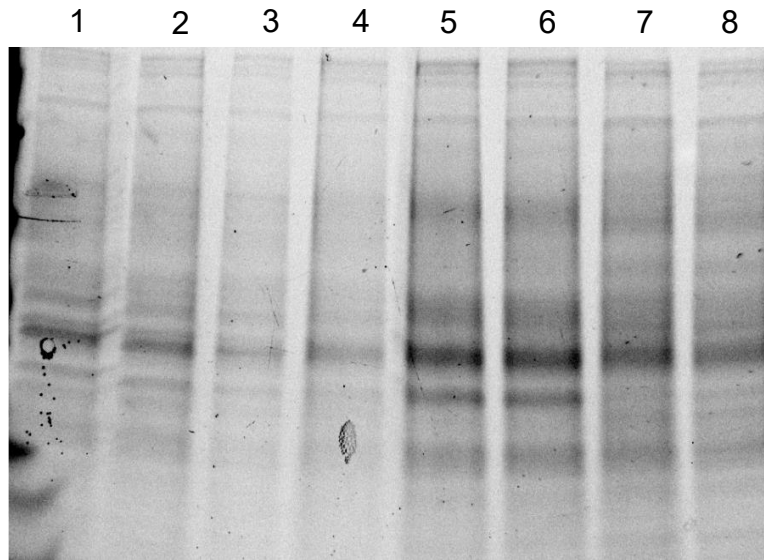
Appendix Figure 3: Gel image showing the total protein of lysates in Appendix Figure1.



Appendix Figure 4: Assessing the glycosylation status of BT-20 using PNGase F and Tunicamycin.

Western blot showing the expression of proteins detected by the KISS1R antibody in BT-20 cell lysates that were either untreated (Lane 1) or treated with a deglycosylation enzyme, PNGaseF (lane 2) or deglycosylation antibiotic, tunicamycin (Lane 3), and the mock control (lane 4), which was incubated with the PNGaseF buffer without the enzyme. The primary antibody was used at 1:1000.
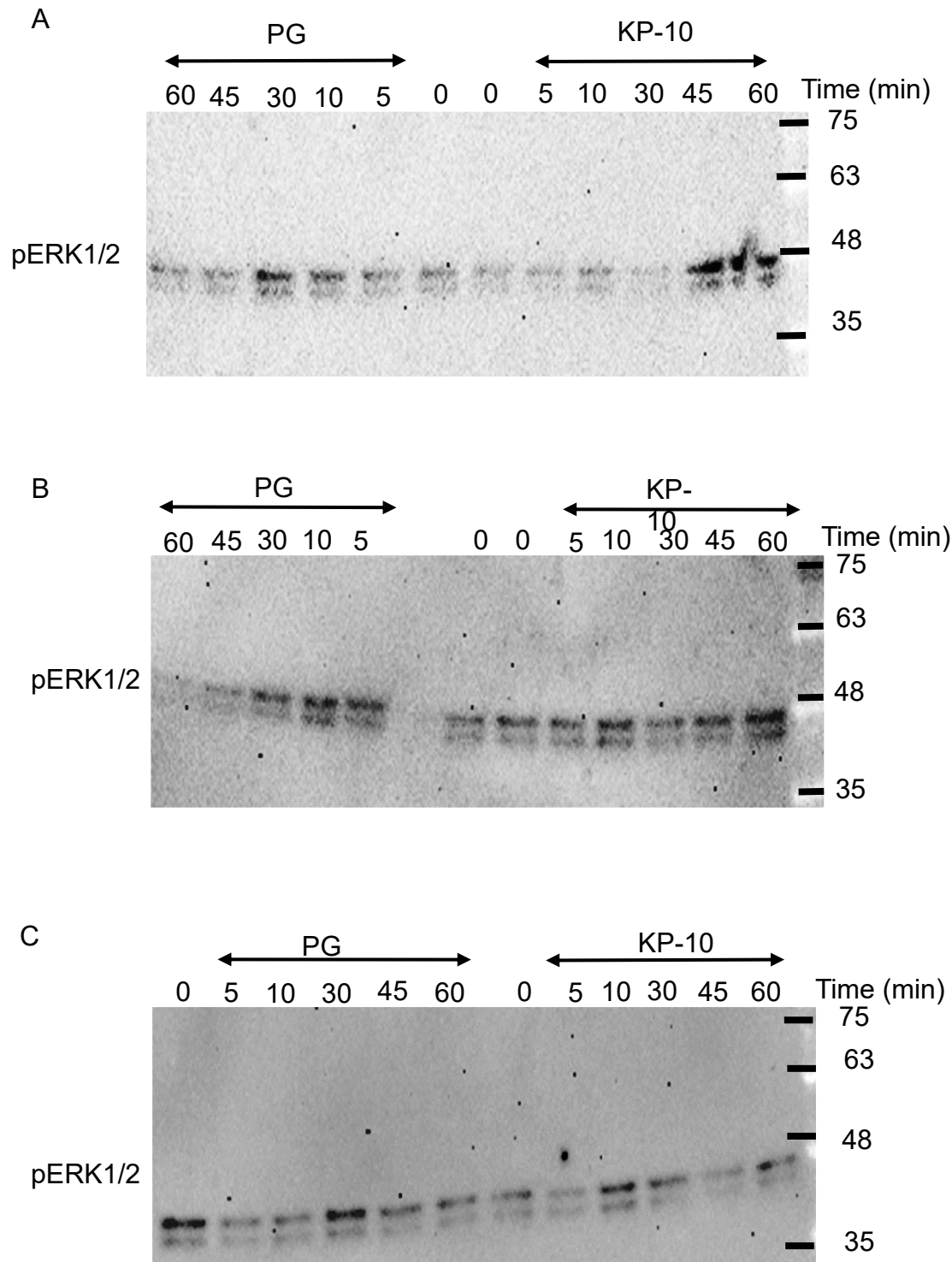
Appendix Figure 5: KISS1R activates ERK phosphorylation a β-arrestin dependent manner in BT-20 cells when stimulated with kisspeptin (KP-10).

(A, B, C, D) BT-20 cells were stimulated with either 100 nM KP-10 or 0.02% propylene glycol (PG) as the vehicle control, for 5, 10, 30, 45 or 60 min. Unstimulated (0) controls were included. After stimulation, the cells were harvested for western blot analysis using rabbit anti-phospho-ERK1/2 antibody. The phospho-ERK antibody was used at 0.25 µg/ml. Three Repeat independent repeats of Figure 3.11.

A

PG ⟷ KP-10

| 60 | 45 | 30 | 10 | 5 | 0 | | 0 | 5 | 10 | 30 | 45 | 60 | Time (min) |

pERK1/2

— 75
— 63
— 48
— 35

B

PG ⟷ KP-10

| 0 | 5 | 10 | 30 | 45 | 60 | | 0 | 5 | 10 | 30 | 45 | 60 | Time (min) |

pERK1/2

— 75
— 63
— 48
— 35
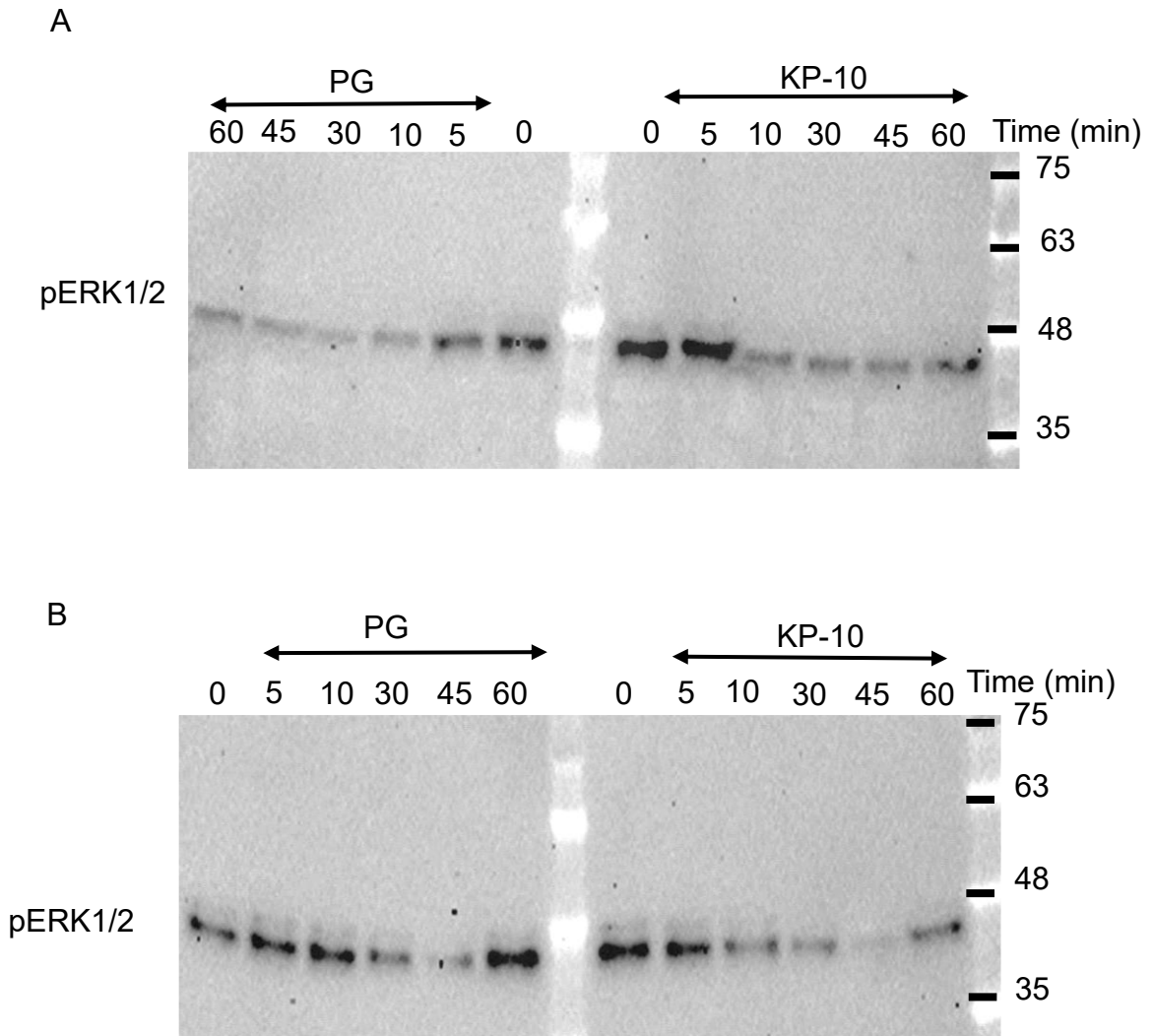
Appendix Figure 6: KISS1R does not activate ERK phosphorylation in MDA-MB-231 cells stimulated with kisspeptin-10 (KP-10).

(A and B) MDA-MB-231 cells were stimulated with either 100 nM KP-10 or 0.02% propylene glycol (PG) as the vehicle control, for 5, 10, 30, 45 or 60 min. Unstimulated (0) controls were included. After stimulation, the cells were harvested for western blot analysis using rabbit anti-phospho-ERK1/2 antibody. The phospho-ERK antibody was used at 0.25 µg/ml. Two independent repeats of Figure 3.12.

134

A



B



C
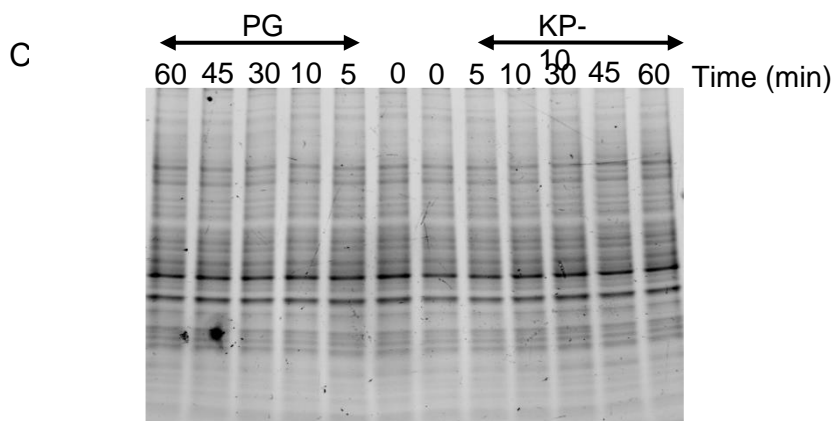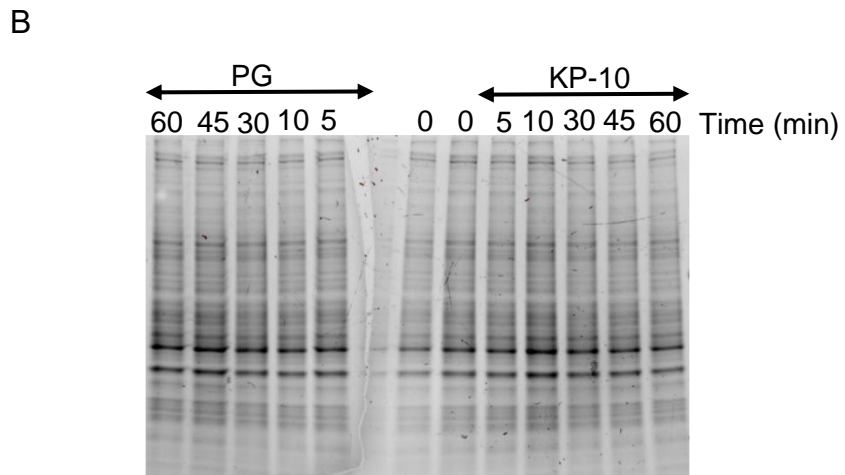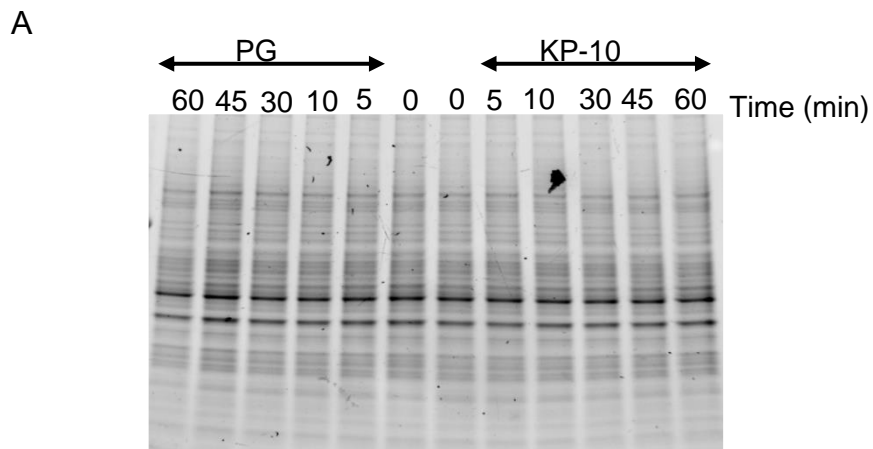


Appendix Figure 7: Gel image for Appendix Figure 5 showing total protein for BT-20 cell lysates stimulated with 100 nM KP-10 at various time points.
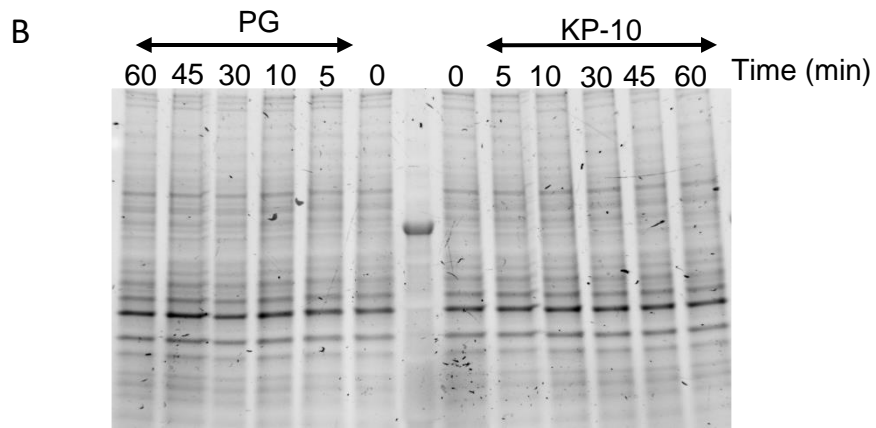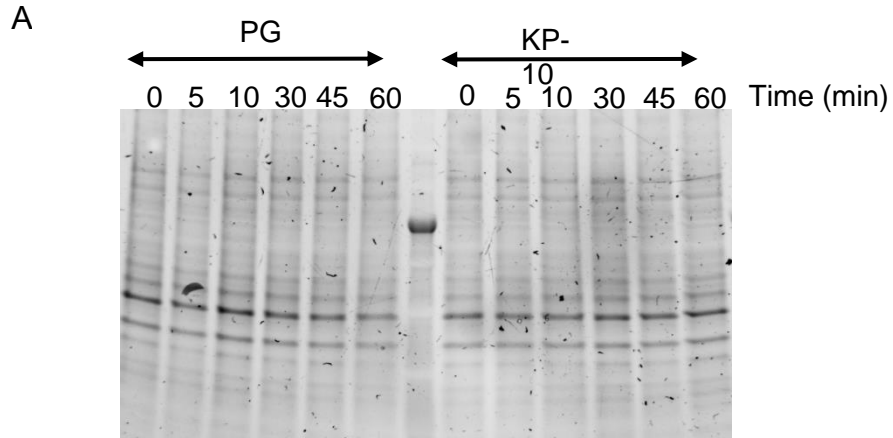
Appendix Figure 8: Gel image for Appendix Figure 6 showing total protein for MDA-MB-231 cell lysates stimulated with 100 nM KP-10 at various time points.
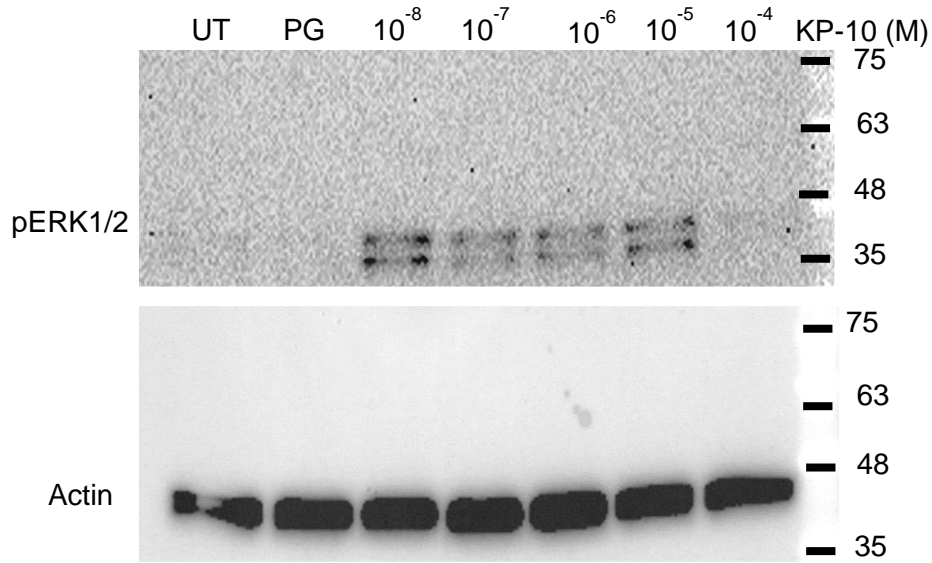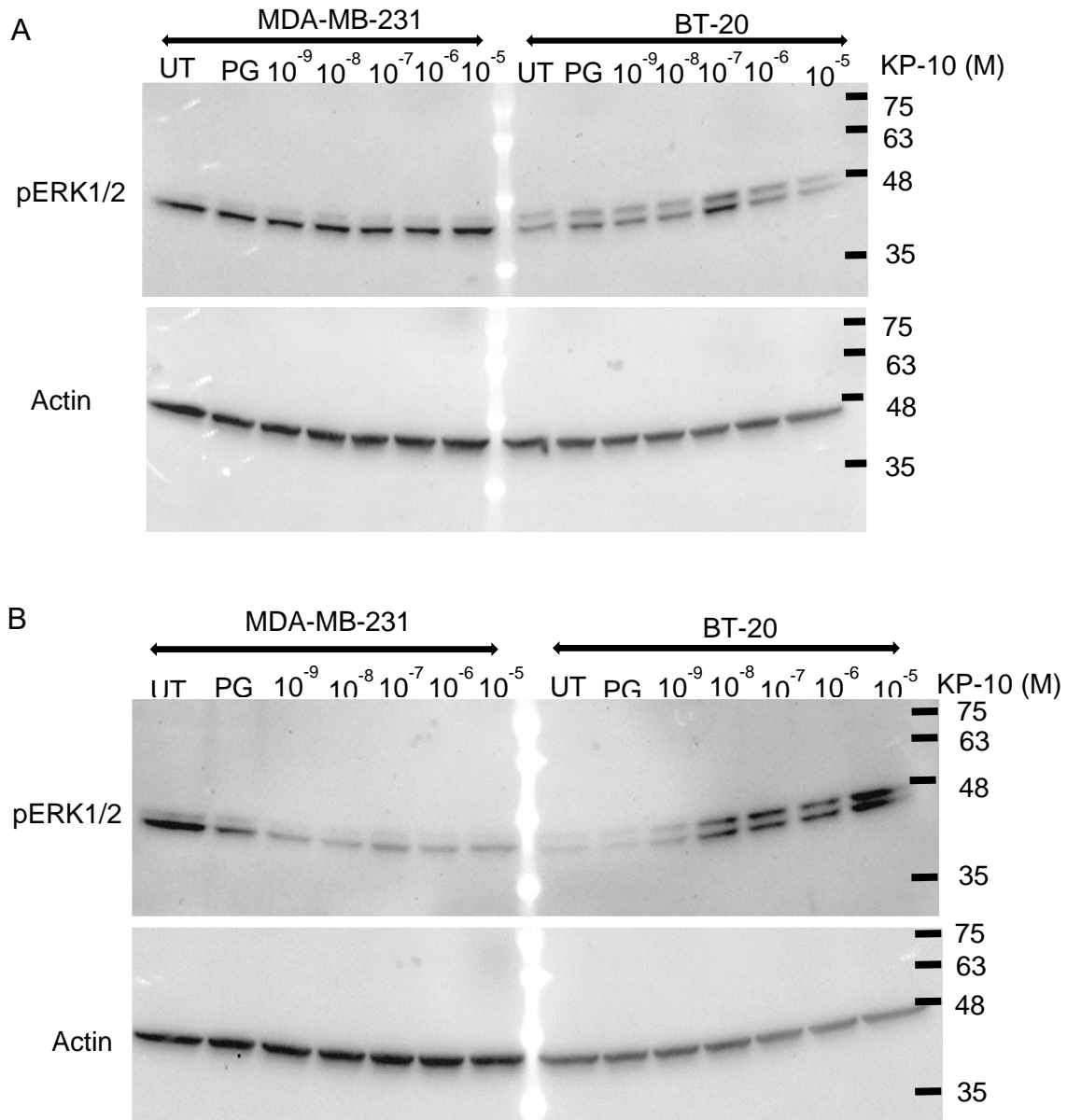
Appendix Figure 9: Endogenous KISS1R in BT-20 cells does not activate ERK1/2 phosphorylation in a dose dependent manner after 5 minutes of stimulation with kisspeptin.

BT-20 cells were stimulated with increasing concentrations ($10^{-8}$ to $10^{-4}$ M or 10 nM to 100 μM KP-10) of KP-10 for 5 min. Unstimulated (UT) and vehicle (PG) controls were included. After stimulation, the cells were harvested for analysis by western blotting using the rabbit phospho-ERK1/2 antibody. Actin (bottom panel) was used as a loading control. Second of Figure 3.15.
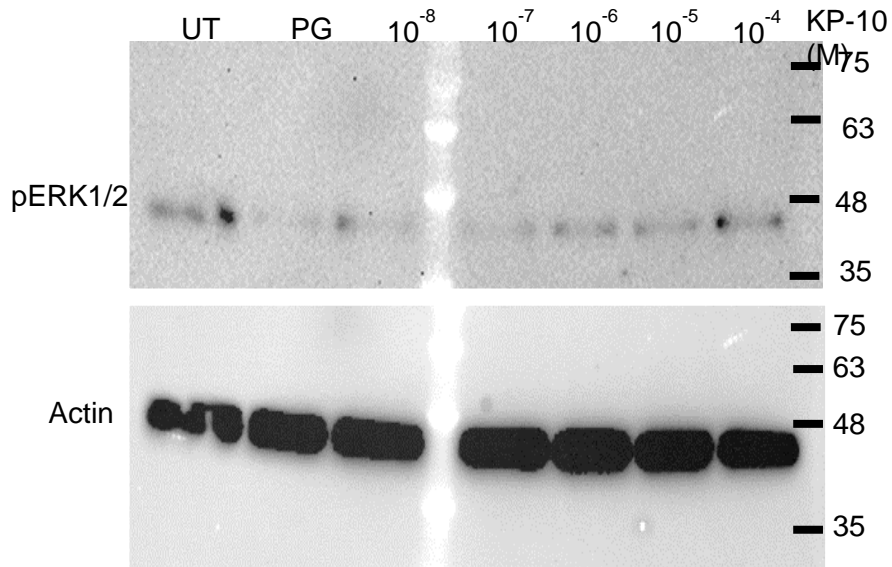
Appendix Figure 10: Endogenous KISS1R in MDA-MB-231 cells does not activate ERK1/2 phosphorylation in a dose dependent manner after 5 minutes of stimulation with kisspeptin.

MDA-MB-231 cells were stimulated with increasing concentrations ($10^{-8}$ to $10^{-4}$ M or 10 nM to 100 µM KP-10) of KP-10 for 5 min. Unstimulated (UT) and vehicle (PG) controls were included. After stimulation, the cells were harvested for analysis by western blotting using the rabbit phospho-ERK1/2 antibody (0.25 µg/ml). Actin (bottom panel) was used as a loading control. Second repeat of Figure 3.16.

Appendix Figure 11: Endogenous KISS1R in MDA-MB-231 and BT-20 cells does not activate ERK phosphorylation in a dose dependent manner after 1 hr stimulation with kisspeptin.

(A and B) MDA-MB-231 (left hand side of the ladder) and BT-20 (right hand side of the ladder) cells were stimulated with increasing concentrations ($10^{-9}$ to $10^{-5}$ M or 1 nM to 10 µM KP-10) of KP-10 for 1 h. Unstimulated (0) and vehicle (PG) controls were included. After stimulation, the cells were harvested for analysis by western blotting using the rabbit phospho-ERK1/2 antibody (0.25 µg/ml). Actin (lower panel) was used as a loading control. Two independent repeats of Figure 3.17.

# Letter of Statistical Clearance

UNIVERSITEIT VAN PRETORIA
UNIVERSITY OF PRETORIA
YUNIBESITHI YA PRETORIA

**Faculty of Health Sciences**
Department of Immunology

## Letter of Statistical Clearance

Thursday, March 14, 2019

This letter is to confirm that the student with the Name; Udochi Felicia Azubuike, Student No: 18278214 studying at the University of Pretoria, discussed the project with the title; *Investigating the*

*Role of the Kisspeptin Receptor, KISS1R, in the Regulation of Breast Cancer Cell Proliferation, Invasion and Migration* with me.

I hereby confirm that I am aware of the project and the statistical analysis of the data generated from the project.

The statistics and analytical tools (Graphpad Prism) that will be used will suffice to achieve the objective(s) of the study.

Yours sincerely

Prof Pieter WA Meyer

Ass. Professor and HoD

Prof PWA Meyer
Head of Department: Immunology
ResCom appointed Biostatistician
University Pretoria

MSc Committee Letter 1

**MSc Committee**
**School of Medicine**
**Faculty of Health Sciences**

UNIVERSITEIT VAN PRETORIA
UNIVERSITY OF PRETORIA
YUNIBESITHI YA PRETORIA

MSc Committee

25 April 2019

Dr I van den Bout

Department of Physiology

Faculty of Health Sciences

Dear Dr,

**Ms F Azuibuike, Student no 18278214**

Please receive the following comments with reference to the MSc Committee submission of the abovementioned student:

| Student name | Ms Felicia Azubuike | Student number | 18278214 |
|---|---|---|---|

| Name of study leader | Dr I van den Bout |
|---|---|
| Department | Physiology |
| Title of MSc | The role of the kisspeptin receptor, KISS1R, in breast cancer cell proliferation, invasion and migration |
| Date of first submission | **March 2019** |
| **Comments to study leader March 2019** | • In the title please remove "Investigating the". Please submit a new MSc form.<br><br>• Ensure that the title on the form and protocol is exactly the same.<br><br>• Please remove the hypotheses.<br><br>• Ensure that you refer correctly to either the gene or protein in the objectives. The gene name needs to be in italics.<br>• The budget needs to be revised as it does not seem to be realistic.<br><br>• The methods lack detail; add detail of procedure to be used. Please remove the background explanation from the methods.<br>• Add a flow diagram of the methodology to be used. |

| | |
|---|---|
| | • The data capturing sheet is incomplete. |
| **April 2019** | ☐ Thank you for submitting the revised protocol and new MSc form. |
| **Decision** | This protocol has been provisionally approved.<br>Please submit the revised protocol to ethics, and supply the MSc committee with proof of acceptance.<br>The internal and external examiners can be nominated and submitted to the MSc<br><br>Committee six months prior to submission of the dissertation. Please ensure that the CV of the examiners includes: supervision, examination and publication records. |

Yours sincerely

Prof Marleen Kock

Chair: MSc Committee

MSc committee Letter 2

MSc Committee

20 June 2019

Dr I van den Bout

Department of Physiology

Faculty of Health Sciences

Dear Dr,

**Ms F Azubuike, Student no 18278214**

Please receive the following comments with reference to the MSc Committee submission of the abovementioned student:

| Student name | Ms Felicia Azubuike | Student number | 18278214 |
|---|---|---|---|
| **Name of study leader** | Dr I van den Bout | | |
| **Department** | Physiology | | |
| **Title of MSc** | The role of the kisspeptin receptor, KISS1R, in breast cancer cell proliferation, invasion and migration | | |
| **Date of first submission** | **March 2019** | | |
| **April 2019** | ☐       Thank you for submitting the revised protocol and new MSc form. | | |
| **June 2019** | ☐       Thank you for submitting the ethics approval letter. | | |

| | This protocol has been approved. |
|---|---|
| **Decision** | Ethics approval has been obtained.<br><br>The internal and external examiners can be nominated and submitted to the MSc Committee six months prior to submission of the dissertation. Please ensure that the CV of the examiners includes: supervision, examination and publication records. |

Yours sincerely

Prof Marleen Kock

Chair: MSc Committee

Ethics Approval Letter 2019





**Faculty of Health Sciences**

The Research Ethics Committee, Faculty Health Sciences, University of Pretoria complies with ICH-GCP guidelines and has US Federal wide Assurance.

• FWA 00002567, Approved dd 22 May 2002 and Expires 03/20/2022.
• IRB 0000 2235 IORG0001762 Approved dd 22/04/2014 and Expires 03/14/2020.

3 June 2019

**Approval Certificate**
**New Application**

**Ethics Reference No.: 271/2019**
**Title: The role of the kisspeptin receptor, KISS1R, in breast cancer cell proliferation, invasion and migration**

Dear Dr JI van den Bout

The **New Application** as supported by documents received between 2019-04-30 and 2019-05-29 for your research, was approved by the Faculty of Health Sciences Research Ethics Committee on its quorate meeting of 2019-05-29.

Please note the following about your ethics approval:
- Ethics Approval is valid for 1 year and needs to be renewed annually by 2020-06-03.
- Please remember to use your protocol number (271/2019) on any documents or correspondence with the Research Ethics Committee regarding your research.
- Please note that the Research Ethics Committee may ask further questions, seek additional information, require further modification, monitor the conduct of your research, or suspend or withdraw ethics approval.

**Ethics approval is subject to the following:**
- The ethics approval is conditional on the research being conducted as stipulated by the details of all documents submitted to the Committee. In the event that a further need arises to change who the investigators are, the methods or any other aspect, such changes must be submitted as an Amendment for approval by the Committee.

We wish you the best with your research.

**Yours sincerely**

_____

**Dr R Sommers**
MBChB  MMed (Int)  MPharmMed  PhD
**Deputy Chairperson** of the Faculty of Health Sciences Research Ethics Committee, University of Pretoria

*The Faculty of Health Sciences Research Ethics Committee complies with the SA National Act 61 of 2003 as it pertains to health research and the United States Code of Federal Regulations Title 45 and 46. This committee abides by the ethical norms and principles for research, established by the Declaration of Helsinki, the South African Medical Research Council Guidelines as well as the Guidelines for Ethical Research: Principles Structures and Processes, Second Edition 2015 (Department of Health)*

Ethics Approval Letter 2020

UNIVERSITEIT VAN PRETORIA
UNIVERSITY OF PRETORIA
YUNIBESITHI YA PRETORIA

**Faculty of Health Sciences**

20 July 2020

**Approval Certificate**
**Annual Renewal**

**Ethics Reference No.:  271/2019**
**Title: The role of the kisspeptin receptor, KISS1R, in breast cancer cell proliferation, invasion and migration**

Dear Dr JI van den Bout

The **Annual Renewal** as supported by documents received between 2020-06-19 and 2020-07-15 for your research, was approved by the Faculty of Health Sciences Research Ethics Committee on its quorate meeting of 2020-07-15.

Please note the following about your ethics approval:
- Renewal of ethics approval is valid for 1 year, subsequent annual renewal will become due on 2021-07-20.
- Please remember to use your protocol number (271/2019 ) on any documents or correspondence with the Research Ethics Committee regarding your research.
- Please note that the Research Ethics Committee may ask further questions, seek additional information, require further modification, monitor the conduct of your research, or suspend or withdraw ethics approval.

**Ethics approval is subject to the following:**
- The ethics approval is conditional on the research being conducted as stipulated by the details of all documents submitted to the Committee. In the event that a further need arises to change who the investigators are, the methods or any other aspect, such changes must be submitted as an Amendment for approval by the Committee.

We wish you the best with your research.

**Yours sincerely**

_____
**Dr R Sommers**
MBChB  MMed (Int)  MPharmMed  PhD
**Deputy Chairperson** of the Faculty of Health Sciences Research Ethics Committee, University of Pretoria

147

# TURNITIN REPORT



## turnitin

### Digital Receipt

This receipt acknowledges that Turnitin received your paper. Below you will find the receipt information regarding your submission.

The first page of your submissions is displayed below.

| | |
|---|---|
| Submission author: | UF (Felicia) Azubuike |
| Assignment title: | Workshop own paper |
| Submission title: | MSc Dissertation |
| File name: | Dissertation_ROSS_EDIT_1.docx |
| File size: | 57.95M |
| Page count: | 156 |
| Word count: | 30,036 |
| Character count: | 164,002 |
| Submission date: | 11-Nov-2020 08:27AM (UTC+0200) |
| Submission ID: | 1442295594 |

UNIVERSITEIT VAN PRETORIA
UNIVERSITY OF PRETORIA
YUNIBESITHI YA PRETORIA

THE ROLE OF THE KISSPEPTIN RECEPTOR, KISS1R, IN BREAST CANCER CELL
PROLIFERATION, INVASION AND MIGRATION

By

UDOCHI FELICIA AZUBUIKE

Submitted in partial fulfilment of the requirements for the Master of Science degree in
Human Physiology

in the

Department of Physiology

Faculty of Health Sciences

UNIVERSITY OF PRETORIA